

K-Ar Age Determination for Quaternary Volcanic Rocks
Based on the Mass Fractionation Correction Method
- Methodology and its Application to Ontake and Aso Volcanoes -

(同位体分別補正法による第四紀火山岩のK-Ar年代測定
- 測定法の開発と御嶽・阿蘇火山への応用 -)

Akikazu Matsumoto

(松本 哲一)

①

K-Ar Age Determination for Quaternary Volcanic Rocks

Based on the Mass Fractionation Correction Method

- Methodology and its Application to Ontake and Aso Volcanoes -

Akikazu Matsumoto

CONTENTS

ABSTRACT

I. INTRODUCTION	1
II. DEVELOPMENT OF K-AR DATING TECHNIQUE FOR QUATERNARY	
VOLCANIC ROCKS	7
II-1 Principle of K-Ar dating technique based on the Mass Fractionation Correction Method	7
II-2 Argon isotopic analysis	10
II-3 Potassium analysis	26
II-4 Error estimation in each analytical procedure	30
II-5 K-Ar age determination for reference materials	33
III. ARGON ISOTOPIC ANALYSES OF HISTORIC VOLCANIC ROCKS	37
III-1 Argon isotopic analyses of historic volcanic rocks	37
III-2 Influence of mass fractionated initial argon on the radiogenic ^{40}Ar analyses	41
III-3 Variation of argon isotopes in a single lava flow	44
III-4 Determination of radiogenic ^{40}Ar by the isochron method	46
III-5 Comparison between historic and late Quaternary volcanic rocks	47
IV. LOWER LIMIT OF MEASURABLE K-AR AGE AND CONCORDANCE	
WITH ^{14}C AGE	51
IV-1 Lower limit of measurable K-Ar age	51
IV-2 Concordance with ^{14}C age	56

V.	K-AR AGE DETERMINATION FOR QUATERNARY VOLCANIC ROCKS ...	58
V-1	K-Ar age determination for Ontake Volcano	58
V-2	K-Ar age determination for Aso Volcano	87
V-3	Eruption ages of some widespread fallout tephras estimated from K-Ar ages of Ontake, Aso and other volcanics	107
V-4	Radiometric ages for Aso-4 ash and Pm-I, and their implications for the late Quaternary sea level fluctuations in South Kanto	116
VI.	CONCLUSIONS	121
	ACKNOWLEDGMENTS	123
	APPENDIX	124
	REFERENCES	146

ABSTRACT

A new K-Ar dating technique based on the "Mass Fractionation Correction Method" (MFCM) has been developed, which is applicable to volcanic rocks that erupted in the order of 10^4 years ago and the gap between the lower limit of K-Ar ages and the upper limit of ^{14}C ages (tens of thousands to hundreds of thousands years ago) could be eliminated. This technique makes it possible to discuss the systematic eruptive histories of Quaternary volcanoes whose lifetimes are within 10^5 - 10^6 years with the combination of ^{14}C dating method.

In the development of analytical procedure, precise argon isotopic analyses have been made on many historic volcanics and it has been concluded that the initial argon isotopic ratios of samples mostly lie on a theoretical mass fractionation line from the present-day atmospheric argon. On the basis of these results, a new K-Ar dating technique has been developed where the initial $^{40}\text{Ar}/^{36}\text{Ar}$ ratio is estimated from a stable $^{38}\text{Ar}/^{36}\text{Ar}$ ratio and the concentration of radiogenic ^{40}Ar is determined by the sensitivity method instead of the conventional isotope dilution method. Potassium analysis has also been improved in its accuracy and precision by the flame emission spectrometry combined with peak integration and lithium internal standard methods.

It has been estimated from argon isotopic ratios of historic volcanics how young volcanics indicate significant K-Ar ages, and the result clarified that the volcanics containing 2% of K_2O indicate significant ages when more than twenty thousand years have passed after their eruptions. K-Ar age determinations for some lavas, which were directly covered with the Aira-Tn ash,

were carried out by the present method and the K-Ar ages obtained are concordant with the ^{14}C age of Aira-Tn ash.

Furthermore, in order to examine the reliability of new K-Ar dating technique for young volcanic rocks, Ontake and Aso Volcanoes were selected and systematic K-Ar age determinations have been made on these volcanics. Their K-Ar ages were concordant with volcanostratigraphies and the following has been clarified.;

(1) Activities of Older Ontake Volcano started at about 700ka and finished before 400ka. It has been clarified that the "Kuragoe-hara Lava", used as a key bed in order to construct the volcanostratigraphy of Older Ontake Volcano, consists of two kinds of lavas that erupted in quite different ages. (2) Activities of Younger Ontake Volcano started at about 80-90ka after more than three hundred thousand years of inactive period. The following activities of the Marishiten Volcano Group started at about 80ka just after finishing of the Mamahahadake Volcano Group and it continued to about 20ka. (3) Aso pyroclastic flows (Aso-1 to 4) indicate significant K-Ar ages (Aso-1: 266 ± 14 ka, Aso-3: 141 ± 5 ka, Aso-3: 123 ± 6 ka and Aso-4: 89 ± 7 ka) from essential lenses, secondary flowed matrixes and vapor phase crystallized part. Activities of nearby coeval monogenetic volcanoes (Akai and Omine Volcanoes) occurred just before the eruption of Aso-2 and Aso-4, respectively. Furthermore, K-Ar ages of central cones clarified that the present shape of Aso caldera formed at least older than 60ka.

Ontake and Aso Volcanoes are the sources of widespread fallout tephras of Pm-I and Aso-4 ash, respectively, and some Ontake and Aso volcanics which gave K-Ar ages were clarified the stratigraphic relations with Pm-I, Aso-4 ash and DKP, so the eruption

ages of Pm-I, Aso-4 ash and DKP have been estimated from K-Ar ages of such volcanics and compared with the ages used in tephrochronology. It has been discussed how these eruption ages have an influence on the time scale used in the late Quaternary sea level fluctuation in South Kanto.

I. INTRODUCTION

Systematic age determinations for volcanoes in Japan clarify temporal and spatial patterns in arc volcanism. However, such age determinations for Quaternary volcanoes having 10^5 - 10^6 years of lifetimes are few in Japan (e.g., Yatsugatake Volcano : Kaneoka et al., 1980 ; Hiruzen Volcano Group and Daisen Volcano : Tsukui et al., 1985 ; Ryohaku-Hida area : Shimizu et al., 1988 ; Shin-etsu Highland : Kaneko et al., 1989 ; Zao Volcano : Takaoka et al., 1989), because it has been difficult for Quaternary volcanics older than the upper limit of ^{14}C dating method (ca. 50ka: Togashi and Matsumoto, 1987) to get accurate eruption ages. Although the fission-track (FT) and ^{238}U - ^{230}Th disequilibrium (Io) dating methods were expected to be applicable to such volcanics, they were not necessarily reliable because of the following reasons.; (1) Quaternary uranium-bearing phenocrysts have few fission tracks and their accurate FT ages can not be expected. (2) Phenocrysts such as zircon used in the Io dating method have a possibility that they had already solidified in a magma chamber (Fukuoka and Kigoshi, 1974) and an isochron age obtained from these phenocrysts may become older than a real eruption age (Fukuoka and Terada, 1984).

Even though the K-Ar dating method technically has been able to date such volcanics by the improvements of electronics and high vacuum techniques (Dalrymple, 1968 ; Hall and York, 1978 ; Gillot et al., 1979, 1982 ; Cassignol and Gillot, 1982), it also remains a serious problem to be solved in order to get meaningful geological ages, i.e., in the conventional K-Ar dating method, the radiogenic ^{40}Ar decayed from ^{40}K has been calculated on the

assumption that the initial $^{40}\text{Ar}/^{36}\text{Ar}$ ratios for all dated samples to be equal to that of the present atmosphere (295.5 : Nier, 1950). Such an uncertainty for the initial ratio has a possibility to make the conventional K-Ar dating of late Quaternary volcanics untrustworthy, because the radiogenic ^{40}Ar accumulated in them is so trace that the present $^{40}\text{Ar}/^{36}\text{Ar}$ ratios are nearly equal to the initial one. It is necessary for K-Ar dating of late Quaternary volcanics to confirm how such an assumption can be assured.

Volcanic products that erupted in historic times have accumulated negligible radiogenic ^{40}Ar , and therefore their present $^{40}\text{Ar}/^{36}\text{Ar}$ ratios can be regarded as representative of initial ratios. Dalrymple (1969) determined $^{40}\text{Ar}/^{36}\text{Ar}$ ratios of historic subaerial volcanic rocks and clarified that their ratios were not necessarily identical to the atmospheric one and were dispersed within 283.5-356.6. This led to the conclusion that accurate K-Ar ages of late Quaternary volcanics could not be obtained by the conventional method assuming the atmospheric initial ratio as shown in Fig. I-1. On the other hand, Krummenacher (1970) and Kaneoka (1980) determined or compiled $^{38}\text{Ar}/^{36}\text{Ar}$ ratios of historic volcanic products in addition to $^{40}\text{Ar}/^{36}\text{Ar}$ ratios and suggested that these ratios generally lay on the theoretical mass fractionation line from the present-day atmospheric one. On the basis of these suggestions, Takaoka et al. (1989) proposed the "Mass Fractionation Correction Method" (MFCM) in order to estimate each initial $^{40}\text{Ar}/^{36}\text{Ar}$ ratio. They presumed the initial argon isotopic ratios of all volcanics to lie on a theoretical mass fractionation line from the atmosphere and

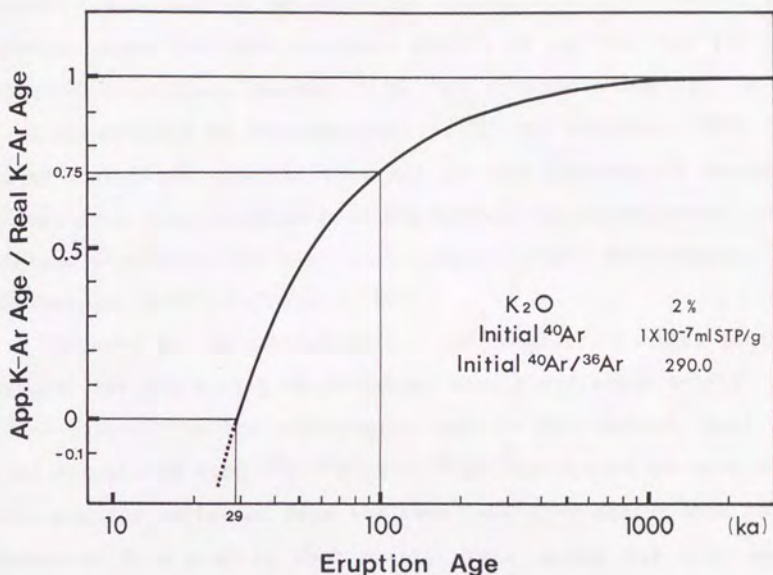


Fig. I -1. Influence of initial $^{40}Ar/^{36}Ar$ ratio different from atmospheric one on conventional K-Ar dating method.

For the sample having 2% of K_2O , $1 \times 10^{-7} \text{ mlSTP/g}$ of initial ^{40}Ar and 290.0 of initial $^{40}Ar/^{36}Ar$ ratio, apparent K-Ar ages in which initial $^{40}Ar/^{36}Ar$ ratio is conventionally assumed to be equal to atmospheric one (295.5), is calculated in each eruption age.

Difference between real eruption age and conventional K-Ar age is significant for the sample younger than 100ka.

estimated initial $^{40}\text{Ar}/^{36}\text{Ar}$ ratio from a stable $^{38}\text{Ar}/^{36}\text{Ar}$ ratio as shown in Fig. I-2. Although MFCM may be one of the most suitable solution to estimate the initial $^{40}\text{Ar}/^{36}\text{Ar}$ ratio, more precise argon isotopic analyses should be carried out for many historic volcanics, because $^{38}\text{Ar}/^{36}\text{Ar}$ ratios of historic volcanics determined by Krummenacher(1970) and Kaneoka(1980) have large analytical uncertainties and are not necessarily enough to accept mass fractionation from the atmosphere. Furthermore, there remains a possibility that such samples might have excess ^{40}Ar (Dalrymple, 1969 ; McDougall, 1969).

Hayatsu and Carmichael(1970) also demonstrated the "Isochron Method" for the dating of volcanics having different initial $^{40}\text{Ar}/^{36}\text{Ar}$ ratios from the atmospheric one. In this method, K-Ar ages were calculated with $^{40}\text{K}/^{36}\text{Ar}$ and $^{40}\text{Ar}/^{36}\text{Ar}$ ratios of some whole rock samples collected from the same lava flow and/or some phases separated from a whole rock sample. This method has been seemed applicable to young volcanics. However, it is not certain whether each sample used in this method should have the same initial $^{40}\text{Ar}/^{36}\text{Ar}$ ratio or not.

In the present study, the following has been done in order to establish a new K-Ar dating technique applicable to volcanics in the range of the upper limit of ^{14}C dating method. ; (1) A new argon analytical system has been constructed to determine $^{38}\text{Ar}/^{36}\text{Ar}$ and $^{40}\text{Ar}/^{36}\text{Ar}$ ratios precisely. (2) More precise $^{38}\text{Ar}/^{36}\text{Ar}$ and $^{40}\text{Ar}/^{36}\text{Ar}$ ratios analyses have been made on many historic volcanic products and stressed the importance of mass fractionation correction for initial $^{40}\text{Ar}/^{36}\text{Ar}$ ratios. (3) It has been estimated how young Quaternary volcanics can be dated when the

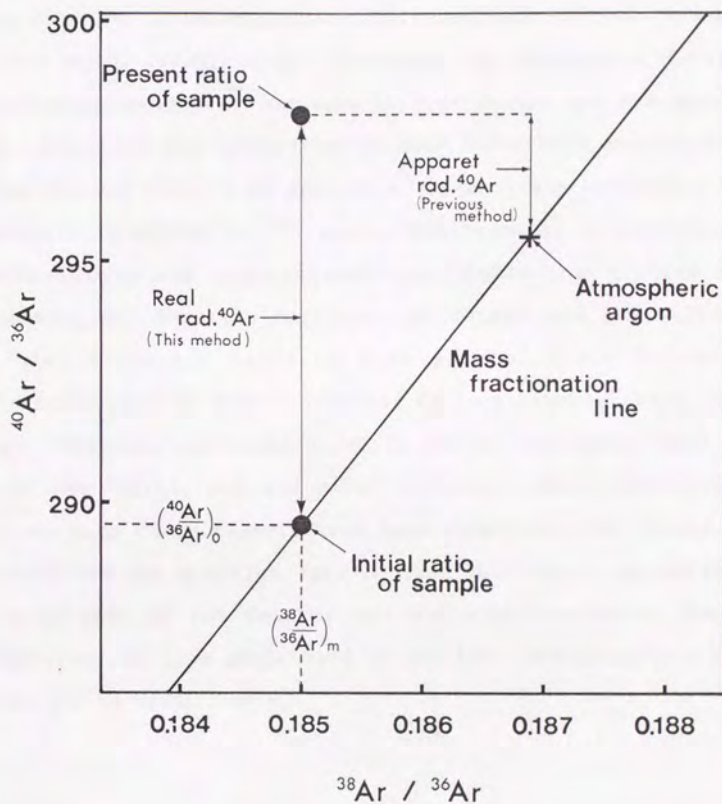


Fig. I-2. Illustration for correction of initial $^{40}\text{Ar}/^{36}\text{Ar}$ ratio by 'Mass Fractionation Correction Method' (Takaoka et al., 1989).

$(^{38}\text{Ar}/^{36}\text{Ar})_m$: $^{38}\text{Ar}/^{36}\text{Ar}$ ratio determined at the present

$(^{40}\text{Ar}/^{36}\text{Ar})_0$: Initial $^{40}\text{Ar}/^{36}\text{Ar}$ ratio estimated from $(^{38}\text{Ar}/^{36}\text{Ar})_m$

Initial argon isotopic ratios are presumed to lie on the theoretical mass fractionation line and the initial $^{40}\text{Ar}/^{36}\text{Ar}$ ratios are estimated from the $^{38}\text{Ar}/^{36}\text{Ar}$ ratios at the present.

initial $^{40}\text{Ar}/^{36}\text{Ar}$ ratio is corrected by MFCM and the concentration of argon is determined by the comparison of peak intensity with the known amount of air standard. (4) Systematic K-Ar age determination using MFCM has been made on Ontake and Aso volcanic rocks. Accuracy and precision of MFCM have been evaluated to confirm whether their K-Ar ages were successively concordant with volcanostratigraphies or ^{14}C ages.; Furthermore, as applications to volcanology and tephrochronology, following studies were performed.; (1) Eruptive histories of Ontake and Aso volcanoes have been discussed based on K-Ar ages of their volcanics. (2) Eruption ages of some widespread fallout tephras (Pm-I, Aso-4 ash and DKP) were estimated directly and/or indirectly from K-Ar ages of the Ontake, Aso and other volcanics whose stratigraphic relations with these tephras have been clarified. (3) It has been discussed how the eruption ages of Pm-I and Aso-4 ash estimated from K-Ar ages of the Ontake, Aso and other volcanics have an influence on the time scale used in the late Quaternary sea level fluctuation in South Kanto.

II. DEVELOPMENT OF K-AR DATING TECHNIQUE FOR QUATERNARY VOLCANIC ROCKS

This chapter describes the development of precise argon isotopic analysis especially for the $^{38}\text{Ar}/^{36}\text{Ar}$ ratio and K-Ar dating technique for young volcanic rocks without using ^{38}Ar spike.

II-1. Principle of K-Ar dating technique based on the Mass Fractionation Correction Method

K-Ar age determination is based on the fact that ^{40}K decays to ^{40}Ar or ^{40}Ca with a half life of 1.25×10^9 years (Steiger and Jäger, 1977). K-Ar age can be calculated by the equation (1), when the concentrations of ^{40}K and radiogenic ^{40}Ar in a sample have been known.

$$t = \frac{1}{(\lambda_{\epsilon} + \lambda_{\beta})} \ln \left[\frac{[\text{Rad. } ^{40}\text{Ar}]}{[^{40}\text{K}]} \left(\frac{\lambda_{\epsilon} + \lambda_{\beta}}{\lambda_{\epsilon}} \right) + 1 \right] \quad (1)$$

t : K-Ar age

λ_{ϵ} : Decay constant from ^{40}K to ^{40}Ar ($0.581 \times 10^{-10}/\text{y}$)

λ_{β} : Decay constant from ^{40}K to ^{40}Ca ($4.962 \times 10^{-10}/\text{y}$)

$[\text{Rad. } ^{40}\text{Ar}]$: Concentration of radiogenic ^{40}Ar (mol/g)

$[^{40}\text{K}]$: Concentration of ^{40}K (mol/g)

The present-day atomic abundance ratio of ^{40}K to total potassium in terrestrial rocks and minerals can be regarded as constant to be 1.167×10^{-4} (Steiger and Jäger, 1977). Therefore, the concentration of ^{40}K can be calculated from the total potassium content. On the other hand, the concentration of radiogenic

^{40}Ar is obtained by argon isotopic analysis, because the abundance ratio of radiogenic ^{40}Ar to total argon varies in each sample. In this study, the radiogenic ^{40}Ar in a sample is calculated by the equation (2), in which the concentration of total ^{40}Ar in a sample is determined by the comparison of total ^{40}Ar peak intensity with the known amount of air standard (sensitivity method) instead of the conventional isotope dilution method using ^{38}Ar spike. The amount of total ^{40}Ar in the air standard is calibrated on the radiogenic ^{40}Ar extracted from a K-Ar dating reference material (JG-1 biotite), and the linearity between amount of ^{40}Ar and ^{40}Ar peak intensity is confirmed by varying the amount of air standard introduced. These analytical procedures will be further described in II-2-2 and 4.

$$[\text{Rad.}^{40}\text{Ar}] = 4.462 \times 10^{-5} [\text{Total}^{40}\text{Ar}] (1 - R_0 / R) \quad (2)$$

$[\text{Rad.}^{40}\text{Ar}]$: Concentration of radiogenic ^{40}Ar (mol/g)

$[\text{Total}^{40}\text{Ar}]$: Concentration of total ^{40}Ar (mlSTP/g)

R_0 : Initial $^{40}\text{Ar}/^{36}\text{Ar}$ ratio

R : $^{40}\text{Ar}/^{36}\text{Ar}$ ratio determined at the present

Although the initial $^{40}\text{Ar}/^{36}\text{Ar}$ ratio (R_0) has been assumed to be equal to the atmospheric ratio (295.5) in the conventional K-Ar method, it is obvious from argon isotopic analyses of historic volcanics that R_0 is not necessarily 295.5 (Dalrymple, 1969 ; Krummenacher, 1970 ; Kaneoka, 1980). R_0 can be estimated by the equations (3) and (4) ("Mass Fractionation Correction Method" (MFCM) : Takaoka et al., 1989) when the initial argon isotopic ratios of dated samples lie on a theoretical mass fractionation

line. Mass fractionation of initial argon isotopes will be discussed in Chapter III based on those of historic volcanic rocks.

$$R_0 = R_A (1 + 4\delta) \quad (3)$$

$$\delta = (r / r_A - 1) / 2 \quad (4)$$

R_0 : Initial $^{40}\text{Ar}/^{36}\text{Ar}$ ratio estimated from $^{38}\text{Ar}/^{36}\text{Ar}$ ratio

R_A : $^{40}\text{Ar}/^{36}\text{Ar}$ ratio of the present-day atmosphere (295.5)

δ : Degree of fractionation per a unit of mass difference

r_A : $^{38}\text{Ar}/^{36}\text{Ar}$ ratio of the present-day atmosphere (0.1869)

r : $^{38}\text{Ar}/^{36}\text{Ar}$ ratio measured of a sample

Analytical uncertainty for the concentration of radiogenic ^{40}Ar and K-Ar age obtained by new dating technique, in which R_0 is estimated by MFCM and the concentration of total ^{40}Ar is determined by the comparison of peak intensity with the air standard, is calculated by the equation (5)-(7). These equations are introduced by the application of "law of propagation of errors" into the equation (1)-(4).

$$\sigma_T^2 = \sigma_K^2 + \sigma_{Ar}^2 \quad (5)$$

$$\sigma_{Ar}^2 = [\sigma_X^2 + \frac{A_c^2}{(1 - A_c)^2} (\sigma_R^2 + \sigma_{Ro}^2)] \quad (6)$$

$$\sigma_{Ro} = [2 r \sigma_r / (2 r - r_A)] \quad (7)$$

$$A_c = [(2 r - r_A) R_A / r_A R] \quad (8)$$

σ_T : Error for calculation of K-Ar age

σ_K : Error for potassium analysis

σ_{Ar} : Error for radiogenic ^{40}Ar analysis

σ_X : Error for total ^{40}Ar analysis

σ_R : Error for $^{40}\text{Ar}/^{36}\text{Ar}$ ratio analysis

- σ_{Ro} : Error for estimation of initial $^{40}\text{Ar}/^{36}\text{Ar}$ ratio
 σ_r : Error for $^{38}\text{Ar}/^{36}\text{Ar}$ ratio analysis
 A_c : Fraction of atmospheric ^{40}Ar

The estimation for these errors indispensable to calculate uncertainties for the concentration of radiogenic ^{40}Ar and the K-Ar ages will be discussed in II-4.

II-2. Argon isotopic analysis

II-2-1. Apparatus

The system for argon isotopic analysis consists of mass spectrometer, extraction furnace and purification system. Most of them are made of stainless steel. Each system is connected by using high vacuum metal valves and ICF flanges sealed with copper gaskets.

< Mass spectrometer >

VG Isotopes 1200C mass spectrometer has been used in this study. The layout is shown in Fig.II-1. This mass spectrometer uses a Nier type ion source equipped with tungsten coil filament. Electro-magnetic analyzer has a 120mm radius and a 60° deflection. Detector provides a Faraday cup (head amplifier is equipped with a $10^{11}\Omega$ resistor) and an electron multiplier. Resolution is larger than 170, when a Faraday cup is used. Adjustment of magnet current, finding of peak center for each argon isotope, and integrations of peak and base line intensities are controlled by a personal computer through the system analyzer. In the normal operation, the vacuum is kept at less than 2×10^{-7} Pa with a 30 l/s

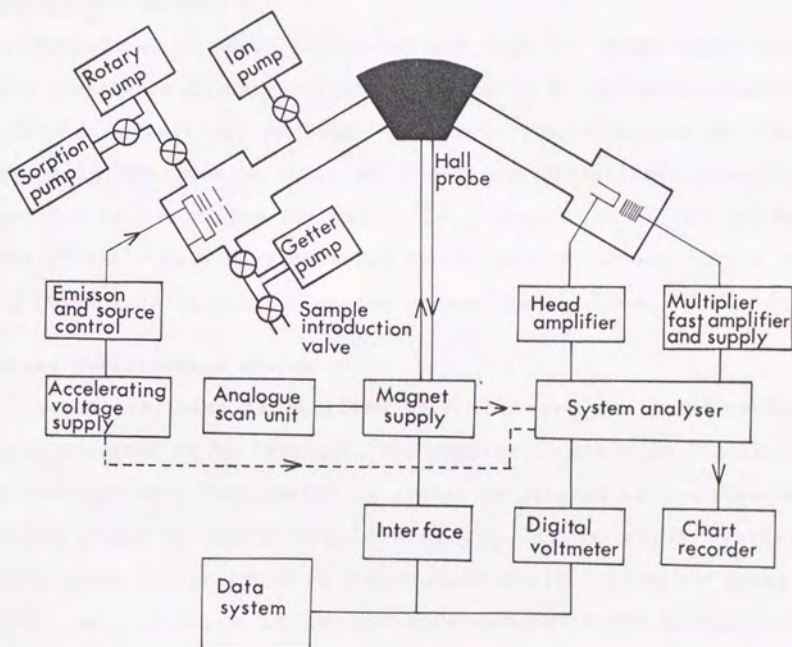


Fig.II-1. Layout of mass spectrometer (VG Isotopes 1200C).

ion pump. Into this mass spectrometer, ^{38}Ar spike has never been introduced in order to determine $^{38}\text{Ar}/^{36}\text{Ar}$ ratios of samples accurately.

< Extraction furnace >

Extraction of argon is carried out with the Ayumi Kogyo tantalum resistance furnace originally designed by Professor Takaoka of Kyushu University. Although the basic specification of this furnace is the same as that of Nagao and Itaya(1988), heating operation is controlled automatically. Temperature of the molybdenum crucible is always measured by the controller and output of this furnace is stabilized at the pre-set temperature.

< Argon purification system >

Argon extracted is purified with the rare gas purification system prepared by VG Isotopes. The outline is shown in Fig.II-2. the U-shaped cold trap, which is soaked in ethanol cooled down to melting point by using liquid nitrogen, traps mainly water. Active gases are adsorbed on two zirconium-aluminum alloy getter pumps, i.e., nitrogen, oxygen and hydrocarbons on the getter pump (G.P.1) heated at 250°C , while hydrogen on that (G.P.2) kept at room temperature. Argon purified is collected on a charcoal trap (C.T.) cooled down with liquid nitrogen. Part A of the purification system (Fig.II-2) is usually pumped with a 30 l/s ion pump, while part B and extraction furnace are pumped with an oil diffusion pump equipped with a liquid nitrogen trap. The vacuum in each part is kept at less than $1 \times 10^{-6}\text{Pa}$.

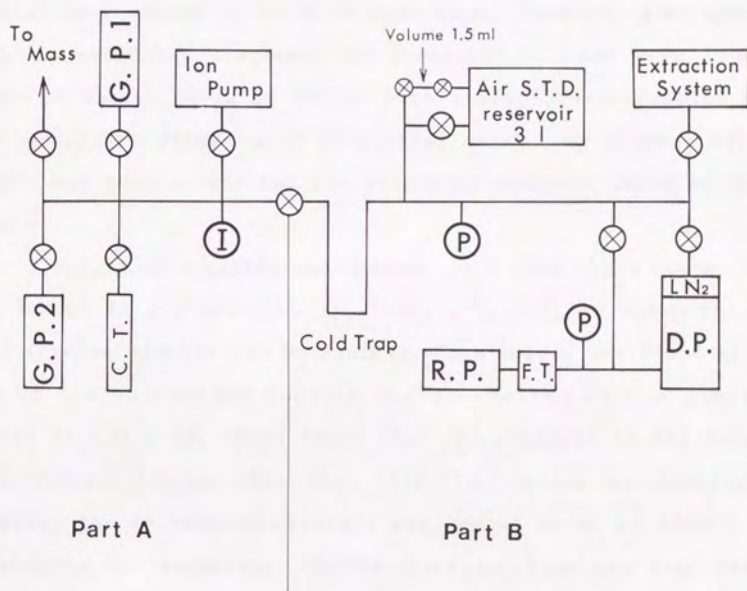


Fig.II-2. Outline of argon purification system.

R.P.: Rotary pump, D.P.: Diffusion pump, F.T.: Foreline trap,
 G.P.1 : Zr-Al alloy getter pump (heated at 250°C),
 G.P.2 : Zr-Al alloy getter pump (kept at room temperature),
 LN₂ : Liquid nitrogen trap, C.T.: Charcoal trap, ①: Ion gauge,
 P: Pirani gauge, X : Metal Valve.

II-2-2. Procedure

< Preparation of samples >

About 100g of whole rock samples were roughly crushed using a stump-mill and then manually crushed using an iron pestle. Most samples were sieved to be 32-60 mesh size, however, some samples such as essential fragments of pyroclastic flows were crushed finer to obtain 60-80 or 80-100 mesh sizes. Sieved samples were ultrasonically rinsed with de-ionized water. An aliquot of the sample was then pulverized for potassium analysis using an agate mortar.

0.1-1.5g of a sample was wrapped in a 10 μ m thick copper foil and loaded in a X'mas-tree type sample holder, as shown in Fig. II-3 (twelve samples can be loaded). This holder was fixed at the top of the extraction furnace and pre-heated with a flexible heater at 125°C for 48-72 hours till the pressure in the extraction furnace became less than 5×10^{-6} Pa. During pre-heating of samples, the molybdenum crucible was heated twice at 1500°C for 30 minutes for degassing. The purification line was also heated at 150°C for 3 hours by flexible heaters at the beginning and the end of pre-heating of samples in order to remove gasses adsorbed on the wall of the line.

< Extraction and purification of argon >

Each sample was dropped into the crucible by moving an iron chip with two magnets. Samples were mostly heated up to 1500°C by 30 minutes and kept at 1500°C for 15 minutes to be melted completely, though the heating speed and maximum temperature were slightly modified on some samples such as rhyolitic rocks. During these procedures, gases extracted were purified with the U-shaped

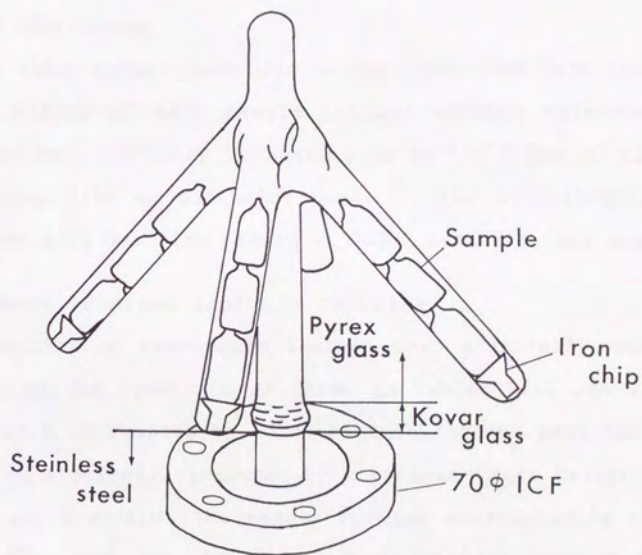


Fig.II-3. Outline of a sample holder.

cold trap and two Zr-Al alloy getter pumps, and argon purified was collected on the charcoal trap cooled down with liquid nitrogen. The pressure of argon was monitored with an ion gauge before the introduction to the mass spectrometer. If the amount of argon exceeded an upper detection limit of detector, it was reduced with valve operations.

Zr-Al alloy getter pumps can be used more than five times in the purification of each sample (ca.2g) without refreshment. These pumps were refreshed by heating up to 750°C for 50 minutes under pumping with an diffusion pump. In the refreshment, the purification line was also heated at 200°C with flexible heaters.

< Measurement of argon isotopic ratios >

Intensities of each argon isotope were statically measured nine times in the condition as shown in Tables II-1 and 2. The magnet current corresponding to each argon isotope peak had been memorized in a personal computer by a program "Mass Calibration" using the air standard. The magnet current corresponding to the center of ^{40}Ar peak was also measured at the beginning of sample analysis to correct a fine drift. The ^{40}Ar intensity, $^{38}\text{Ar}/^{36}\text{Ar}$ and $^{40}\text{Ar}/^{36}\text{Ar}$ ratios in each cycle were calculated by the equation of Dodson(1978), and were extrapolated back to the zero time when argon was introduced to the mass spectrometer. Argon blank and discrimination of argon isotopes which occurred in the mass spectrometer were corrected by the means which will be described in the sections II-2-3 and 4.

< Calibration of the air standard >

Calibration of the air standard was carried out by the

Table II-1. Analytical condition for argon isotopic analysis.

Ion accelerating voltage	4.02 KV
Filament current	2.55 A
Trap current	230 μ A
Emission current	1.5 mA
Repeller voltage	- 6.85 V
Magnet current	2.10~2.20 A
Collector	Faraday cup

Table II-2. Program for argon isotopic analysis.

No.	Mass No.	Integration time (sec.)	Comment
1	35.568	4 (10)*	baseline for ^{36}Ar
2	35.968	7 (10)	^{36}Ar peak
3	36.468	4 (10)	baseline for ^{36}Ar and ^{38}Ar
4	37.963	12 (15)	^{38}Ar peak
5	38.463	4 (15)	baseline for ^{38}Ar and ^{40}Ar
6	39.962	4	^{40}Ar peak

* Numbers in parenthesis are integration time of blank measurement.

following procedure. JG-1 biotite (Uchiumi and Shibata, 1980) was used as the standard material and the weight used was 17-20mg.

- (a) 17-20mg of JG-1 biotite was weighed. Argon was extracted and purified by the same procedure as mentioned in the previous section. The ^{40}Ar intensity and the $^{40}\text{Ar}/^{36}\text{Ar}$ ratio were determined.
- (b) The air standard introduced from a reservoir was purified by the same procedure as (a). Then, the ^{40}Ar intensity and the $^{40}\text{Ar}/^{36}\text{Ar}$ ratio were determined.
- (c) Sensitivity of the mass spectrometer at that time (mlSTP/V) was calculated with the concentration of radiogenic ^{40}Ar in JG-1 biotite (2.49×10^{-5} mlSTP/g ; Uchiumi and Shibata, 1980), and with the ^{40}Ar intensity (V/g) and the $^{40}\text{Ar}/^{36}\text{Ar}$ ratio of JG-1 biotite determined in (a).
- (d) The amount of ^{40}Ar in the air standard introduced from a reservoir was calculated with the sensitivity obtained in (c) and the ^{40}Ar intensity of the air standard determined in (b). Depletion of the air standard in a reservoir was corrected with the equations (9) and (10).

$$\delta = V_T / (V_P + V_T) \quad (9)$$

$$\text{Air}_{(t)} = \text{Air}_{(i)} \delta^{(t-1)} \quad (10)$$

V_P : Volume of pipettes (1.5 ml)

V_T : Volume of reservoir (3 l)

t : The number of times used

$\text{Air}_{(i)}$: Initial amount of air introduced from the reservoir

$\text{Air}_{(t)}$: The amount of air at the t -th introduction

< Calculation of radiogenic ^{40}Ar >

The ^{40}Ar intensity of a sample (V/g) was converted into the amount of total ^{40}Ar (mlSTP/g) to compare with that of the air standard calibrated. The amount of radiogenic ^{40}Ar was calculated by using the amount of total ^{40}Ar , $^{38}\text{Ar}/^{36}\text{Ar}$ and $^{40}\text{Ar}/^{36}\text{Ar}$ ratios from the equations (2)-(4) of II-1.

Analytical procedures mentioned in this section remains some factors to be evaluated more precisely in order to get accurate argon isotopic ratios, e.g., system blanks and discrimination of the mass spectrometer. It will be evaluated in the next sections how such factors influence argon isotopic analysis.

II-2-3. System blank analysis

System blanks produced during argon isotopic analyses have possibilities to disturb accurate argon isotopic analyses. In this section, these blanks are individually determined and their influences on an actual sample analysis are evaluated.

< Background in the mass spectrometer itself >

A background output profile scanned around mass numbers 35 to 40 in a static condition is shown in Fig.II-4. There are three distinct peaks at the mass numbers 35 (8.4×10^{-12} mlSTP), 37 (2.8×10^{-12} mlSTP) and 40 (1.5×10^{-11} mlSTP), and also two trace peaks at 36 (1.3×10^{-12} mlSTP) and 38 (4×10^{-13} mlSTP). As both ratios of (37/35) and (38/36) are about 1:3, respectively, this implies that two distinct peaks at the mass numbers 35 and 37 are derived from ^{35}Cl and ^{37}Cl , respectively, and that two trace peaks at the mass numbers 36 and 38 would be attributed to $^1\text{H}^{35}\text{Cl}$ and $^1\text{H}^{37}\text{Cl}$ which

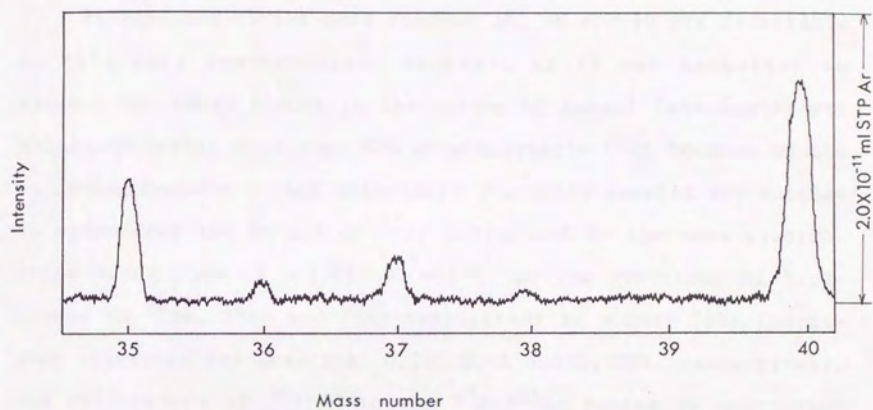


Fig.II-4. Mass spectrometer background around mass numbers 35-40 in the static condition.

are formed by the combination of hydrogen with chlorine. Peaks derived from $^1\text{H}^{35}\text{Cl}$ and $^1\text{H}^{37}\text{Cl}$ can not be separated from ^{36}Ar and ^{38}Ar , respectively, in the resolution of this mass spectrometer (170). On the other hand, another distinct peak at the mass number 40 is derived from memory effect of ^{40}Ar .

Backgrounds at the mass numbers 36, 38 and 40 are detectable in this mass spectrometer. However, it is not necessary to correct for these blanks in the dating of normal late Quaternary volcanics having more than 80% of atmospheric ^{40}Ar because of the following reasons ; late Quaternary volcanics samples are weighed in order that the amount of ^{40}Ar introduced to the mass spectrometer may become $(2.0-5.0) \times 10^{-7} \text{ mlSTP}$, so the fractions of background to ^{36}Ar , ^{38}Ar and ^{40}Ar intensities in normal late Quaternary volcanics are less than 0.23, 0.41 and 0.008%, respectively, and differences of $^{38}\text{Ar}/^{36}\text{Ar}$ and $^{40}\text{Ar}/^{36}\text{Ar}$ ratios by correction of the background are much less than their analytical errors.

< Hot blank >

During heating and purification procedures, argon and other gasses come from the crucible and the wall of lines in addition to gasses released from a sample itself. Such background gasses derived in such a condition are so called "hot blank" gasses. Argon isotopic analysis in the empty condition was made in the same procedure as actual sample analyses in order to estimate this blank. Table II-3 shows the amount of ^{40}Ar and argon isotopic ratios in fifteen hot blank analyses determined before and after actual sample analyses during one month. It should be noticed that the values given in the table are those from which backgrounds in the mass spectrometer itself were previously sub-

Table II-3. Argon isotopic analysis in hot blank.

$^{38}\text{Ar}/^{36}\text{Ar}$	$^{40}\text{Ar}/^{36}\text{Ar}$	^{40}Ar (10^{-9}mlSTP)
0.187 ± 0.007	294 ± 2	21.1
0.191 ± 0.004	293 ± 2	18.3
0.181 ± 0.007	291 ± 5	11.3
0.191 ± 0.010	296 ± 4	6.8
0.185 ± 0.010	294 ± 9	4.8
0.196 ± 0.017	300 ± 8	2.6
0.187 ± 0.022	294 ± 7	5.3
0.197 ± 0.027	302 ± 6	3.7
0.168 ± 0.022	306 ± 10	2.8
0.209 ± 0.030	298 ± 4	2.8
0.193 ± 0.007	291 ± 3	16.6
0.174 ± 0.017	304 ± 8	4.7
0.208 ± 0.034	282 ± 15	2.0
0.182 ± 0.024	282 ± 15	1.8
0.212 ± 0.034	287 ± 7	2.4

Analytical errors in each analysis are given in 1σ .

Table II-4. Argon in metal foils ($10\mu\text{m}$ thick).

Sample	^{40}Ar (mlSTP/g)
Al	3.0×10^{-7}
Sn	4.9×10^{-8}
Cu	9.7×10^{-10}

tracted and corrected for the discrimination of mass spectrometer (mass discrimination correction method will be described in the next section). The amounts of ^{40}Ar are in the range of $(1.8-20) \times 10^{-9} \text{ mlSTP}$ and tend to be larger when a new crucible is used and/or many samples remain in the sample holder. $^{38}\text{Ar}/^{36}\text{Ar}$ and $^{40}\text{Ar}/^{36}\text{Ar}$ ratios are in the range of 0.174-0.212 and 282-306, respectively. These ratios can be regarded as equal to the atmospheric ratios, when the errors in each analysis (1σ) and the deviations of fifteen analyses are considered. In this study, hot blank is always checked before and after actual sample analyses and it is subtracted from peak intensities of argon isotopes obtained in the sample analysis (see APPENDIX I). In the correction of hot blank, the intensity of ^{40}Ar in hot blank [$(^{40}\text{Ar})_b$] is averaged with those determined before and after sample analysis, and it is presumed that the $^{38}\text{Ar}/^{36}\text{Ar}$ and $^{40}\text{Ar}/^{36}\text{Ar}$ ratios of hot blank are the same as those of the atmospheric argon when the ratios determined before and after sample analysis are within their deviations during one month.

< Argon in metal foils >

A metal foil for wrapping crushed samples should have a lower melting point than that of rock samples and have low argon blank. The amount of argon in copper, tin and aluminum foil (10 μm thick), which are commercially available, were determined. The result is shown in Table II-4. Copper foil showed the lowest value, hence samples are wrapped in copper foil. Argon released from copper foil is estimated to be $1.7 \times 10^{-10} \text{ mlSTP } ^{40}\text{Ar}$ when 1 g of sample is extracted, because about 0.18 g of copper foil is necessary to wrap each of samples (ca. 1 g). As the effect of argon

from copper foil to actual sample analysis is less than 0.1%, the effect of argon from copper foil can be negligible in the present study.

II-2-4. Air standard analysis

A long-term stability of the mass spectrometer, a good linearity between the amount of argon and the peak intensity, and an accurate calibration for the air standard also should be confirmed to achieve an accurate argon isotopic analysis, because the concentration of radiogenic ^{40}Ar is obtained by the comparison of peak intensity with a known amount of the air standard. This section describes sufficiencies for these necessary conditions.

< Stability of the mass spectrometer >

A long-term stability of the mass spectrometer was evaluated by replicate analyses of the ^{40}Ar intensity, $^{38}\text{Ar}/^{36}\text{Ar}$ and $^{40}\text{Ar}/^{36}\text{Ar}$ ratios in the air standard. Table II-5 shows their reproducibilities of thirty-five analyses during one month. Their average and standard deviation (1 σ) were $^{38}\text{Ar}/^{36}\text{Ar}=0.1895\pm0.0003$, $^{40}\text{Ar}/^{36}\text{Ar}=298.9\pm0.2$ and $^{40}\text{Ar}=8.846\pm0.047$, respectively. Furthermore, $^{38}\text{Ar}/^{36}\text{Ar}$ and $^{40}\text{Ar}/^{36}\text{Ar}$ ratios were within analytical uncertainties whatever the amount of argon introduced was varied to 1/3, 1/2 and 1.5 times as much as that in Table II-5. Replicate analyses of ^{40}Ar intensity, $^{38}\text{Ar}/^{36}\text{Ar}$ and $^{40}\text{Ar}/^{36}\text{Ar}$ ratios in the air standard suggest that this mass spectrometer has an enough stability to determine radiogenic ^{40}Ar . However, they are somewhat discriminated from the known atmospheric value ($^{38}\text{Ar}/^{36}\text{Ar}=0.1869$ and $^{40}\text{Ar}/^{36}\text{Ar}=295.5$: Nier,1950). In the actual sample

Table II-5. Reproducibility of air standard analyses.

$^{36}\text{Ar}/^{36}\text{Ar}$	$^{40}\text{Ar}/^{36}\text{Ar}$	^{40}Ar intensity* (V)	Times
0.1895 ± 0.0003 (CV. 0.153%)	298.9 ± 0.2 (CV. 0.065%)	8.846 ± 0.047 (CV. 0.528%)	35

* The depletion of air standard in the reservoir is corrected.
 ^{40}Ar introduced to the mass spectrometer is 3.68×10^{-7} mlSTP.

The errors are given in 1σ .

Table II-6. Calibration of ^{40}Ar in the air standard using JG-1 biotite.

^{40}Ar in the air standard (10^{-9} mlSTP)			
373	378	365	370
357	365	371	366
Average	368 ± 7 (CV. 1.8%)		

analysis, this discrimination is corrected by comparing the ratios of the air standard determined during one month with those of Nier(1950) (see APPENDIX I). The drift of sensitivity is estimated to be about 0.5% on the result that the deviation of ^{40}Ar intensity during a month (1σ) is 0.53%.

< Linearity between the amount of argon and the peak intensity >

A linearity between the amount of argon introduced to the mass spectrometer and the intensity is evaluated by varying the amount of argon introduced to 1/3, 1/2 and 1.5 times as much as that in a normal air standard analysis. The result (Fig.II-5) indicates that there is a good linearity in this range, because the regression coefficient between the amount of argon and the intensity is 0.999.

< Calibration of the air standard >

The amount of argon in the air standard is calibrated by the procedure mentioned in II-2-2. In this calibration, hot blank, discrimination of the mass spectrometer and depletion of the air standard are corrected. The result is shown in Table II-6. The mean of eight calibrations is $3.68 \times 10^{-7} \text{ ml STP } ^{40}\text{Ar}$ and the standard deviation (1σ) is 1.8%. In the following determination of radiogenic ^{40}Ar , the sensitivity of the mass spectrometer for argon isotopes at that time is calculated with this value ($3.68 \times 10^{-7} \text{ ml STP } ^{40}\text{Ar}$) and the ^{40}Ar intensity of the air standard at that time.

II-3. Potassium analysis

II-3-1. Apparatus

A flame photometer (Kotaki FIP-3D) has been used in this

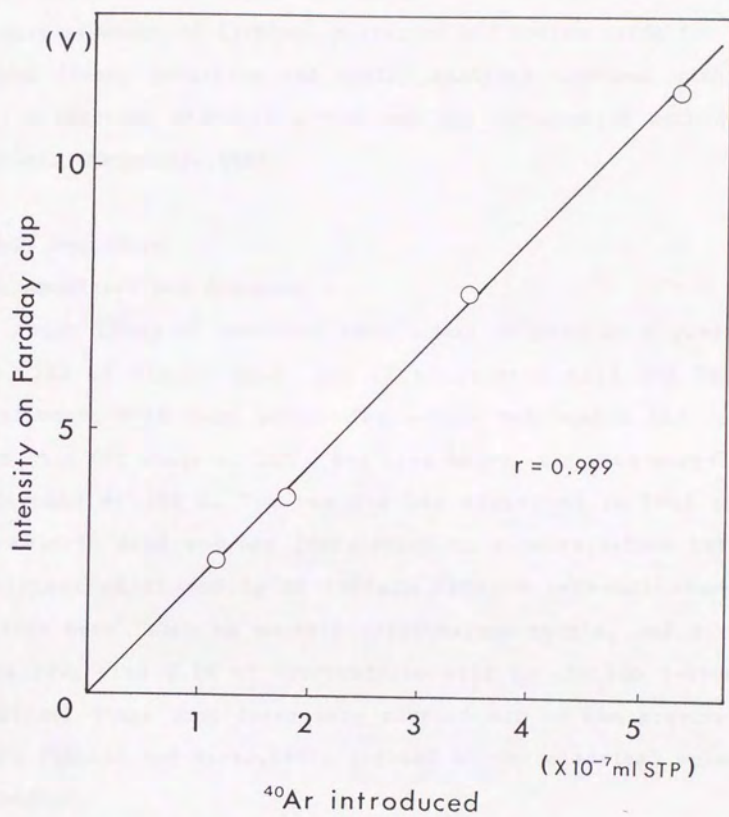


Fig.II-5. Linearity between the amount of argon and the peak intensity.

study. Although this flame photometer is the exclusive one for the determination of lithium, potassium and sodium using the air-propane flame, potassium and sodium analyses combined with the lithium internal standard method and the integration method are available (Matsumoto,1989).

II-3-2. Procedure

< Decomposition and dilution >

About 150mg of powdered sample was weighed in a platinum dish. 3ml of nitric acid, 1ml of perchloric acid and 5ml of hydrofluoric acid were added. The sample was heated and decomposed on a hot plate at 100° C for five hours, and then evaporated to dryness at 200° C. The residue was dissolved in 10ml of 2M hydrochloric acid and was transferred to a polyethylene bottle. An aliquot of it and 2g of 1000ppm lithium internal standard solution were taken to another polyethylene bottle, and diluted up to 100g with 0.1M of hydrochloric acid to contain 1-8ppm of potassium. These procedures were carried out by the gravimetric method (Uchida and Hirao,1987) instead of the classical volumetric method.

< Determination of potassium >

Six potassium standard solutions with concentration of 0, 2, 4, 6, 8, 10 ppm were prepared. These solutions contain 20 ppm of lithium as an internal standard material. The calibration line between the concentration and the relative intensity integrated was obtained as follows. the lithium intensity of the 0ppm K standard was integrated for ten seconds in the condition given in Table II-7. Integration of potassium and lithium intensities in

Table II-7. Analytical condition for flame emission spectrometry of potassium.

Apparatus	KOTAKI Flame photometer FIP-3D
Fuel gas	Propane
Oxidant gas	Air
Fuel gas flow rate	0.28 l/min (2.6 kg/cm ²)
Oxidant gas pressure	1.2 kg/cm ²
Wave length selection	K, Li filter
Sample flow rate	3 ml/min
Integral time	10 sec

* Fuel gas flow and oxidant gas pressure were measured by a flow meter and a pressure gauge, respectively, equipped in the apparatus.

other standards were started at the same condition and were finished when the lithium intensity integrated became the same as that of the Oppm K standard. The calibration line indicates the regression coefficient of more than 0.9999. Sample solutions were also analyzed at the same condition with frequent analyses of the monitor standard solution to check a fine drift of the sensitivity. The concentrations of potassium in sample solutions were calculated from the calibration line.

< Accuracy and precision >

Concentrations of potassium in six USGS and sixteen GSJ reference rock samples were determined in order to evaluate an accuracy and a precision of this method. More than five analyses were independently done in each sample, in which the weights of samples were varied in the range of 100-200mg. The results are shown in Table II-8 and errors for each sample are given in lo. The values obtained are in good agreement with recommended values (Ando et al., 1989 ; Gladney and Burns, 1983) and their standard deviations are less than 0.7%. These results suggest that this method has an accuracy and a precision enough for the determination of potassium in K-Ar dating.

II-4. Error estimation in each analytical procedure

Errors in each analytical procedure should be estimated accurately, because analytical uncertainties for K-Ar ages are calculated from these errors as mentioned in II-1. These errors are estimated as follows.

Table II-8. Comparison of potassium concentrations in reference rock samples.

Samples	K ₂ O concentration, %	
	This work*	Recommended Value**
AGV-1	2.92 ± 0.01	2.90 ± 0.10
BCR-1	1.71 ± 0.01	1.69 ± 0.08
G-1	5.58 ± 0.01	5.48 ± 0.14
G-2	4.52 ± 0.01	4.49 ± 0.14
GSP-1	5.53 ± 0.01	5.51 ± 0.14
W-1	0.641 ± 0.002	0.639 ± 0.041
JG-1	3.99 ± 0.02	3.97 ± 0.058
JG-1a	4.03 ± 0.02	4.01 ± 0.068
JG-2	4.73 ± 0.02	4.72 ± 0.048
JG-3	2.62 ± 0.01	2.63 ± 0.039
JR-1	4.46 ± 0.02	4.41 ± 0.112
JR-2	4.51 ± 0.01	4.45 ± 0.103
JA-1	0.770 ± 0.002	0.775 ± 0.037
JA-2	1.77 ± 0.01	1.80 ± 0.040
JA-3	1.41 ± 0.01	1.41 ± 0.026
JB-1	1.42 ± 0.01	1.43 ± 0.051
JB-1a	1.40 ± 0.01	1.42 ± 0.033
JB-2	0.415 ± 0.002	0.418 ± 0.013
JB-3	0.774 ± 0.002	0.778 ± 0.028
JGb-1	0.230 ± 0.001	0.240 ± 0.012
JF-1	9.90 ± 0.03	10.07 ± 0.022
JF-2	13.07 ± 0.03	13.11 ± 0.087

* Errors are given in 1σ .

** Ando et al., 1989 ; Gladney and Burns, 1983

< Error for potassium analysis >

Replicate determinations of potassium for reference rock samples indicate that their standard deviations (1σ) are less than 0.7%. The error for potassium analysis (σ_K), therefore, is estimated to be 0.7%.

< Error for total ^{40}Ar analysis >

The error for total ^{40}Ar analysis (σ_X) is estimated to be 4% on the basis of following reasons, i.e., the standard deviation (1σ) for calibration of the air standard is 1.8%, the sensitivity of the mass spectrometer for ^{40}Ar varies 0.53% during one month of air standard analyses and the analytical error for the ^{40}Ar intensity in each air standard analysis is less than 0.1%. σ_X (1σ) can be estimated to be about 2% from these results. However, it is assumed to be 4% for safety in the error estimations.

< Error for $^{40}\text{Ar}/^{36}\text{Ar}$ and $^{38}\text{Ar}/^{36}\text{Ar}$ ratio analyses >

Although σ_K and σ_X are fixed as 0.7 and 4%, respectively, errors for $^{40}\text{Ar}/^{36}\text{Ar}$ and $^{38}\text{Ar}/^{36}\text{Ar}$ ratio analyses (σ_R and σ_r) are estimated in each sample analysis. They include not only each analytical error, but also errors produced through the correction for hot blank and discrimination of the mass spectrometer. These errors are calculated on the "law of propagation of errors" (Appendix I: Matsumoto et al., 1989), in which the deviations for $^{38}\text{Ar}/^{36}\text{Ar}$ and $^{40}\text{Ar}/^{36}\text{Ar}$ ratios of hot blank and the air standard compiled during one month are adopted as the errors for these ratios in hot blank and air standard analyses (Appendix I : $\sigma_{(m/m')b}$ and $\sigma_{(m/m')air}$). σ_R and σ_r are usually less than 0.23 and 0.45%, respectively, in the determinations of volcanics

younger than 100ka.

II-5. K-Ar age determination for reference materials

Replicate K-Ar age determinations have been made on some reference materials to evaluate precisions (reproducibilities) of the new technique without using ^{38}Ar spike, in which the initial argon isotopic ratios are presumed to lie on a theoretical mass fractionation line and the initial $^{40}\text{Ar}/^{36}\text{Ar}$ ratios of samples are estimated by the "Mass Fractionation Correction Method".

< Bern 4B >

Bern 4B is a well-known reference material for the conventional K-Ar dating which was prepared at the Bern University and the concentration of radiogenic ^{40}Ar is recommended to be $5.33 \times 10^{-6} \text{ mlSTP/g}$ (Flish, 1982). K-Ar ages were determined independently four times and the results are shown in Table II-9. Uncertainties for $^{38}\text{Ar}/^{36}\text{Ar}$ ratio analyses (σ_r) are considerably large as 0.7-1.2%. However, as is clear from the equations (6)-(8) of II-1, σ_r hardly shows an influence on the dating of this sample and it can be negligible compared with other uncertainties when the fraction of atmospheric ^{40}Ar is low as less than 20%. The concentration of radiogenic ^{40}Ar in each determination can be obtained within 5% errors and the mean is in good agreement with Flish(1982).

< Fish Canyon Tuff biotite >

Fish Canyon Tuff in southwestern U.S.A. has been well dated by the K-Ar, ^{40}Ar - ^{39}Ar and fission-track methods and its age is $27.2 \pm 0.37 \text{ Ma}$ (Hurford and Hammerschmidt, 1985). Zircon and apatite

Table II-9. K-Ar age determination of some reference materials.

Sample Name	Sample wt. (g)	K ₂ O (%)	³⁹ Ar/ ³⁹ Ar	⁴⁰ Ar/ ³⁹ Ar	Total ⁴⁰ Ar (10 ⁻⁹ mlSTP/g)	Rad. ⁴⁰ Ar	Atm. ⁴⁰ Ar (%)	Age (ka)
Bern 4B	0.0667		0.1859 ± 0.0020	1953 ± 10	5910 ± 240	5020 ± 200	15.0	16400 ± 700
	0.0656		0.1863 ± 0.0022	2000 ± 10	6130 ± 250	5230 ± 210	14.7	17100 ± 700
	0.0687	9.47 ± 0.02	0.1867 ± 0.0017	1411 ± 7	6700 ± 270	5300 ± 210	20.9	17300 ± 700
	0.0656		0.1872 ± 0.0014	1836 ± 4	6040 ± 240	5070 ± 200	16.1	16600 ± 700
		9.53*			AV. 5150 ± 100			16900 ± 300
					5530*			
Fish Canyon Tuff biotite	0.0554		0.1885 ± 0.0016	2362 ± 8	9070 ± 360	7920 ± 320	12.7	27600 ± 1100
	0.0553		0.1860 ± 0.0023	2439 ± 10	8770 ± 350	7720 ± 310	12.0	26900 ± 1100
	0.0628	8.90 ± 0.04	0.1867 ± 0.0018	1830 ± 7	9310 ± 370	7810 ± 310	16.1	27200 ± 1100
	0.0626		0.1861 ± 0.0025	2563 ± 6	9150 ± 370	8110 ± 330	11.4	28200 ± 1100
	0.0634		0.1863 ± 0.0022	2306 ± 11	9120 ± 360	7960 ± 320	12.7	27700 ± 1100
		8.92**			AV. 7900 ± 140			27500 ± 500
					7877**			27150 ± 370**
BB-6	2.029		0.1866 ± 0.0010	388.0 ± 1.5	1220 ± 50	295 ± 16	75.9	451 ± 25
	3.017	2.02 ± 0.01	0.1864 ± 0.0006	407.2 ± 0.7	1010 ± 40	281 ± 12	72.2	430 ± 19
	2.994		0.1868 ± 0.0008	403.6 ± 0.8	1070 ± 40	287 ± 10	73.1	440 ± 21
					AV. 286 ± 8			438 ± 13
		2.02 ± 0.04*			288.4 ± 7.6*			441 ± 13*
YZ-1	1.019		0.1873 ± 0.0033	371.1 ± 1.5	610 ± 24	122 ± 18	80.0	223 ± 33
	3.002	1.70 ± 0.01	0.1869 ± 0.0006	368.0 ± 0.8	604 ± 24	119 ± 6	80.3	217 ± 10
	3.025		0.1866 ± 0.0008	375.9 ± 0.9	585 ± 23	122 ± 6	78.4	222 ± 12
					AV. 120 ± 7			219 ± 12
		1.70**			114 ± 7**			208 ± 13**

* Flish (1982)

** N.Takaoka (Personal Communications)

Jäger et al. (1985)

** Hurford and Hammerschmidt (1985)

Rad. ⁴⁰Ar is the concentration of radiogenic ⁴⁰Ar. Atm. ⁴⁰Ar is the fraction of atmospheric ⁴⁰Ar. The means are given in a weighted mean and the errors are in 1σ.

crystals separated from this tuff have become widely distributed standards for the fission-track method. In this study, biotite separated from the sample collected at the same outcrop as used for the fission-track standard, was dated for comparison. This sample contains the same order of radiogenic and atmospheric ^{40}Ar as Bern 4B. K-Ar ages in each determination can be obtained within 5% errors and the mean is in good agreement with Hurford and Hammerschmidt(1985).

< BB-6 and YZ-1 >

BB-6 is a Quaternary reference material of Bern University and YZ-1 is that of Yamagata University for K-Ar dating. K-Ar ages of BB-6 and YZ-1 are $441 \pm 13\text{ka}$ (Jäger et al., 1985) and $208 \pm 13\text{ka}$ (Takaoka, Personal communications), respectively. Four independent potassium analyses and three radiogenic ^{40}Ar analyses were carried out on each sample. The results are shown in Table II-9. The $^{38}\text{Ar}/^{36}\text{Ar}$, $^{40}\text{Ar}/^{36}\text{Ar}$ ratios and the amount of radiogenic ^{40}Ar can be determined within errors of $\sigma_r=0.45$, $\sigma_R=0.2$ and $\sigma_{Ar}=5\%$, respectively, when the weight of a sample for radiogenic ^{40}Ar analysis is 3g. The concentration of radiogenic ^{40}Ar and the K-Ar age in each sample are in good agreement with those reported by Jäger et al.(1985) and Takaoka (Personal communications).

A good precision of new K-Ar dating technique has been confirmed for older than 200ka by replicate determinations of these reference materials. However, the accuracy of this technique for late Quaternary volcanics can not be evaluated without confirming that the initial argon isotopic ratios lie on a theoretical mass fractionation line. In the next chapter, the distribution of initial argon isotopic ratios will be evaluated from those of

historic volcanics. Furthermore, the accuracy and the precision for ages younger than 200ka will be evaluated indirectly as follows. (1) K-Ar age determinations are made on some volcanics covering or covered with widespread fallout tephras which are well dated by the ^{14}C dating method. It has been confirmed whether their K-Ar ages are concordant with ^{14}C ages or not. (2) Systematic K-Ar age determinations for Ontake and Aso volcanics were carried out and the concordance with their volcano-stratigraphies are evaluated.

III. ARGON ISOTOPIC ANALYSES OF HISTORIC VOLCANIC ROCKS

K-Ar dating technique developed in the previous chapter does not use ^{38}Ar spike and the initial $^{40}\text{Ar}/^{36}\text{Ar}$ ratio can be estimated from the stable $^{38}\text{Ar}/^{36}\text{Ar}$ ratio when the initial argon isotopes lie on a theoretical mass fractionation line from the atmosphere. In this chapter, precise argon isotopic analyses are made on many historic volcanic rocks from Japan and it is confirmed that the "Mass Fractionation Correction Method" (MFCM) is useful for the estimation of the initial $^{40}\text{Ar}/^{36}\text{Ar}$ ratio. Furthermore, the influence of mass fractionated initial argon on radiogenic ^{40}Ar analyses and the variation of argon isotopes in a single lava flow are discussed by using these results.

III-1. Argon isotopic analyses of historic volcanic rocks

Twenty-four lava flows and three pyroclastic materials were collected from many parts of Japan. Their eruption ages are well known from records except for the Shessho Lava of Kusatsu-shirane Volcano. The Shessho Lava is estimated to have erupted approximately three thousand years ago (Hayakawa and Yui, 1989). Argon isotopic analyses were carried out by the procedure mentioned in the previous chapter.

The results are shown in Table III-1. The errors for each analysis are given in 1 σ and they include errors produced in the correction of hot blank and discrimination of the mass spectrometer. Analytical errors for the $^{38}\text{Ar}/^{36}\text{Ar}$ ratio are 0.2-0.3% and those for the $^{40}\text{Ar}/^{36}\text{Ar}$ ratio are 0.1-0.2%. These errors for the $^{38}\text{Ar}/^{36}\text{Ar}$ ratio (0.2-0.3%) are one third or less of those (1%) in

Table III-1. Argon isotopic analysis of historic lavas and pyroclastics.

Sample	$^{38}\text{Ar}/^{36}\text{Ar}$	$^{40}\text{Ar}/^{36}\text{Ar}$	Total ^{40}Ar (10^{-9}mlSTP/g)
[Miyakejima Vol.]			
1962 83MY04	0.1867 ± 0.0006	295.1 ± 0.5	140
1983 84MY214	0.1872 ± 0.0006	295.8 ± 0.4	83.5
1983 84MYDH-A	0.1862 ± 0.0003	292.8 ± 0.4	406
1983 84MYDH-B	0.1860 ± 0.0006	292.3 ± 0.5	470
1983 84MYDH-C	0.1860 ± 0.0004	293.1 ± 0.5	186
1983 84MYDH-D	0.1862 ± 0.0005	293.9 ± 0.5	426
1983 84MYDH-E	0.1865 ± 0.0004	293.9 ± 0.3	302
[Izu-Oshima Vol.]			
1951 OH-1	0.1863 ± 0.0006	292.7 ± 0.4	260
1986 LA OSM118	0.1871 ± 0.0005	296.5 ± 0.5	481
1986 LB 80SM302	0.1863 ± 0.0006	293.9 ± 0.6	225
1986 Scoria 358	0.1867 ± 0.0005	295.3 ± 0.5	770
[Fuji Vol.]			
864 560713-1	0.1859 ± 0.0004	292.4 ± 0.3	435
[Akita-Komagatake Vol.]			
1970 NI70101301	0.1860 ± 0.0004	293.2 ± 0.5	122
1970 70SI925-01 (Bomb)	0.1853 ± 0.0006	290.8 ± 0.5	83.7
[Asama Vol.]			
1783 AS-01	0.1857 ± 0.0004	290.9 ± 0.5	340
1783 R14182	0.1870 ± 0.0005	296.0 ± 0.5	397
1783 ONI-21	0.1862 ± 0.0005	292.9 ± 0.3	3120
1783 ONI-22	0.1855 ± 0.0006	291.1 ± 0.5	1290
1108 SA87073105*	0.1851 ± 0.0005	289.3 ± 0.4	366
1108 SA87073107*	0.1865 ± 0.0005	293.3 ± 0.3	1560
1783 R14181 (Pyroclastic)	0.1865 ± 0.0004	294.6 ± 0.5	1080
[Usu Vol.]			
1944 R15244	0.1860 ± 0.0006	292.3 ± 0.4	84.5
1977 77USU	0.1857 ± 0.0005	291.0 ± 0.5	402
[Sakurajima Vol.]			
1946 R12414	0.1849 ± 0.0005	290.2 ± 0.4	274
1475-1476	0.1849 ± 0.0004	296.5 ± 0.6	91.8
R12412	0.1846 ± 0.0005	297.1 ± 0.4	92.5
[Niijima Vol.]			
886 NI77102602	0.1858 ± 0.0006	292.5 ± 0.4	1140
[Kusatsu-shirane Vol.]			
Shessho Lava KS01*	0.1835 ± 0.0005	285.4 ± 0.3	136

The errors are given in 1σ . * SA87073105 is the Kamino-butai Lava and SA87073107 is the Shimono-butai Lava. # The eruption of the Shessho Lava is estimated to be a few thousands years ago.

historic lavas compiled by Kaneoka(1980). Fig.III-1 also shows argon isotopic ratios of these samples. $^{40}\text{Ar}/^{36}\text{Ar}$ ratios are given in the axis of ordinates and $^{38}\text{Ar}/^{36}\text{Ar}$ ratios in that of abscissas. + shows argon isotopic ratios of the atmosphere and the line through + is a theoretical mass fractionation line from the atmosphere.

Of these twenty-seven samples, only four samples shown by open circles can be regarded to have the same argon isotopic ratios as the atmosphere when the errors are considered. Other samples shown by closed circles have the ratios different from the atmospheric ones. These samples except for the Bunmeni Lava (R12412) of Sakurajima Volcano, can be regarded to lie on a mass fractionation line and are mostly fractionated toward the enrichment in lighter isotopes. These results support Krummenacher (1970) and Kaneoka(1980), and it may be presumed that the initial argon isotopic ratio of age-unknown samples mostly lie on a theoretical mass fractionation line and their initial $^{40}\text{Ar}/^{36}\text{Ar}$ ratios can be estimated from the stable $^{38}\text{Ar}/^{36}\text{Ar}$ ratio. The Mass fractionation toward the enrichment to lighter isotopes might occur during the gathering of volatiles into a magma chamber from the ground water and relatively shallow crustal materials containing the atmospheric gases as discussed by Kaneoka(1980).

On the other hand, an exception, i.e., the Bunmeni Lava of Sakurajima Volcano (R12412), would be caused by the existence of excess ^{40}Ar , because the $^{40}\text{Ar}/^{36}\text{Ar}$ ratio measured is distinctly higher than the ratio estimated from the $^{38}\text{Ar}/^{36}\text{Ar}$ ratio. As R12412 is a glassy andesitic lava flow, it might be important for such a glassy sample to check whether excess ^{40}Ar exists or not.

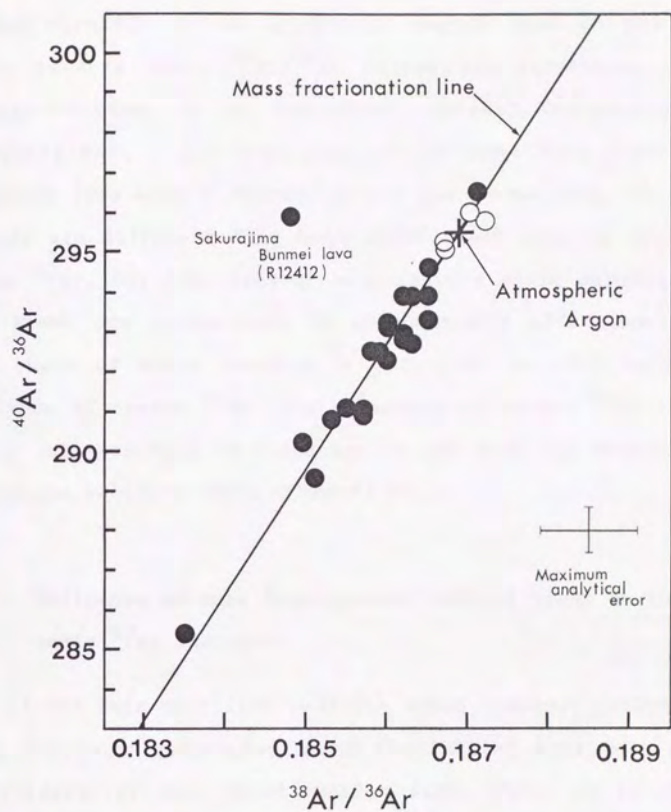


Fig. III-1. Argon isotopic ratios of historic lavas and pyroclastics in Japan.

+ shows argon isotopic ratio of the atmosphere. The line through + is the theoretical mass fractionation line from the atmospheric argon. The range of error shows a maximum deviation (1σ).

However, the excess ^{40}Ar contained in dated samples can not be checked directly by the analytical method used in the present study, because their $^{40}\text{Ar}/^{36}\text{Ar}$ ratios are increasing with the passage of time. It is, therefore, checked indirectly by the following way. ; (1) K-Ar ages of the same lava flow samples collected from some different points are determined. If their K-Ar ages are different from each other, such samples may contain excess ^{40}Ar . (2) K-Ar ages of some samples whose stratigraphy is well known are determined. If an extremely older age compared with those of other samples is obtained, it will indicate an existence of excess ^{40}Ar . The existence of excess ^{40}Ar in actual sample analyses will be discussed in the K-Ar age determinations for Ontake volcanic rocks (Chapter V).

III-2. Influence of mass fractionated initial argon on the radiogenic ^{40}Ar analyses

It has been clarified that the argon isotopic ratios of historic volcanics corresponding to the initial ones mostly lie on the theoretical mass fractionation line. Then, it is evaluated how fractionated initial argon has an influence on the radiogenic ^{40}Ar analyses.

A relationship between the amount of total ^{40}Ar and the degree of mass fractionation [$f = (^{38}\text{Ar}/^{36}\text{Ar})_{\text{sample}} / (^{38}\text{Ar}/^{36}\text{Ar})_{\text{air}}$] is given in Fig. III-2. Their degrees are almost within $f=0.99-1$ independent of total ^{40}Ar . Based on these results, it is estimated how mass fractionated initial argon has an influence on the radiogenic ^{40}Ar analysis when the initial argon is fractio-

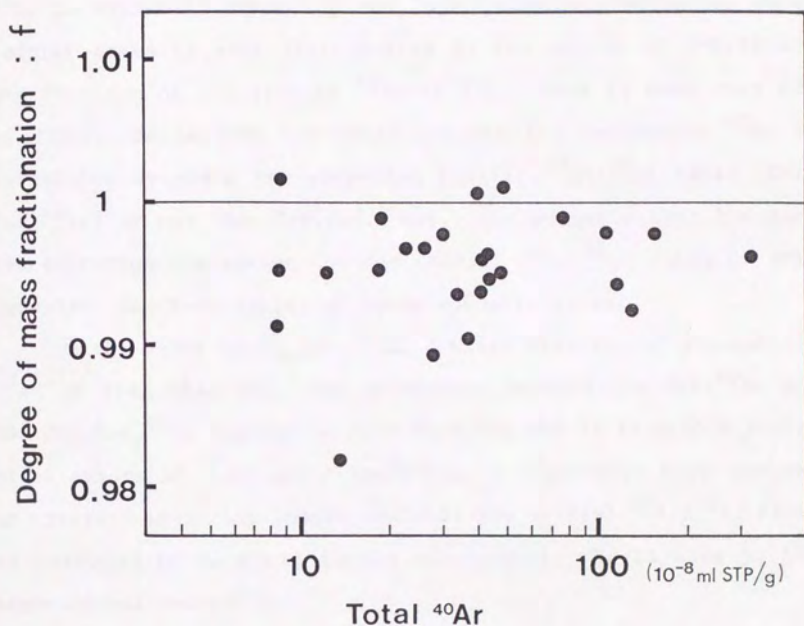


Fig. III-2. Relationship between the amount of total ^{40}Ar and the degree of mass fractionation in historic volcanic products.

f is the degree of mass fractionation and is defined by $(^{38}\text{Ar}/^{36}\text{Ar})_{\text{sample}} / (^{38}\text{Ar}/^{36}\text{Ar})_{\text{air}}$.

nated in the degree of $f=0.99$. The result is given in Fig.III-3.

The fraction of atmospheric ^{40}Ar in late Quaternary volcanic rocks usually exceed 95%, because the accumulation of radiogenic ^{40}Ar is extremely trace. In the late Quaternary volcanics whose initial argon is mass fractionated in the degree of $f=0.99$ and the fraction of atmospheric ^{40}Ar is 95%, there is more than 60% of difference between the cases whether the radiogenic ^{40}Ar is calculated by using the corrected initial $^{40}\text{Ar}/^{36}\text{Ar}$ ratio (Cor. Rad. ^{40}Ar) or not (Non Cor.Rad. ^{40}Ar). This suggests that the mass fractionation correction for the initial $^{40}\text{Ar}/^{36}\text{Ar}$ ratio is very important for K-Ar dating of young volcanic rocks.

On the other hand, in a sample whose fraction of atmospheric ^{40}Ar is less than 80%, the difference between Cor.Rad. ^{40}Ar and Non Cor.Rad. ^{40}Ar reduces to less than 10% and it is within analytical errors of K-Ar ages. Therefore, a reasonable K-Ar age can be obtained in such a sample whatever the initial $^{40}\text{Ar}/^{36}\text{Ar}$ ratio is presumed to be equal to the atmospheric one as done by the conventional method.

III-3. Variation of argon isotopes in a single lava flow

Even in a single lava flow, the surface cools down faster than the interior. Although volatiles gathered in a magma chamber would mostly be degassed and the isotopic equilibrium with the atmospheric argon would be achieved in the part cooled down slowly, yet in the part cooled down faster, such volatiles would mostly be left and their argon isotopes would be in disequilibrium with the atmospheric one. Thus, there is a possibility that

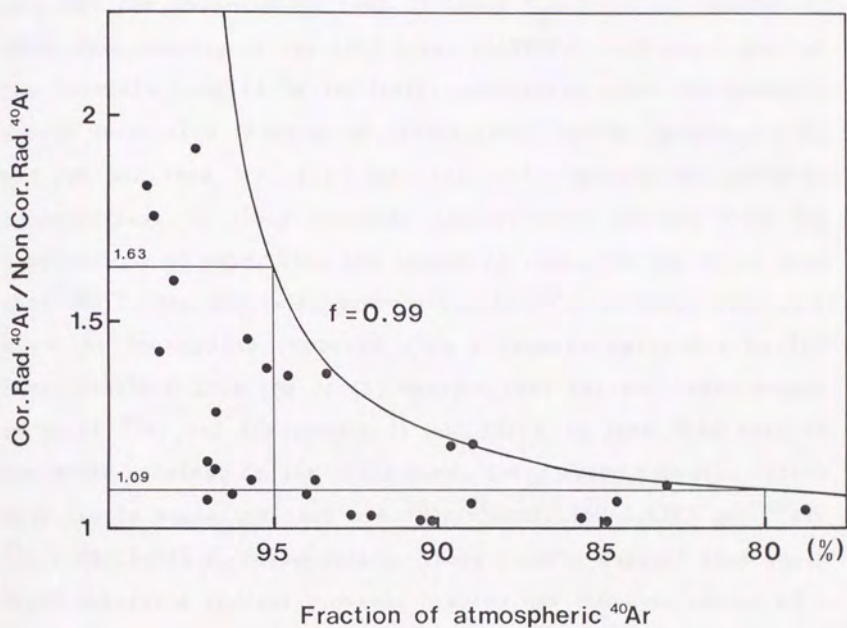


Fig.III-3. Influence of mass fractionated initial argon on radiogenic ^{40}Ar analysis.

Cor.Rad. ^{40}Ar is radiogenic ^{40}Ar calculated with the initial $^{40}\text{Ar}/^{36}\text{Ar}$ ratio, corrected on the basis of $^{38}\text{Ar}/^{36}\text{Ar}$ ratio.

Non Cor.Rad. ^{40}Ar is radiogenic ^{40}Ar calculated with atmospheric $^{40}\text{Ar}/^{36}\text{Ar}$ ratio.

Closed circles show relationships between fraction of non radiogenic ^{40}Ar and Cor.Rad. ^{40}Ar /Non Cor.Rad. ^{40}Ar in actual sample analysis.

the concentration of argon and argon isotopic ratios might be different from place to place even in a single lava flow.

In the present study, the variation of argon isotopes in a single lava flow is checked by the 1983 Lava of Miyakejima Volcano and the Onioshidashi Lava of Asama Volcano that erupted in 1783. Five samples of the 1983 Lavas (84MYDH-A - E) are a part of the borehole core (5.5m in depth) penetrated into the previous ground vertically (Suto et al., 1984). Each sample (84MYDH-A - E) was cut off from 0.7, 2.1, 3.8, 4.2, 5.1m beneath the surface, respectively. As these borehole samples were chilled with the large amount of water when the inside of lava flow was still more than 500° C, the degassing process and isotope exchange reactions might be incomplete compared with a case as naturally cooled lava. 84MYDH-C from the center massive part has the least amount of total ^{40}Ar and its amount is one third or less than that of the other samples. On the other hand, their argon isotopic ratios have little variation that are $^{38}\text{Ar}/^{36}\text{Ar}=0.1860-0.1865$ and $^{40}\text{Ar}/^{36}\text{Ar}=292.3-293.9$, respectively. These results suggest that their argon degassing process proceeds keeping the isotopic ratios of a magma chamber and the secondary mass fractionation hardly occurs during cooling process in the ground surface. Although Itaya and Nagao(1988) also found such a tendency in the lava flow of Aso Volcano, it is not necessarily applicable to all samples, because the sample (84MY214) collected from a different point has a higher ratio than those of borehole samples. In such a sample, the secondary fractionation toward the enrichment in heavier isotopes might occur during degassing process in the ground surface.

Four samples of the Onioshidashi Lava (AS-01, R14182, ONI-

21, ONI-22) were collected from different points of the surface to check horizontal variation of argon isotopes. Although their argon isotopic ratios lie on the fractionation line, a meaningful relationship can not be found between the amount of total ^{40}Ar and the argon isotopic ratios, i.e., AS-01 and R14182 have similar amounts of total ^{40}Ar (AS-01 : 3.40×10^{-7} mlSTP/g, R14182 : 3.97×10^{-7} mlSTP/g), but the $^{40}\text{Ar}/^{36}\text{Ar}$ ratios (AS-01 : 290.9 ± 0.5 , R14182 : 296.0 ± 0.5) are different beyond 1 σ of analytical uncertainties. On the other hand, AS-01 and ONI-22 have a similar argon isotopic ratio (AS-01 : 290.9 ± 0.5 , ONI-22 : 291.1 ± 0.5), but the amount of total ^{40}Ar in ONI-22 (1.29×10^{-6} mlSTP/g) is four times as much as that in AS-01 (3.40×10^{-7} mlSTP/g).

In the present study, vertical and horizontal variations of argon isotopes in a single lava flow have been checked with only two kinds of lava flows. It has been clarified that the amount of total ^{40}Ar and the argon isotopic ratios are not necessarily constant and they vary in a complicated way. A more intensive research should be done to make clear the mechanism for these variations.

III-4. Determination of radiogenic ^{40}Ar by the isochron method

Hayatsu and Carmichael (1970) demonstrated a K-Ar dating technique by the isochron method. This method has been seemed applicable to young volcanics. In this method, K-Ar ages of young volcanics are obtained by the following ways. (1) Some whole rock samples expected to have different potassium or total ^{40}Ar content, are collected from the same lava flow and an isochron age

is calculated with their $^{40}\text{K}/^{36}\text{Ar}$ and $^{40}\text{Ar}/^{36}\text{Ar}$ ratios. (2) Some phases are separated from a whole rock sample and an isochron age is calculated with their ratios.

Fig.III-4 shows $^{40}\text{K}/^{36}\text{Ar}$ and $^{40}\text{Ar}/^{36}\text{Ar}$ ratios of the 1983 Lava of Miyakejima Volcano and the Onioshidashi Lava of Asama Volcano. Two solid lines mean the isochrons of 100ka when the initial $^{40}\text{Ar}/^{36}\text{Ar}$ ratios are 290.9 and 292.3, respectively. $^{40}\text{Ar}/^{36}\text{Ar}$ ratios of such lava flows vary beyond the isochrons of 100 Ka, so the real K-Ar ages younger than 100ka can not be expected in the way of (1). Also in the way of (2), it is unexpected to get real K-Ar ages, because Takaoka(1985) and Itaya and Nagao (1988) suggested that the $^{40}\text{Ar}/^{36}\text{Ar}$ ratios of phenocrysts (e.g., olivine, quartz, plagioclase) were higher than those of ground-mass and their ratios were different from each other because of the existence of excess ^{40}Ar . It is, therefore, concluded that the isochron method is useful only for old samples whose present $^{40}\text{Ar}/^{36}\text{Ar}$ ratios are large enough to neglect the variation of initial $^{40}\text{Ar}/^{36}\text{Ar}$ ratio.

III-5. Comparison between historic and late Quaternary volcanic rocks

In this study, it has been presumed that the volcanic rocks which erupted tens of thousands years ago would be subjected to the similar solidification and cooling processes as historic volcanics, and that the argon isotopic ratios of historic volcanics would be representative of the initial ratios in dated samples. These assumptions were evaluated indirectly by comparing the

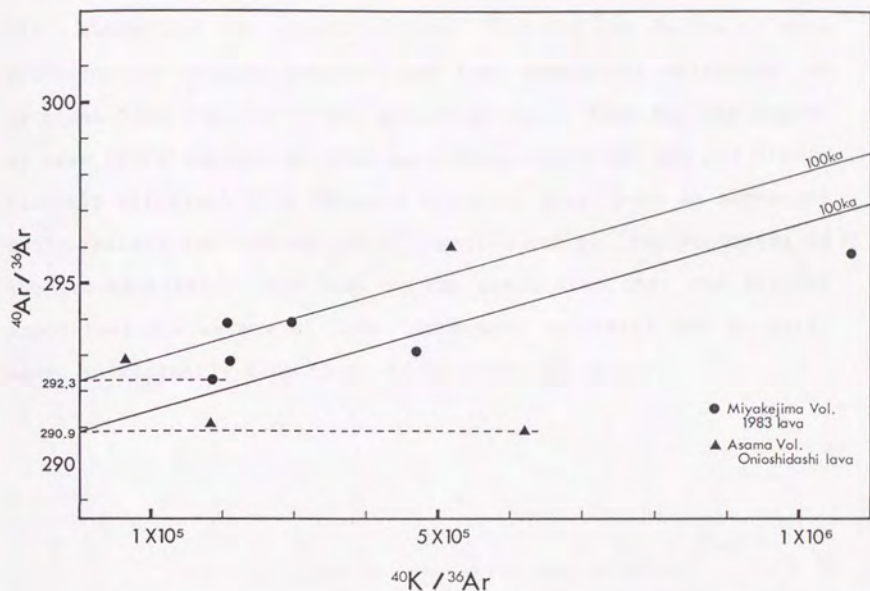


Fig.III-4. K-Ar isochron of a single historic lava flow.

Two kinds of samples were collected from the 1983 Lava of Miyakejima Volcano and the Onioshidashi Lava of Asama Volcano that erupted in 1783.

Two solid lines mean the isochrons of 100ka when the initial $^{40}\text{Ar} / ^{36}\text{Ar}$ ratio is assumed to be 290.9 and 292.3, respectively.

amount of total ^{40}Ar and the degree of mass fractionation between historic and late Quaternary (pre-historic) volcanic rocks. Fig. III-5 summarizes the amount of total ^{40}Ar and the degree of mass fractionation between historic and late Quaternary volcanics. As is clear from Fig. III-5, the amount of total ^{40}Ar and the degree of mass fractionation in late Quaternary volcanics are not significantly different from those of historic ones. Such an agreement would reflect the similar solidification and cooling processes in the ground surface, and lead to the conclusion that the initial argon isotopic ratios of late Quaternary volcanics can be estimated sufficiently from those of historic volcanics.

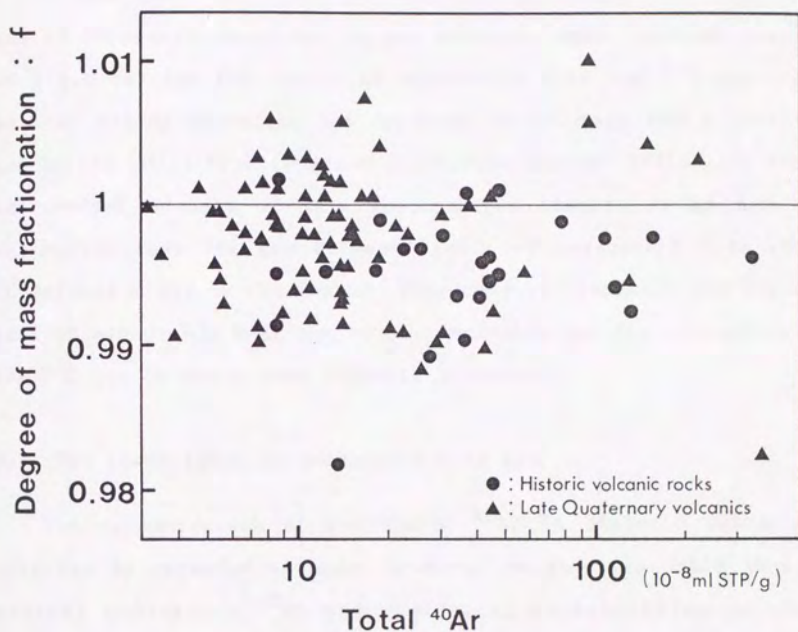


Fig. III-5. Relationship between amount of total ^{40}Ar and degree of mass fractionation in historic and late Quaternary volcanic rocks.

f is the degree of mass fractionation and is defined by $(^{38}\text{Ar}/^{36}\text{Ar})_{\text{sample}} / (^{38}\text{Ar}/^{36}\text{Ar})_{\text{air}}$.

IV. LOWER LIMIT OF MEASURABLE K-AR AGE AND CONCORDANCE WITH ^{14}C AGE

It has been difficult for volcanic products that erupted tens of thousands years ago to get accurate ages, because there was a gap between the limits of measurable K-Ar and ^{14}C ages. A new K-Ar dating technique has improved an accuracy and a precision by the "Mass Fractionation Correction Method" (MFCM) and the instrumental advance of mass spectrometer itself, so it has a possibility that the gap between limits of measurable K-Ar and ^{14}C methods might be eliminated. This chapter describes the lower limit of measurable K-Ar age by new technique and the concordance with ^{14}C age by using some volcanic materials.

IV-1. The lower limit of measurable K-Ar age

The concentration of radiogenic ^{40}Ar in historic volcanic rocks can be regarded as zero. However, as shown in Table IV-1, apparent radiogenic ^{40}Ar and analytical uncertainties can be calculated with the equations of Appendix II (Matsumoto et al., 1989), because their argon isotopic ratios are plotted around the mass fractionation line having uncertainties of $\sigma_r=0.2-0.3\%$ and $\sigma_R=0.1-0.2\%$ as shown in Fig.III-1.

Fig.IV-1 also shows apparent radiogenic ^{40}Ar of historic volcanics, correlated with the amount of total ^{40}Ar . Apparent radiogenic ^{40}Ar are expressed in the absolute values and the corresponding apparent K-Ar ages that are normalized to 1% of K_2O is given in another axis of ordinates. Some of their analytical uncertainties (1 σ) are given in vertical lines and the solid line

Table IV-1. Apparent radiogenic ^{40}Ar and K-Ar ages in historic volcanic rocks.

Sample	$^{39}\text{Ar}/^{36}\text{Ar}$	$^{40}\text{Ar}/^{36}\text{Ar}$	App. Ini. $^{40}\text{Ar}/^{36}\text{Ar}^*$ (10^{-9}mlSTP/g)	Total ^{40}Ar (10^{-9}mlSTP/g)	K ₂ O (%)	App. Rad. ^{40}Ar (10 ⁻⁹ mlSTP/g)	App. Age*** (ka)
【 Miyakejima Vol. 】							
1962 83MY04	0.1867±0.0006	295.1±0.5	294.9±1.9	140	0.620	+ 0.10±0.90	+ 5±50
1983 84MY214	0.1872±0.0006	295.8±0.4	296.4±1.9	83.5	0.548	- 0.20±0.80	- 10±40
1983 84MYDH-A	0.1862±0.0003	292.8±0.4	293.3±1.1	406	0.518	- 0.70±1.60	- 40±90
1983 84MYDH-B	0.1860±0.0006	292.3±0.5	292.7±2.0	470	0.541	- 0.60±3.20	- 40±190
1983 84MYDH-C	0.1860±0.0004	293.1±0.5	292.7±1.4	186	0.538	+ 0.30±1.00	+ 20±60
1983 84MYDH-D	0.1862±0.0005	293.9±0.5	293.3±1.6	426	0.538	+ 0.90±2.40	+ 50±140
1983 84MYDH-E	0.1865±0.0004	293.9±0.3	294.2±1.2	302	0.545	- 0.30±1.30	- 20±80
【 Izu-Oshima Vol. 】							
1951 OH-1	0.1863±0.0006	292.7±0.4	293.6±1.9	260	0.411	- 0.80±1.70	- 60±130
1986 LA OSM118	0.1871±0.0005	296.5±0.5	296.1±1.8	481	0.405	+ 0.70±3.00	+ 50±230
1986 LB 80SM302	0.1863±0.0006	293.9±0.6	293.6±1.8	225	0.457	+ 0.20±1.40	+ 20±100
1986 Scoria 358	0.1867±0.0005	295.3±0.5	294.9±1.7	770	0.452	+ 1.00±4.60	+ 70±310
【 Fuji Vol. 】							
864 560713-1	0.1859±0.0004	292.4±0.3	292.3±1.4	435	0.905	+ 0.20±2.10	+ 5±70
【 Akita-Komagatake Vol. 】							
1970 NI70101301	0.1860±0.0004	293.2±0.5	292.7±1.2	122	0.481	+ 0.20±0.60	+ 10±30
1970 70S1925-01 (Bomb)	0.1853±0.0006	290.8±0.5	290.4±1.9	83.7	0.506	+ 0.10±0.60	+ 7±30

* App. Ini. $^{40}\text{Ar}/^{36}\text{Ar}$ indicates the apparent initial $^{40}\text{Ar}/^{36}\text{Ar}$ ratio calculated by the equation of Appendix I on the basis of the observed $^{39}\text{Ar}/^{36}\text{Ar}$ ratio.

** App. Rad. ^{40}Ar indicates the concentration of apparent radiogenic ^{40}Ar that is calculated with the amount of total ^{40}Ar , $^{40}\text{Ar}/^{36}\text{Ar}$ observed and App. Ini. $^{40}\text{Ar}/^{36}\text{Ar}$.

*** App. Age indicates the apparent K-Ar age that is calculated with K₂O content and App. Rad. ^{40}Ar . The decay constants used in the age calculation are $\lambda = 4.962 \times 10^{-10}/\text{y}$, $\lambda_s = 0.561 \times 10^{-10}/\text{y}$ and $^{40}\text{K}/\text{K} = 0.01167$ atom %.

Table IV-1. (continued)

Sample	$^{39}\text{Ar}/^{36}\text{Ar}$	$^{40}\text{Ar}/^{36}\text{Ar}$	App. Ini. $^{40}\text{Ar}/^{36}\text{Ar}$	Total ^{40}Ar (10^{-9}mlSTP/g)	K ₂ O (%)	App. Rad. ^{40}Ar (10^{-9}mlSTP/g)	App. Age (ka)
【Asama Vol.】							
1783 AS-01	0.1857 ± 0.0004	290.9 ± 0.5	291.7 ± 1.3	340	1.30	-0.90 ± 1.60	-20 ± 40
1783 R14182	0.1870 ± 0.0005	296.0 ± 0.5	295.8 ± 1.7	397	1.24	$+0.30 \pm 2.40$	$+7 \pm 60$
1783 ONI-21	0.1862 ± 0.0005	292.9 ± 0.3	293.3 ± 1.6	3120	1.25	-4.30 ± 17.0	-110 ± 430
1783 ONI-22	0.1855 ± 0.0006	291.1 ± 0.5	291.1 ± 2.0	1290	1.44	0	0
1108 SA87073105	0.1851 ± 0.0005	289.3 ± 0.4	289.8 ± 1.5	366	1.22	-0.60 ± 2.00	-20 ± 50
1108 SA87073107	0.1865 ± 0.0005	293.3 ± 0.3	294.2 ± 1.4	1560	1.42	-4.80 ± 7.80	-110 ± 170
1783 R14181 (Pyroclastic)	0.1865 ± 0.0004	294.6 ± 0.5	294.2 ± 1.1	1080	1.05	$+1.50 \pm 4.50$	$+40 \pm 130$
【Usu Vol.】							
1944 R15244	0.1860 ± 0.0006	292.3 ± 0.4	292.7 ± 1.8	84.5	0.986	-0.10 ± 0.60	-4 ± 20
1977 770SU	0.1857 ± 0.0005	291.0 ± 0.5	291.7 ± 1.7	402	1.27	-1.00 ± 2.50	-20 ± 60
【Sakurajima Vol.】							
1946 R12414	0.1849 ± 0.0005	290.2 ± 0.4	289.2 ± 1.7	274	1.81	$+0.90 \pm 1.70$	$+20 \pm 30$
1475-1476 R12412	0.1849 ± 0.0004	296.5 ± 0.6	289.2 ± 1.2	91.8	2.47	$+2.30 \pm 0.40$	$+28 \pm 5$
	0.1846 ± 0.0005	297.1 ± 0.4	288.2 ± 1.5	92.5		$+2.80 \pm 0.50$	$+35 \pm 6$
【Niijima Vol.】							
886 NI7102602	0.1858 ± 0.0006	292.5 ± 0.4	292.0 ± 1.9	1140	3.28	$+2.00 \pm 7.50$	$+20 \pm 70$
【Kusatsu-shirane Vol.】							
Shesho Lava KS01	0.1835 ± 0.0005	285.4 ± 0.3	284.7 ± 1.5	136	1.82	$+0.30 \pm 0.70$	$+6 \pm 10$

is drawn along the upper limits of 1 σ uncertainties for apparent radiogenic ^{40}Ar . As is clear from Fig.IV-1, apparent radiogenic ^{40}Ar and the solid line drawn along the upper limits of 1 σ of uncertainties for apparent radiogenic ^{40}Ar are increasing with the amount of total ^{40}Ar . Such a tendency results from the fact that the apparent radiogenic ^{40}Ar is calculated by the multiplication of total ^{40}Ar (see Appendix II). As the solid line mentioned above corresponds to the maximum apparent radiogenic ^{40}Ar of historic volcanics in any amount of total ^{40}Ar , it can be regarded as the minimum requirement to distinguish dated samples from historic volcanics, i.e., as far as the radiogenic ^{40}Ar has been accumulated beyond the line, it is impossible to distinguish dated samples from historic volcanics at 68% confidence.

The amount of total ^{40}Ar in pre-historic (late Quaternary) volcanics dated in the present study are usually within (3-300) $\times 10^{-8}\text{mlSTP/g}$ and their mean is about $1 \times 10^{-7}\text{mlSTP/g}$. If the sample contains $1 \times 10^{-7}\text{mlSTP/g}$ of total ^{40}Ar and 1% of K_2O , the minimum radiogenic ^{40}Ar and K-Ar age to distinguish from historic volcanics are estimated to be $1 \times 10^{-9}\text{mlSTP/g}$ and 30ka, respectively. However, it is a matter of course that such a minimum requirement to distinguish from historic volcanics can be improved by selecting the sample having higher potassium content and/or lower amount of total ^{40}Ar . The amount of total ^{40}Ar varies even in a single lava flow as mentioned in III-3. It is, therefore, indispensable to establish a convenient guideline to select a sample having the total ^{40}Ar as little as possible.

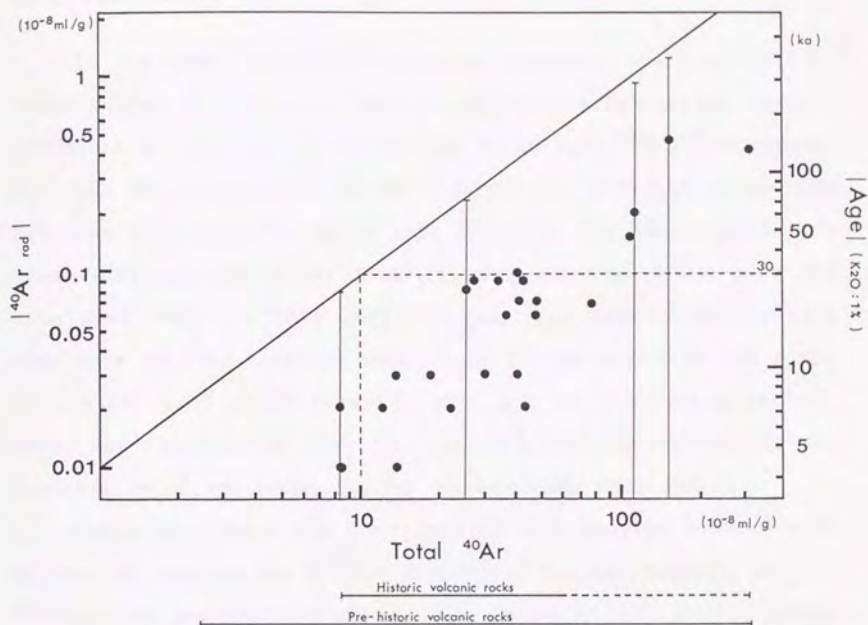


Fig.IV-1. Concentration of apparent radiogenic ^{40}Ar in historic volcanic rocks correlating to the amount of total ^{40}Ar .

Apparent radiogenic ^{40}Ar are expressed in absolute value.

Age indicates the apparent K-Ar age of historic volcanics containing 1% of K_2O .

Some analytical uncertainties (1σ) for apparent radiogenic ^{40}Ar are given in vertical lines and the solid line is drawn along the upper limits of 1σ of uncertainties for apparent radiogenic ^{40}Ar .

The ranges of total ^{40}Ar in historic and pre-historic (late Quaternary) volcanics are shown below the figure.

IV-2. Concordance with ^{14}C age

It has been clarified from argon isotopic analyses of historic volcanics that the "Mass Fractionation Correction Method" (MFCM) is useful for the estimation of initial $^{40}\text{Ar}/^{36}\text{Ar}$ ratios. Although the reliability of new K-Ar dating technique using MFCM has been confirmed for older than 200ka by the determination of some reference materials, that for younger than 200ka have not been confirmed. In this section, K-Ar age determinations have been made on some volcanic rocks directly covered with the Aira-Tn ash (AT ash) which is well dated by the ^{14}C dating method. Then, the concordance with ^{14}C age is evaluated to confirm the reliability of new technique for ages younger than 200ka.

Table IV-2 shows the K-Ar ages of five samples covered with AT ash. AT ash is one of the widespread fallout tephras and its ^{14}C age is recommended to be 22ka (Endo et al., 1986). Three samples were collected from the Yonnoike Lava (Yamada and Kobayashi, 1988) of Ontake Volcano, others from the Sawatsuno and Haku-sui Lavas (Ono and Watanabe, 1985) of Aso Volcano. Their K-Ar ages (34 ± 5 , 37 ± 8 , 31 ± 7 , 36 ± 4 , 27 ± 6 and 30 ± 6 ka) are concordant with the ^{14}C age of AT ash even between the different volcanoes. These results suggest that a new K-Ar dating technique using MFCM has a capability to get a reasonable K-Ar age even in the order of 10ka.

Table IV-2. K-Ar ages of the samples covered with the Aira-Tn (AT) ash.

Sample Name	Sample Wt. (g)	K ₂ O (%)	$^{39}\text{Ar}/^{36}\text{Ar}$	$^{40}\text{Ar}/^{39}\text{Ar}$	Total ^{40}Ar (10^{-9} ml STP/g)	Rad. ^{40}Ar (10^{-9} ml STP/g)	Atm. ^{40}Ar (%)	Age (ka)
【Yonnoike Lava】								
PEAK-145	2.065	2.88	0.1867 \pm 0.0006	303.7 \pm 0.4	107 \pm 4	3.10 \pm 0.65	97.1	33 \pm 7
	3.011		0.1865 \pm 0.0005	303.6 \pm 0.2	105 \pm 4	3.24 \pm 0.53	96.9	35 \pm 6
								AV. 34 \pm 5
PEAK-146	2.057	2.87	0.1865 \pm 0.0003	298.6 \pm 0.2	235 \pm 9	2.65 \pm 0.65	98.8	31 \pm 7
NIGRG-206	2.128	2.83	0.1867 \pm 0.0006	307.2 \pm 0.4	85.0 \pm 3.4	3.40 \pm 0.55	96.0	37 \pm 6
	3.010		0.1872 \pm 0.0005	309.3 \pm 0.2	76.8 \pm 3.1	3.20 \pm 0.43	95.8	35 \pm 5
								AV. 36 \pm 4
【Sawatsuno Lava】								
KWK736	2.039	4.06	0.1858 \pm 0.0005	299.5 \pm 0.2	140 \pm 6	3.50 \pm 0.76	97.5	27 \pm 6
【Hakusui Lava】								
KWAS609	2.168	4.25	0.1868 \pm 0.0016	321.0 \pm 0.8	50.8 \pm 2.0	4.07 \pm 0.81	92.0	30 \pm 6

The ^{14}C age of AT ash is recommended to be 22ka (Endo et al., 1986).

V. K-AR AGE DETERMINATION FOR QUATERNARY VOLCANIC ROCKS

K-Ar dating technique for Quaternary volcanic rocks has been developed and reasonable K-Ar ages can be obtained for some lavas covered with AT ash (^{14}C :22ka ; Endo et al.,1986) as discussed in the foregoing chapters. However, it has not been confirmed whether K-Ar ages obtained are successively concordant with their volcanostratigraphies. In this chapter, systematic K-Ar age determinations are made on Ontake and Aso Volcanoes to confirm successive concordances with volcanostratigraphies and it aims to construct eruptive histories on the basis of their K-Ar ages. Furthermore, eruption ages of some widespread fallout tephtras (Pm-I, Aso-4 ash and DKP) are estimated directly and/or indirectly from K-Ar ages of Ontake, Aso and other volcanic products, and compared with the ages used in tephrochronology.

V-1. K-Ar age determination for Ontake Volcano

V-1-1. Geology and volcanic history of Ontake Volcano

Ontake Volcano is located in the south margin of Norikura volcanic zone. It has a conspicuous cone whose top is Ken-ga-Mine 3063.4m in altitude, resting on mountains 1500-1900m in altitude (Fig.V-1). The edifice, which contains two overlapping bodies of compound volcanoes with caldera almost buried down, consists of about 80km^3 of volcanic products (Kobayashi,1974 ; Yamada and Kobayashi,1988). The summit of edifice consists of a series of smaller stratocones with or without crater basins arranged in roughly N-S trend.

The volcanostratigraphy of Ontake Volcano has been research-

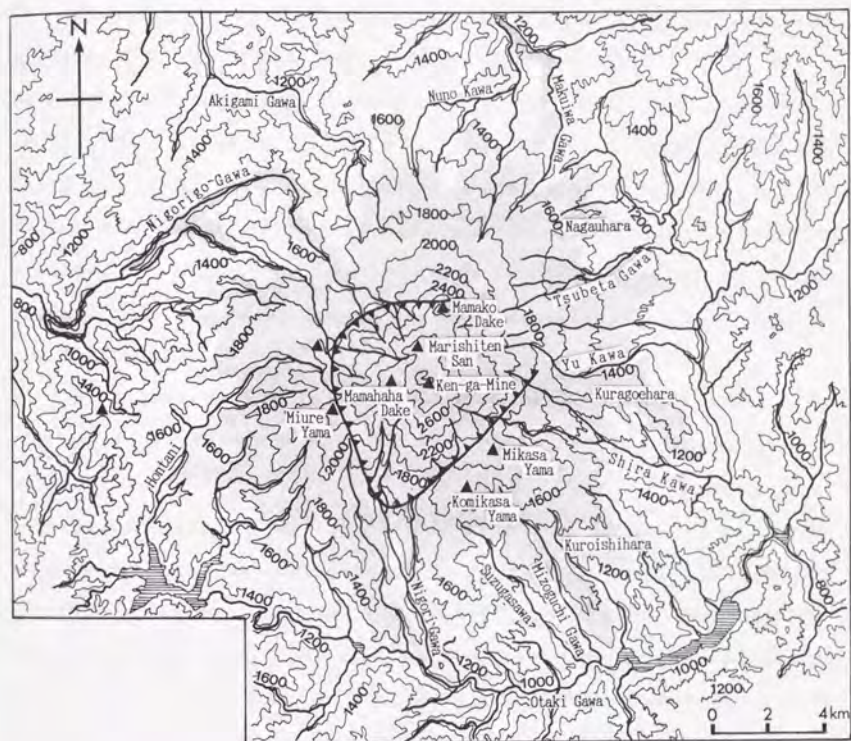


Fig.V-1. Distribution of Ontake volcanic rocks.

ed by Kozu(1907), Samejima(1958) and Shibata(1963), and it was recently reconstructed by Yamada and Kobayashi(1988) on the basis of geological researches for Ontake Volcano itself and the stratigraphy of Ontake Tephra Group (Kobayashi,1974,1980,1982 ; Kobayashi and Soya,1981 ; Kobayashi et al.,1975,1977 ; Takemoto et al.,1987) as shown in Table V-1 and Fig.V-2. They divided the volcanism of Ontake Volcano into two active periods (Older Ontake Period and Younger Ontake Period) and two alternatively inactive periods. The outline of geology and eruptive history in Ontake Volcano constructed by Yamada and Kobayashi(1988) is described in the following.

The first active period (Older Ontake Period) initiated in the middle Pleistocene and volcanic products seem to build up a single cone of stratovolcano up to about 80km^3 in volume. They consist of lavas and volcanoclastic deposits. Lavas are mainly of augite-hypersthene andesite with or without small amounts of hornblende and/or olivine (SiO_2 :59-63%), ranging from augite-olivine basalt (SiO_2 :50%) to augite-hypersthene-hornblende dacite (SiO_2 :67%). After such an active period, there had been a long inactive period and the volcanic edifice of Older Ontake Volcano had been dissected intensively to form radial valleys before the following activity of Younger Ontake Volcano. The central part of Older Ontake Volcano was also lost with the following caldera formation in Younger Ontake Period. The volcanostratigraphy of Older Ontake volcanic rocks was constructed as given in Table V-2, in which the "Kuragoehara Lava" distributed in an extremely wide area was selected as a key bed and the stratigraphy was estimated from the relations to the lava. K-Ar ages of Older

Table V-1. Outline of the volcanism in Ontake Volcano (after Yamada and Kobayashi, 1988).

Age	Period	Stage	Magmatic products	Volcanic activity	Landform	Remarks		
PLEISTOCENE	(ka)			1979 Explosion		1984 Earthquake		
	Holocene	Inactive Period		Phreatic explosion Hot spring Fumarole	Explosion craters Large-scale landslides	1975-78 Earthq. swarm Akahoya Ash (6300y B.P.) AT Ash (22000y B.P.)		
			22					
	50-60	48	Younger	Marishiten Volcano Group	Andesite	Andesite lava, pyroclastic flow and air-fall tephra	Composite stratovolcano	Kisagawa Mudflows DKP Pumice ca. 48000y B.P.)
			Ontake					
		70-90	Period	Mamahaha-dake Volcano Group	Dacite	Viscous lava, pyroclastic flow and air-fall tephra	Lava dome	Asa-4 Ash
					Rhyolite	Rhyolitic pumice	Caldera formation	Pm-1 Pumice (7-9 X 10 ³ y B.P.)
				Inactive Period			Heavily dissected	Wamura Mudflows
	Older Ontake Period	Late	Andesite	Lava, pyroclastic flow and air-fall tephra	Single cone of stratovolcano	Yamada and Kobayashi (1988)		
Middle		Andesite Basalt Basaltic andesite						
Early		Dacite Andesite Basaltic andesite						

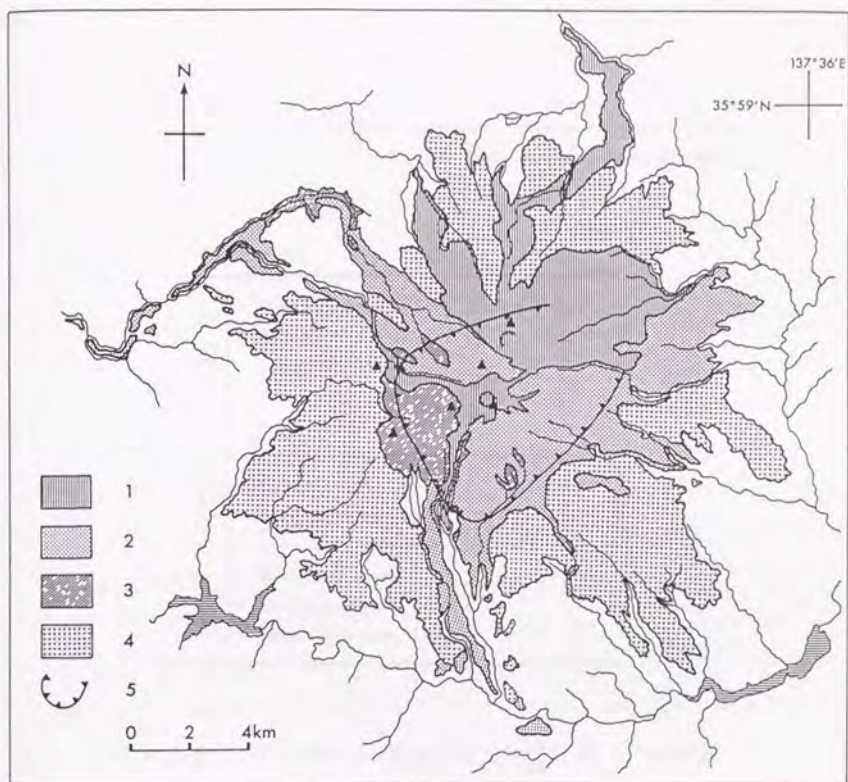


Fig.V-2. Geological map of Ontake Volcano (simplified after Yamada and Kobayashi,1988).

- | | |
|---|---|
| 1 : Marishiten Volcano Group
with craters (IV Stage) | 3 : Mamahahadake Volcano Group (II Stage) |
| 2 : Marishiten Volcano Group
without craters (III Stage) | 4 : Older Ontake Volcano Group (I Stage) |
| | 5 : Caldera wall |

TableV-2. Volcanostratigraphy of Older Ontake volcanic rocks.
(after Yamada and Kobayash,1988)

Late	Mikasayama Lava (390±20ka)*
	Mizoguchigawa Lava (420±20ka)*
	Nunokawa Lava
	Suzugasawa Lava
	Sengendaru Lava
Middle	Kuragoehara Lava
	Makuiwagawa Lava
Early	Hakodani Lava
	Shiranunodani Lava
	Tsuchiurazawa Lava

* K-Ar ages were determined by Shimizu et al.(1988)

Ontake volcanic rocks were obtained only for the Mikasayama and the Mizoguchigawa Lavas whose ages were 390 ± 20 and 420 ± 20 ka, respectively (Shimizu et al., 1988). Systematic K-Ar age determination for Older Ontake volcanic rocks is necessary to estimate the initiation and the period of Older Ontake volcanism.

The Younger Ontake Period can be subdivided into two stages by a sudden change of products without an evident cessation of activities : the earlier stage is called the "Mamahahadake Volcano Group" and the later one is the "Marishiten Volcano Group". Activities of the Mamahahadake Volcano Group started by successive eruptions of enormous amount of rhyolitic pumice falls (SiO_2 :70-73%) accompanied by the formation of a caldera. Among these extensive tephra layers, a pumice fall layer called the "Pm-I Pumice Fall" covered of a wide area more than $3 \times 10^4 \text{ km}^2$. The following activities ejected dacitic products : thick lava flows, pyroclastic flows and air-fall pumice. They buried up the major part of new-born caldera, resulting in the formation of a composite shield volcano with dacite lavas (SiO_2 :66-69%), Mamahaha-Dake. Products of the Mamahahadake Volcano Group are estimated to be about 50 km^3 in volume. The Marishiten Volcano Group ejected about 10 km^3 of andesitic products (SiO_2 :59-63% for the most parts), are formed small stratocones overlapped each other and arranged in a roughly N-S trend. The upper parts of cones are composed mainly of mantles of dense welded agglutinate with small amounts of lava flows except for the latest crater of Sannoike Volcano. the volcanostratigraphy of Younger Ontake volcanic rocks (Yamada and Kobayashi, 1988) is shown in Table V-3 and Fig.V-3.

The Younger Ontake Tephra Group also has been researched by

Table V-3. Volcanostratigraphy of Younger Ontake volcanic rocks.
(after Yamada and Kobayash, 1988)

Younger Ontake volcanic rocks	Marishiten Vol. Group	Sannoike Volcanic Product
		Yonnoike Volcanic Product
		Ichinoike Volcanic Product
		Mamakodake Volcanic Product
		Kuaskidani Volcanic Product
		Okunoin Volcanic Product
		Kongodo Volcanic Product
		Nigorigo Volcanic Product
	Mamahadake Vol. Group	Miureyama Lava
		Nigoridaki Pyroclastic Flow Deposit
		Yunotani Lava
		Shintani Lava
		[Caldera Formation]
		Pm-I Pumice Fall Deposit

Older Ontake volcanic rocks

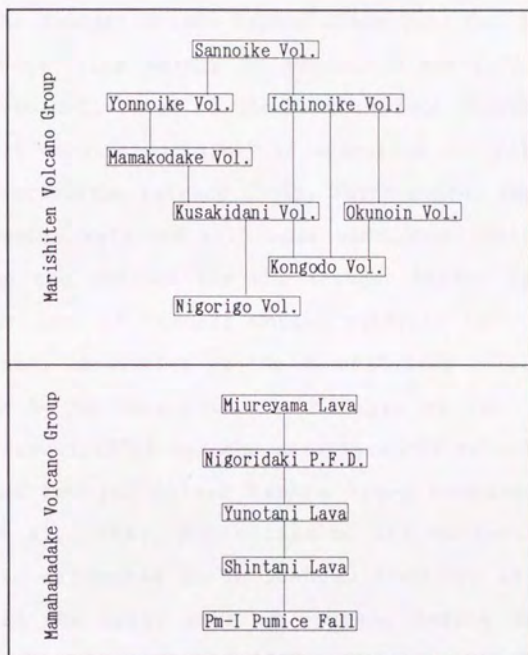


Fig.V-3. Volcanostratigraphy of Younger Ontake volcanic rocks.
(after Yamada and Kobayashi,1988)

many workers (e.g., Momose and Kobayashi, 1972 ; Kobayashi, 1982 ; Kobayashi et al., 1977 ; Sakai, 1981 ; Takemoto et al., 1987). They subdivided the Younger Ontake Tephra Group into two stages ; the lower part consisting mainly of rhyolitic air-fall pumice was corresponded to activities of the Mamahahadake Volcano Group and the upper part consisting mainly of andesitic air-fall scoria to that of the Marishiten Volcano Group. Furthermore, they clarified the stratigraphic relation with some widespread fallout tephras and estimated the sources for the Younger Ontake Tephra Group. Although K-Ar ages of Younger Ontake volcanic rocks have never been determined, activities of the Mamahahadake Volcano Group is estimated to be 60-90ka from the FT ages of Pm-I (70-90ka : Machida and Suzuki, 1971) and the stratigraphic relation that the lower part of Younger Ontake Tephra Group includes Aso-4 ash (Takemoto et al., 1988). Activities of the Marishiten Volcano Group is also estimated to be 30-60ka from the stratigraphic relation that the upper part of Younger Ontake Tephra Group includes DKP (Machida and Arai, 1979 ; Takemoto et al., 1988) and is covered with AT ash whose ^{14}C age was recommended to be 22ka (Endo et al., 1986).

After the last magmatic eruption of Marishiten Volcano Group, Ontake Volcano has been in the second inactive period, during which the superficial phenomena are restricted to phreatic activities : hot springs, fumaroles and intermittent phreatic explosions with the average interval of about 1500 years. The last phreatic explosion, but the first historical one, occurred in 1979.

V-1-2. Experiment

K-Ar age determination for Ontake Volcano has been made on all of the twenty-three volcanic products classified by Yamada and Kobayashi(1988). These samples were collected from lava flows or dense welded agglutinates, except for the Nigoridaki Pyroclastic Flow (NGRG-240 : an essential fragment in pyroclastic flow) and the Pm-I Pumice Fall (800N-08 : phenocrysts in a pumice fall). Their localities are shown in Fig.V-4 and 5, and petrographic descriptions are given in Appendix III. In most of these volcanic products, samples of the same unit were collected from different places and analyzed to confirm reliabilities of K-Ar ages. Some samples were also analyzed twice to know reproducibilities of analyses.

Although the preparation of samples, argon isotopic analysis and potassium analysis were carried out by the procedure mentioned in II-2 and 3, phenocrysts larger than 60 mesh in lava flow or dense-welded agglutinate samples were removed as much as possible by hand-picking, or separation using an isodynamic separator and/or heavy liquid to minimize a possibility for the existence of excess ^{40}Ar .

V-1-3. Result of K-Ar dating

K-Ar ages of Ontake volcanic rocks are shown in Table V-4 and 5 with uncertainties of 1 σ . Uncertainties for concentration of radiogenic ^{40}Ar and K-Ar ages are calculated by the equations (5) to (8) of II-1, in which errors for each analytical procedure (σ_K , σ_X , σ_r and σ_R) follow the estimation of II-4. The concordance of K-Ar ages with volcanostratigraphies and the eruptive his-

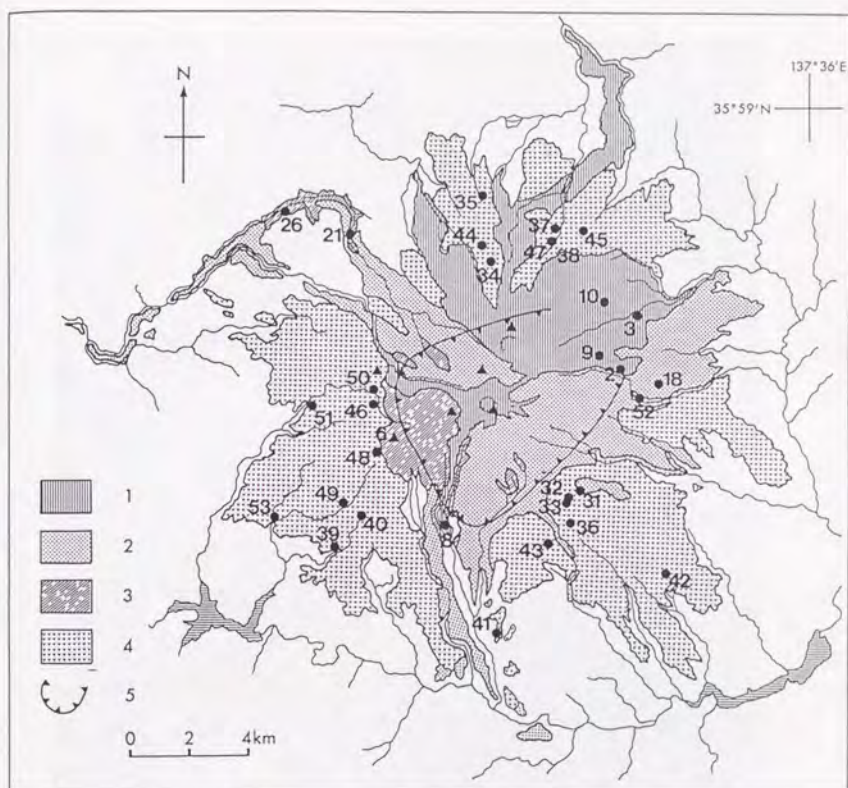


Fig.V-4. Localities of samples at the foot of Ontake Volcano.

Geological map is after Yamada and Kobayashi(1988).

The number in the figure corresponds to Sample No of TableV-4 and 5.

Legend of the map is the same with that of Fig.V-2.

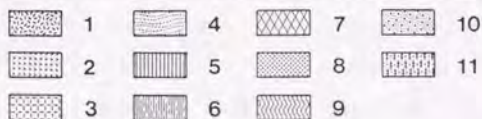
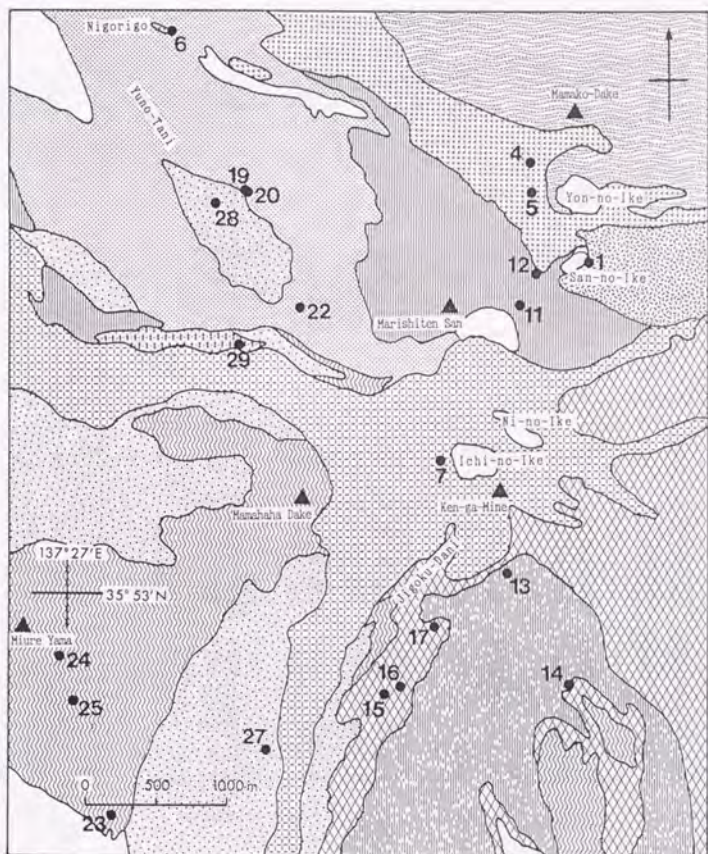


Fig.V-5. Localities of samples at the top of Ontake Volcano.

Geological map is after Yamada and Kobayashi(1988).

Numbers in the figure corresponds to Sample No of Table V-4 and 5.

- | | | |
|-----------------------------|-----------------------------|--------------------|
| 1 : Sunnoike Vol. Product | 5 : Kusakidani Vol. Product | 9 : Miureyama Lava |
| 2 : Yonnoike Vol. Product | 6 : Okunoin Vol. Product | 10 : Yunotani Lava |
| 3 : Ichinoike Vol. Product | 7 : Kogodo Vol. Product | 11 : Shintani Lava |
| 4 : Mamakodake Vol. Product | 8 : Nigorigo Vol. Product | |

Table V-4. K-Ar ages of Younger Ontake Volcanic rocks.

Sample Name	Sample Wt. (g)	K ₂ O (%)	³⁹ Ar/ ³⁹ Ar	⁴⁰ Ar/ ³⁹ Ar	Total ⁴⁰ Ar (10 ⁻⁶ mlSTP/g)	Rad. ⁴⁰ Ar (10 ⁻⁶ mlSTP/g)	Atm. ⁴⁰ Ar (%)	Age (ka)
【Sannoike Volcano】								
1. PEAK-6'-1 LV	3.016	2.78	—	—	>190	—	—	—
2. PEAK-16 LV	3.030	2.38	—	—	>150	—	—	—
3. NITK-72 LV	2.035	2.72	0.1858±0.0006	296.9±0.3	99.2±4.0	1.64±0.61	98.4	19±7
	3.015		0.1861±0.0004	298.1±0.2	104±4	1.78±0.49	98.3	20±6
								Av. 20±5
【Yonnoike Volcano】								
4. PEAK-145 LV	2.065	2.88	0.1867±0.0006	303.7±0.4	107±4	3.10±0.65	97.1	33±7
	3.011		0.1865±0.0005	303.6±0.2	105±4	3.24±0.53	96.9	35±6
							Av. 34±5	
5. PEAK-146 LV	2.057	2.87	0.1865±0.0003	298.6±0.2	235±9	3.46±0.78	98.5	37±8
6. NGRG-206 LV	2.128	2.83	0.1867±0.0006	307.2±0.4	85.0±3.4	3.40±0.55	96.0	37±6
	3.010		0.1872±0.0005	309.3±0.2	76.8±3.1	3.20±0.43	95.8	35±5
							Av. 36±4	
【Ichinoike Volcano】								
7. PEAK-170 LV	3.016	3.22	—	—	>190	—	—	—
8. NGRKW-20 LV	2.148	2.69	0.1852±0.0003	293.5±0.2	229±9	2.65±0.65	98.8	31±7
【Mamakodake Volcano】								
9. NITK-11 LV	3.019	2.40	0.1856±0.0005	312.2±0.2	56.8±2.3	3.78±0.30	93.3	49±4
10. NITK-134 LV	2.045	2.79	0.1857±0.0005	299.7±0.3	143±6	3.81±0.84	97.3	42±9
【Kusakidani Volcano】								
11. PEAK-180 LV	2.156	2.01	0.1862±0.0004	299.3±0.2	190±8	3.81±0.88	98.0	59±14
12. PEAK-185 AG	2.174	2.11	0.1850±0.0004	293.8±0.2	263±11	3.85±1.11	98.5	57±16

LV: Lava flow, AG: Dense-welded agglutinate.

The number in Sample Name corresponds to localities of samples in Fig. V-4 and 5.

(continued)

Sample Name	Sample Wt. (g)	K ₂ O (%)	³⁹ Ar/ ³⁶ Ar	⁴⁰ Ar/ ³⁶ Ar	Total ⁴⁰ Ar (10 ⁻⁹ mlSTP/g)	Rad. ⁴⁰ Ar (10 ⁻⁹ mlSTP/g)	Atm. ⁴⁰ Ar (%)	Age (ka)
[Okunoin Volcano]								
13. PEAK-178 LV	2.170	1.57	0.1876±0.0004	307.0±0.3	94.2±3.8	2.85±0.44	97.0	57±9
14. TNHR-09 AG	2.124	2.42	0.1865±0.0005	304.0±0.2	150 ± 6	4.82±0.77	96.8	62±10
[Kongodo Volcano]								
15. AKGW-05 LV	2.997	1.91	0.1875±0.0005	314.7±0.2	74.3±3.0	4.08±0.43	94.5	66±7
16. AKGW-06 LV	2.025	2.62	0.1851±0.0004	295.9±0.3	295 ± 12	6.08±1.36	97.9	72±16
17. AKGW-10 AG	2.029	2.49	—	—	>190	—	—	—
18. NITK-116 LV	2.019	3.19	0.1856±0.0006	306.1±0.3	139 ± 6	6.63±0.86	95.2	65±8
[Nigorigo Volcano]								
19. NGRG-28-3 LV	2.997	2.02	0.1864±0.0003	—	>160	—	—	—
20. NGRG-28-4 LV	2.976	2.11	0.1868±0.0005	314.8±0.3	82.7±3.3	5.15±0.49	93.8	76±7
21. NGRG-106 LV	3.012	1.54	0.1870±0.0003	305.9±0.2	126 ± 5	4.16±0.39	96.7	84±8
22. NGRG-118 LV	3.015	2.15	0.1866±0.0007	324.6±0.4	60.2±2.4	5.57±0.46	90.8	80±7
[Miureyama Lava]								
23. SKRSW-13 LV	2.060	3.00	0.1864±0.0011	330.1±0.7	76.2±3.0	8.36±0.87	89.0	86±9
24. SKRSW-19 LV	3.006	3.16	0.1859±0.0009	345.7±0.4	55.7±2.2	8.61±0.59	84.6	84±6
25. SKRSW-20 LV	3.014	3.14	0.1852±0.0006	298.0±0.6	306 ± 12	8.12±1.92	97.4	80±19
[Nigoridaki Pyroclastic Flow]								
26. NGRG-240 EF	2.068	3.35	0.1868±0.0012	354.8±0.7	55.4±2.2	9.30±0.72	83.2	86±7
[Yunotani Lava]								
27. NGRG-25 LV	3.011	3.25	0.1871±0.0010	362.7±0.7	47.8±1.9	8.77±0.56	81.6	84±5
28. NGRG-28-1 LV	2.018	3.50	0.1855±0.0003	297.5±0.2	457 ± 18	9.84±1.52	97.9	87±13

LV: Lava flow, AG: Dense-welded agglutinate, EF: Essential fragment in pyroclastic flow.

(continued)

Sample Name	Sample Wt. (g)	K ₂ O (%)	³⁹ Ar/ ³⁶ Ar	⁴⁰ Ar/ ³⁶ Ar	Total ⁴⁰ Ar (10 ⁻⁹ mlSTP/g)	Rad. ⁴⁰ Ar (10 ⁻⁹ mlSTP/g)	Atm. ⁴⁰ Ar (%)	Age (ka)	
【Shintani Lava】									
29. NGRG-127	LV	2.146	3.26	0.1853±0.0007	329.7±0.3	74.3±3.0	8.85±0.59	88.1	84±6
【Pm-I Pumice Fall】									
30. 800N-08	Hb*	1.018	0.600	0.1869±0.0003	314.5±0.2	383±15	23.2±1.5	94.0	1200±80
	Bi-1*	0.435	7.05	0.1875±0.0004	381.7±0.2	2220±89	490±21	77.9	2160±90
	Bi-2*	0.418	7.30	0.1877±0.0004	344.0±0.2	1500±60	200±10	86.6	854±40

* Phenocrysts in Pm-I Pumice Fall ; Hb : 32-100 mesh of hornblende, Bi-1 : 16-32 mesh of biotite, Bi-2 : 32-60 mesh of biotite.

Table V-5. K-Ar ages of Older Ontake Volcanic rocks.

Sample Name	Sample Wt. (g)	K ₂ O (%)	³⁹ Ar/ ³⁶ Ar	⁴⁰ Ar/ ³⁶ Ar	Total ⁴⁰ Ar (10 ⁻⁹ mlSTP/g)	Rad. ⁴⁰ Ar (10 ⁻⁹ mlSTP/g)	Atm. ⁴⁰ Ar (%)	Age (ka)
[Mikasayama Lava]								
31. OHTK-25 LV	2.043	3.43	0.1868±0.0009	449.6±0.3	137 ± 5	47.1±2.1	65.7	430±20
32. MZCGW-09 LV	2.027	3.82	0.1854±0.0014	565.6±0.5	112 ± 4	54.6±2.4	51.4	440±20
[Mizoguchigawa Lava]								
33. MZCGW-05 LV	2.116	2.80	0.1860±0.0003	322.8±0.2	581 ± 23	54.2±2.9	90.7	600±30
[Nunokawa Lava]								
34. ASH-27 LV	2.108	1.91	0.1861±0.0004	395.6±0.3	150 ± 6	38.8±1.6	74.7	630±30
35. TKN-51 LV	2.102	1.43	0.1853±0.0008	388.8±0.3	142 ± 6	35.9±1.7	74.7	780±40
[Suzugasawa Lava]								
36. MZCGW-03 LV	2.123	1.73	0.1864±0.0006	380.8±0.4	160 ± 6	36.5±1.7	77.2	650±30
[Sengendaru Lava]								
37. TKN-29 LV	2.116	2.04	0.1850±0.0003	293.1±0.2	433 ± 17	5.3±1.5	98.8	81±14
38. TKN-46 LV	2.036	3.15	0.1859±0.0003	293.0±0.3	>1300	—	—	—
[Kuragochara Lava]								
39. TCUR-22 LV	2.028	3.74	0.1874±0.0008	628.1±1.0	121 ± 5	63.7±2.6	47.3	530±20
40. TCUR-33 LV	2.034	3.74	0.1867±0.0004	511.1±0.5	152 ± 6	64.4±2.6	57.7	530±20
41. NGRKW-73 LV	2.041	3.25	0.1860±0.0010	657.9±0.5	106 ± 4	59.0±2.4	44.5	560±20
42. OHTK-18 LV	2.035	2.78	0.1872±0.0004	556.1±0.4	133 ± 5	62.2±2.5	53.3	690±30
43. SZGSW-06 LV	2.030	3.50	0.1868±0.0003	408.0±0.3	302 ± 12	83.6±3.4	72.4	740±30
44. ASH-20 LV	2.032	2.18	0.1881±0.0006	446.2±0.4	143 ± 6	47.2±2.0	67.1	670±30
45. TKN-41 LV	2.156	3.33	0.1853±0.0004	470.6±0.3	203 ± 8	77.9±3.2	61.7	720±30

LV: Lava flow

(Continued)

Sample Name	Sample Wt. (g)	K ₂ O (%)	³⁶ Ar/ ³⁶ Ar	⁴⁰ Ar/ ³⁶ Ar	Total ⁴⁰ Ar (10 ⁻⁹ mlSTP/g)	Rad. ⁴⁰ Ar (%)	Atm. ⁴⁰ Ar (%)	Age (ka)
【Makuiwagawa Lava】								
46. HNTN-36	LV 2.090	1.38	0.1881±0.0009	427.5±0.6	81.4±3.3	24.4±1.1	70.0	550±30
47. TKN-30	LV 2.105	1.27	0.1862±0.0007	401.1±0.5	106±4	28.5±1.3	73.1	700±30
【Hakodani Lava】								
48. TCUR-14	LV 2.109	3.92	0.1865±0.0007	625.6±0.5	152±6	80.7±3.3	47.0	640±30
【Shiranunodani Lava】								
49. TCUR-09	LV 2.130	2.86	0.1877±0.0003	429.8±0.3	189±8	58.1±2.4	69.3	630±30
50. HNTN-16	LV 2.113	3.32	0.1874±0.0010	684.2±1.4	123±5	69.5±2.8	43.4	650±30
【Tsuchiurazawa Lava】								
51. HNTN-12	LV 2.022	1.98	0.1870±0.0007	386.1±0.3	178±7	41.6±1.9	76.6	650±30
52. YKW-13	LV 2.011	1.49	0.1868±0.0006	401.4±0.4	131±5	34.5±1.5	73.5	720±30
53. TCUR-01	LV 2.031	1.46	—	—	>1500	—	—	—

LV: Lava flow

tory of Ontake Volcano based on K-Ar ages are discussed in the following.

< Younger Ontake Period >

As is clear from Table V-4, K-Ar ages of the Younger Ontake volcanic products in which more than one samples were dated, are in good agreement one another within 1σ of uncertainties except for the Pm-I Pumice Fall (800N-08Hb, Bi-1 and Bi-2), and the samples determined twice (NITK-72, PEAK-145 and NGRG-206) have good reproducibilities. K-Ar ages of the Marishiten and Mamahadake Volcano Group are summarized in Fig.V-6 and 7, consisting with their volcanostratigraphies (Yamada and Kobayashi, 1988). In these figures, K-Ar ages of the volcanic products in which more than one samples were dated and the same sample was dated twice, are given in weighted means. Furthermore, Fig.V-6 shows another K-Ar ages calculated by the conventional method that the initial $^{40}\text{Ar}/^{36}\text{Ar}$ ratio is assumed to be equal to the atmospheric one, to evaluate the importance of "Mass Fractionation Correction Method" (MFCM) for young volcanics.

K-Ar ages of the Marishiten and Mamahadake Volcano Group dated by MFCM are successively concordant with volcanostratigraphies and their eruption ages can be distinguished one another within 1σ of uncertainties when their K-Ar ages have a time interval of more than 10^4 years, while K-Ar ages calculated by the conventional method (given in parentheses of Fig.V-6) are often inconsistent with the volcanostratigraphy. These results suggest that the mass fractionation correction for the initial $^{40}\text{Ar}/^{36}\text{Ar}$ ratio is indispensable for volcanics younger than 100ka to get a reasonable concordance with volcanostratigraphies.

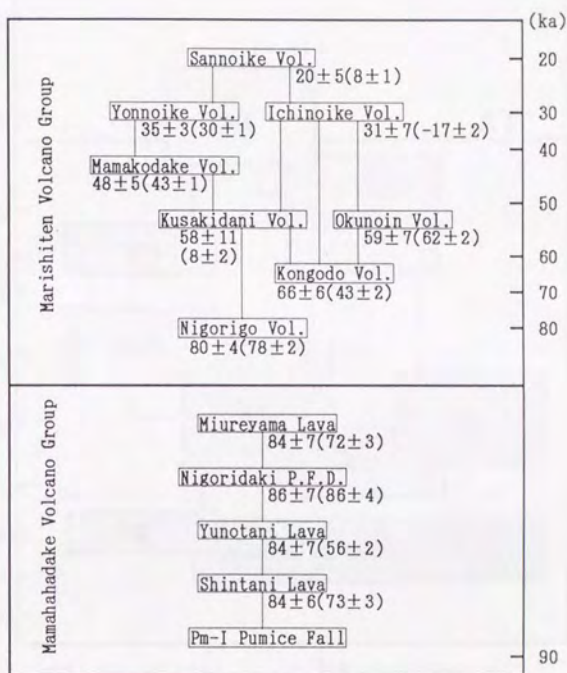


Fig.V-6. K-Ar ages of Younger Ontake volcanic rocks, consisting with volcanostratigraphy.

Volcanostratigraphy is after Yamada and Kobayashi(1988).
Values in parentheses mean K-Ar ages calculated by the conventional method.

K-Ar age of each volcanic product is given in weighted mean.

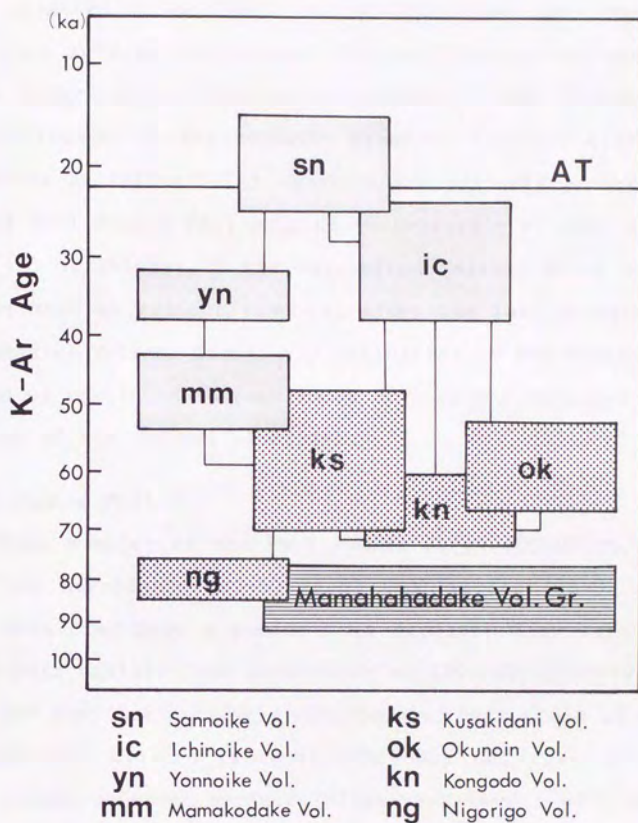


Fig.V-7. K-Ar ages of Younger Ontake volcanic rocks, consisting with volcanostratigraphy.

Volcanostratigraphy is after Yamada and Kobayashi(1988).

Vertical range in each product corresponds to 1σ of uncertainty for each K-Ar age.

Activities of the Marishiten and Mamahahadake Volcano Group were estimated to be 30-60 and 60-90ka from the stratigraphic positions of some widespread fallout tephras in the Younger Ontake Tephra Group (Yamada and Kobayashi,1988). However, K-Ar ages of Younger Ontake volcanic products directly clarify their activities as follows. (1) Mamahahadake volcanic products except for the Pm-I Pumice Fall erupted successively at most within 80-90ka. (2) Activities of the Marishiten Volcano Group started at 80ka without an evident time lag after the last eruption of the Mamahahadake Volcano Group. (3) Activities of the Marishiten Volcano Group continued through about 80-20ka and finished around at the time of the fallout of AT ash.

< Pm-I Pumice Fall >

Three samples of the Pm-I Pumice Fall (800N08 Hb, Bi-1 and Bi-2) are hornblende (32-80 mesh) and biotite (16-32 and 32-60 mesh) extracted from a pumice fall deposit. K-Ar ages of these phenocrysts deviate from each other as 1200 ± 80 , 2160 ± 90 and 850 ± 40 ka, and they are extremely old compared with those of the other Mamahahadake volcanic products (80-90ka) and that of the last Older Ontake volcanic product (Mikasayama Lava : 440 ± 10 ka). Such extremely old ages would be caused by the existence of excess ^{40}Ar , because as it has been discussed for large phenocrysts (>5 mm) in lava flows (Takaoka,1985 ; Itaya and Nagao,1988), phenocrysts in the Pm-I Pumice Fall also have a possibility that they had already solidified in a magma chamber without enough mixing with volatiles diffused from the ground water or crustal materials containing the atmospheric argon and that they kept excess ^{40}Ar trapped at the depths.

Although the Pm-I Pumice Fall could not give reasonable K-Ar ages on phenocrysts (hornblende and biotite), it can be estimated from K-Ar ages of the other Mamahahadake Volcano Group that the Pm-I Pumice Fall erupted at least older than 80ka. The eruption age of Pm-I will be further discussed in the next section by comparing with K-Ar ages of some volcanic products whose stratigraphic relations with the Pm-I tephra layer have been clarified.

< Older Ontake Period >

The volcanostratigraphy of Older Ontake Volcano was constructed on the basis of relations with the "Kuragoehara Lava" distributed in an extremely wide area (Yamada and Kobayashi, 1988). K-Ar age determinations for Older Ontake volcanic rocks have firstly been made on the Kuragoehara Lava in order to confirm whether such widely distributed lavas erupted at the same age or not. Fig.V-8 shows the distribution of Older Ontake volcanic products divided into three areas (West, South-East and North) and localities of the Kuragoehara Lava samples. K-Ar ages of these lavas are summarized in Table V-6. K-Ar ages of the Kuragoehara Lava can be divided into two eruption ages as the lavas distributed in the West Area are about 550ka, while those in the South-East and North Areas about 700ka. It is, therefore, no doubt that the Kuragoehara Lava classified by Yamada and Kobayashi(1988) consists of two kinds of lavas erupted in quite different ages. Based on these results, K-Ar age determinations for the other Older Ontake volcanic rocks have been made on each product distributed in the three areas.

K-Ar ages of Older Ontake volcanic rocks distributed in each area are shown in Fig.V-9, consisting with volcanostratigraphies.

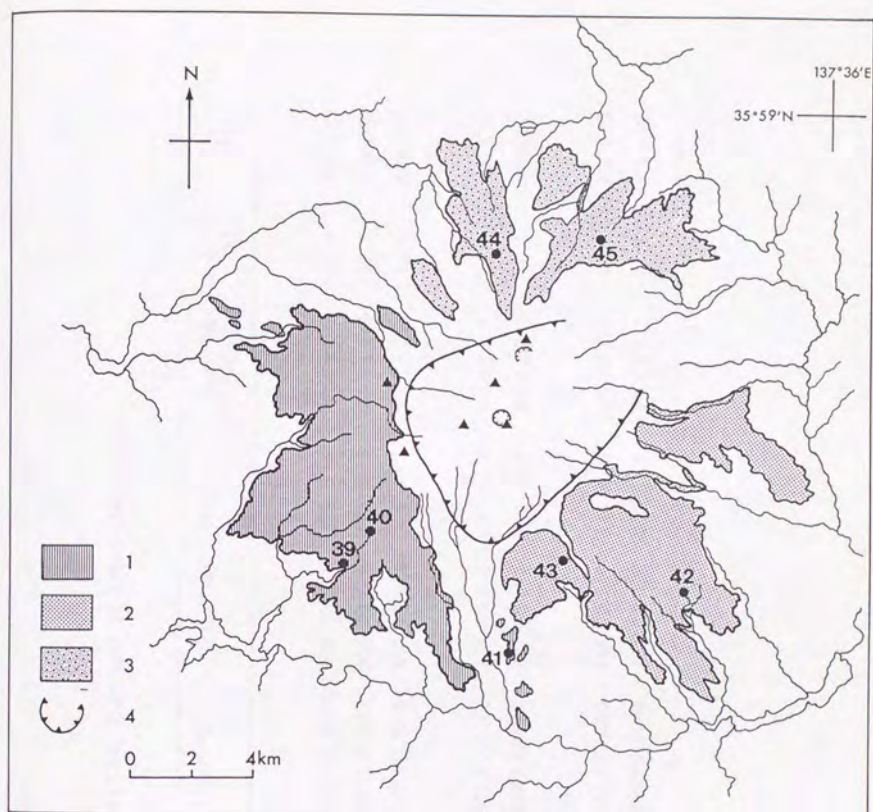


Fig.V-8. Distribution of Older Ontake volcanic rocks and localities of samples from the Kuragoebara Lava.

1 : West Area 2 : South-East Area 3 : North Area

The number in the figure corresponds to Sample No of Table V-5.

Table V-6. K-Ar ages of Kuragoehara Lava.

Sample Name	Sample Wt. (g)	K ₂ O (%)	$^{39}\text{Ar}/^{36}\text{Ar}$	$^{40}\text{Ar}/^{36}\text{Ar}$	Total ^{40}Ar (10^{-9}mlSTP/g)	Rad. ^{40}Ar (10^{-9}mlSTP/g)	Atm. ^{40}Ar (%)	Age (ka)
【West Area】								
39. TOUR-22	2.028	3.74	0.1874 ± 0.0008	628.1 ± 1.0	121 ± 5	63.7 ± 2.6	47.3	530 ± 20
40. TOUR-33	2.034	3.74	0.1867 ± 0.0004	511.1 ± 0.5	152 ± 6	64.4 ± 2.6	57.7	530 ± 20
41. NGRKW-73	2.041	3.25	0.1860 ± 0.0010	657.9 ± 0.5	106 ± 4	59.0 ± 2.4	44.5	560 ± 20
【South-East Area】								
42. OHTK-18	2.035	2.78	0.1872 ± 0.0004	556.1 ± 0.4	133 ± 5	62.2 ± 2.5	53.3	690 ± 30
43. SZGSW-06	2.030	3.50	0.1868 ± 0.0003	408.0 ± 0.3	302 ± 12	83.6 ± 3.4	72.4	740 ± 30
【North Area】								
44. ASH-20	2.032	2.18	0.1881 ± 0.0006	446.2 ± 0.4	143 ± 6	47.2 ± 2.0	67.1	670 ± 30
45. TKN-41	2.156	3.33	0.1853 ± 0.0004	470.6 ± 0.3	203 ± 8	77.9 ± 3.2	61.7	720 ± 30

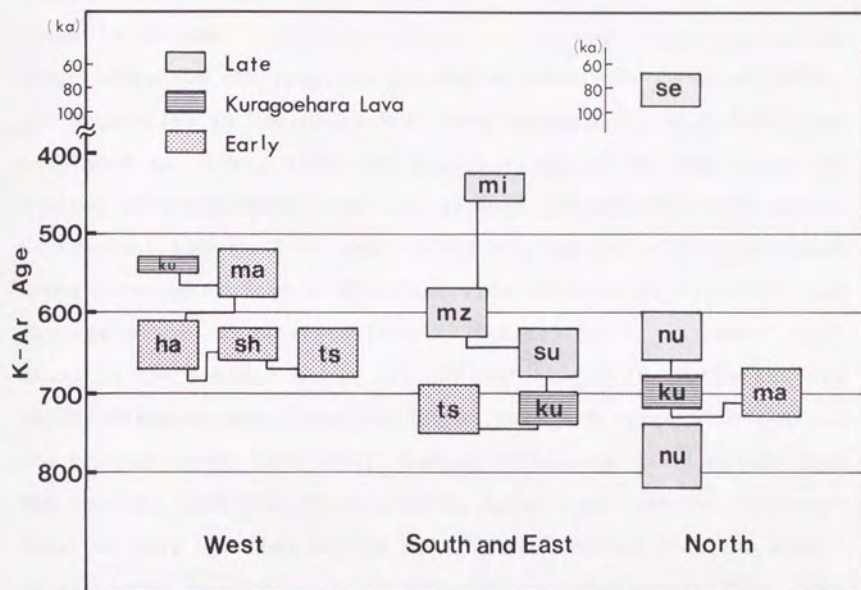


Fig.V-9. K-Ar ages of Older Ontake volcanic rocks, consisting with volcanostratigraphy.

Lines connected with each volcanic product mean the stratigraphic relations after Yamada and Kobayashi(1988).

mi : Mikasayama Lava	se : Sengendaru Lava	sh : Shiranunodani Lava
mz : Mizoguchigawa Lava	ku : Kuragoehara Lava	ts : Tsuchiurazawa Lava
nu : Nunokawa Lava	ma : Makuiwagawa Lava	
su : Suzugasawa Lava	ha : Hakodani Lava	

Their K-Ar ages are concordant with the stratigraphies in each area except for the Nunokawa Lava distributed in the North Area. The activity of Older Ontake volcano in each area can be summarized as follows ; (1) Activities in the West Area started at about 650ka and the products erupted successively to about 500ka. (2) Activities in the South-East Area started at about 700ka and suspended at 600ka. After an inactive period of more than one hundred thousand years, the last product (Mikasayama Lava) erupted at about 450ka ; K-Ar ages of the Mikasayama and Mizoguchigawa Lavas were determined independently by Shimizu et al.(1988) and the age of the Mikasayama Lava (390 ± 20 ka) is in agreement with those in the present study (430 ± 20 and 440 ± 20 ka), while the age of the Mizoguchigawa Lava (420 ± 20 ka) does not agree with that in the present study (600 ± 30 ka). Such a difference would result from the reasons that the Mizoguchigawa Lava consisted of different lavas of more than one as the Kuragoehara Lava or that the sample dated in the present study (MZGCGW-05) included excess ^{40}Ar . The reason will be clarified by intensive dating for these lavas collected from many places. (3) In the North Area, K-Ar ages of the Nunokawa Lava (ASH-27: 630 ± 30 ka ; TKN-51: 780 ± 40 ka) are significantly different from each other beyond 1 σ of uncertainty and K-Ar age of TKN-51 is inconsistent with the value expected from the volcanostratigraphy. These would result from the same reasons as mentioned in (2) that the Nunokawa Lava consisted of different lavas of more than one or that the older sample (TKN-51) might include excess ^{40}Ar . On the other hand, K-Ar age of the Sengendaru Lava is extremely young compared with other products as 81 ± 14 ka. This lava is not covered with any other Older Ontake volca-

nic products and subjected to no alteration. The Sengendaru Lava might have erupted during the Younger Ontake Period. Other products in the North Area erupted during 600-700ka.

It has been concluded that activities of Older Ontake Volcano started at least older than 700ka and finished at about 450 ka. Inactive period between the Older and Younger Ontake Periods continued for more than three hundred thousand years. K-Ar ages of volcanics classified into the Makuiwagawa and Tsuchiurazawa Lavas are different in each area. These lavas were classified into the same layers on the basis of their stratigraphic relations with the Kuragoehara Lava and petrologies, so they must be the materials that erupted in quite different ages. The volcano-stratigraphy of Older Ontake Volcano constructed by Yamada and Kobayashi(1988) should be revised based on K-Ar ages of volcanics distributed in each area.

< Summary >

Systematic K-Ar age determinations for Younger Ontake volcanic products have shown successive concordance with the volcano-stratigraphy and clarified the usefulness of K-Ar dating technique based on the "Mass Fractionation Correction Method" (MFCM) for volcanics in the order of 10ka. Activity of the Younger Ontake Volcano Group started at about 90ka and finished at about 20ka. The last eruption of the Mamahahadake Volcano Group and the initiation of the Marishiten Volcano Group would have occurred successively at about 80ka without an evident time lag.

K-Ar age determinations for Older Ontake volcanics in each area have clarified that the eruption ages of some volcanics classified into the same lavas show different ages in each place,

and that the Sengendaru Lava might have erupted in the Younger Ontake Period. The volcanostratigraphy of Older Ontake Volcano constructed by Yamada and Kobayashi(1988) should be partially revised on the basis of their K-Ar ages.

V-2. K-Ar age determination for Aso Volcano

V-2-1. Geology and volcanic history of Aso Volcano

Aso Volcano is a large caldera volcano located in the south margin of central Kyushu volcanic field where voluminous calc-alkaline volcanic rocks erupted in the late Pliocene to early Pleistocene. The Aso caldera is 25km north to south and 18km east to west in diameters. Central cones, more than seventeen in numbers, are clustered near the center of caldera, dividing the caldera floor into two valleys (Fig.V-10). These valleys are joined and drained to the west through a gorge (Tateno Barranco) at the west rim of the caldera. Geology and petrology of Aso Volcano have been studied by some workers (e.g. Ono, 1965 ; Watanabe and Ono, 1969 ; Ono et al., 1981, 1982) and they were recently summarized by Ono and Watanabe (1985). The volcanostratigraphy of Aso Volcano constructed by Ono and Watanabe (1985) is shown in Fig.V-11. The outline of geology and the eruptive history are described as follows.

Activities of Aso Volcano commenced in the middle Pleistocene. Four times of large-scale eruption of pyroclastic flows, Aso-1 to Aso-4 in the order of time sequence, caused a large caldera. These pyroclastic flows covered wide areas to form plateaus of very gentle slope, 1-2°, around the caldera and were distributed along valleys in the central to northern Kyushu and even in the Amakusa Islands and the western Honshu across the sea. Enormous amount of air fall ashes erupted with these pyroclastic flows and the one (Aso-4 ash) that accompanied the Aso-4 pyroclastic flow is famous as one of the widespread fallout tephtras (Machida et

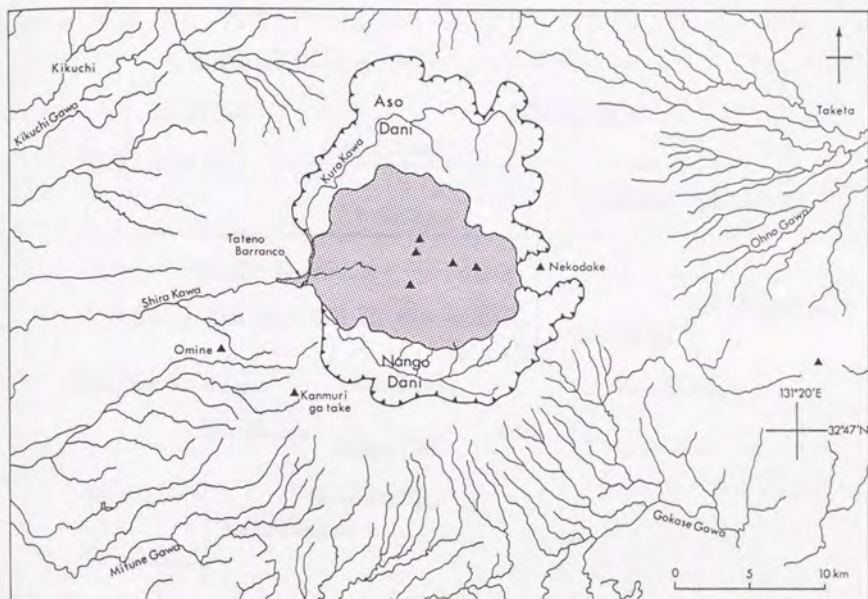


Fig. V-10. Location of Aso Volcano.

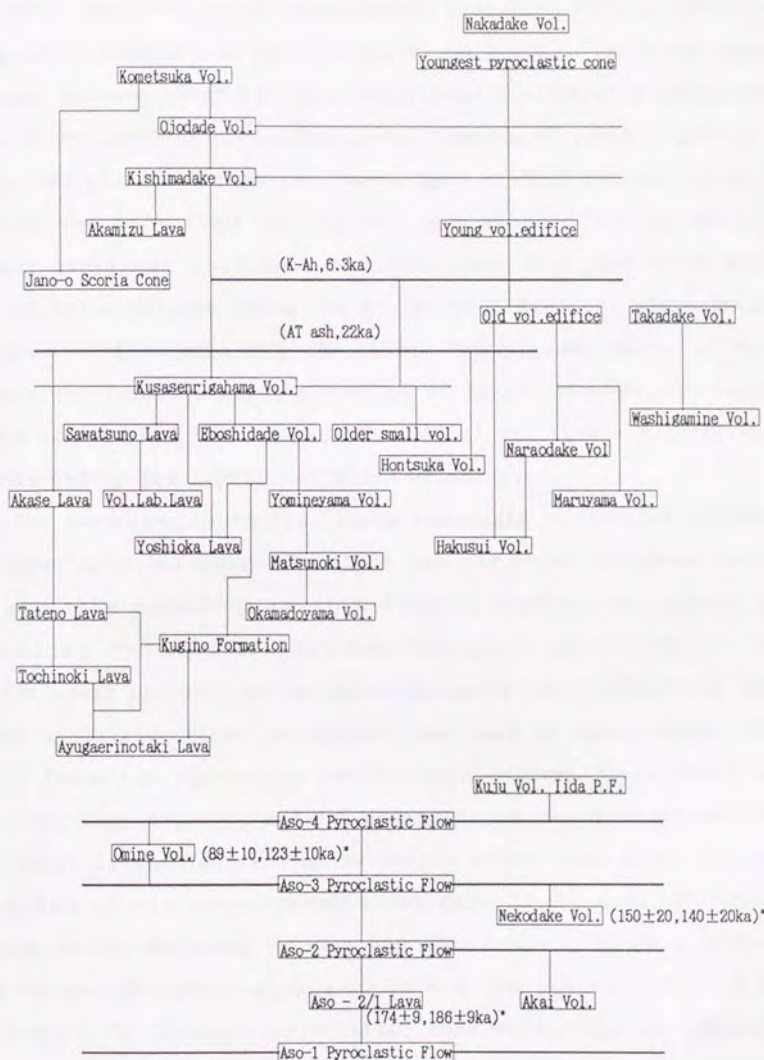


Fig. V-11. Volcanostratigraphy of Aso and nearby coeval volcanic rocks (partially modified after Ono and Watanabe, 1988). * K-Ar ages are after Itaya et al. (1984).

al.,1985). Detailed field observations clarified that a few lava flows were intercalated between Aso-1 and 2 (Ono, 1965) and that Nekodake Volcano which had been classified into central cones was built at the earlier stage than Aso-3 (Ono et al.,1982). Furthermore, they clarified that the Togawa Lava of Akai Volcano located 16km to the west from the caldera rim erupted in the period between Aso-1 and 2 (Ono et al.,1981) and that the Takayubaru Lava of Omine Volcano lying 5km to the west from the rim between Aso-3 and 4 (Watanabe and Ono,1969). The present shape of Aso caldera was formed after the outflow of Aso-4, however, it seems that a caldera had been formed after Aso-1 and it was successively enlarged by the successive major eruptions.

The formation of central cones commenced without an evident cessation of volcanism. The shape and structure of these cones are variable depending on chemistry of rocks. The outlet of valleys at the west rim (Tateno Barranco) was formed in an earlier stage probably by tectonic movements and, thereafter, was dammed up by lava flows to deposit lake beds at least twice. The Kugino Formation exposed in the southern valley (Nango Dani) is the older lake deposit, and the sediments in the northern valley (Aso Dani) is the younger one estimated to be older than 22ka on the basis of the stratigraphic relation to AT ash. Of these central cones, Nakadake Volcano has been active. It is a composite volcano of basic andesite to basalt. The active crater is at the top of the Youngest pyroclastic cone consisting of agglutinate and layers of ash, and this cone and the Young volcanic edifice were formed to the west of half-destroyed large old volcanic edifice of Nakadake.

Aso volcanic rocks range from basalt (SiO_2 :49%) to rhyolite (SiO_2 :72%) and constitute a single rock suite which is chemically and mineralogically distinct from rocks of either older volcanoes exposed at the caldera rim or nearby coeval volcanoes. Aso volcanic rocks are characteristically high in content of alkalies, especially in K_2O .

K-Ar age determinations for Aso and nearby coeval volcanic rocks have been made on only the Aso-2/1 Lava, Tenguyama dike of Nekodake Volcano and Takayubaru Lava of Omine Volcano (Fig.V-11 : Itaya et al.,1984). Although FT ages (Okaguchi,1978 ; Tamanyu, 1979) on the Aso pyroclastic flows (Aso-1 to Aso-4) have been obtained, they had so large analytical uncertainties that it is impossible to discuss their accurate eruption ages as given in Table V-7. Central cones have never been dated by any radiometric methods and only the stratigraphic relation with widespread fallout tephras (AT ash and K-Ah) was known.

V-2-2. Experiment

K-Ar age determinations for Aso Volcano have been made on the eleven volcanic products that erupted before the fallout of AT ash. The Togawa Lava of Akai Volcano and the Takayubaru Lava of Omine Volcano whose stratigraphic relations to the Aso pyroclastic flows were clarified (Ono et al.,1981 ; Watanabe and Ono, 1969), also have been dated. These samples were collected from lava flows, dikes or pyroclastic flows. Their localities are shown in Fig.V-12 to 14. The samples of Omine Volcano (MF72A1 and MF72B2) and Nekodake Volcano (82AS786T1) are the same ones dated by Itaya et al.(1984). The samples collected from lava flows and

TableV-7. Fission-Track ages of Aso pyroclastic flows.

	Fission-Track age (ka)	
Aso-4	$29 \pm 14^{(1)}$	$84 \pm 25^{(2)}$
Aso-3	$103 \pm 42^{(1)}$	
Aso-2	$154 \pm 60^{(1)}$	$185 \pm 46^{(2)}$
Aso-1	$260 \pm 76^{(1)}$	$358 \pm 72^{(1)}$

(1) Okaguchi(1978) (2) Tamayu(1979)

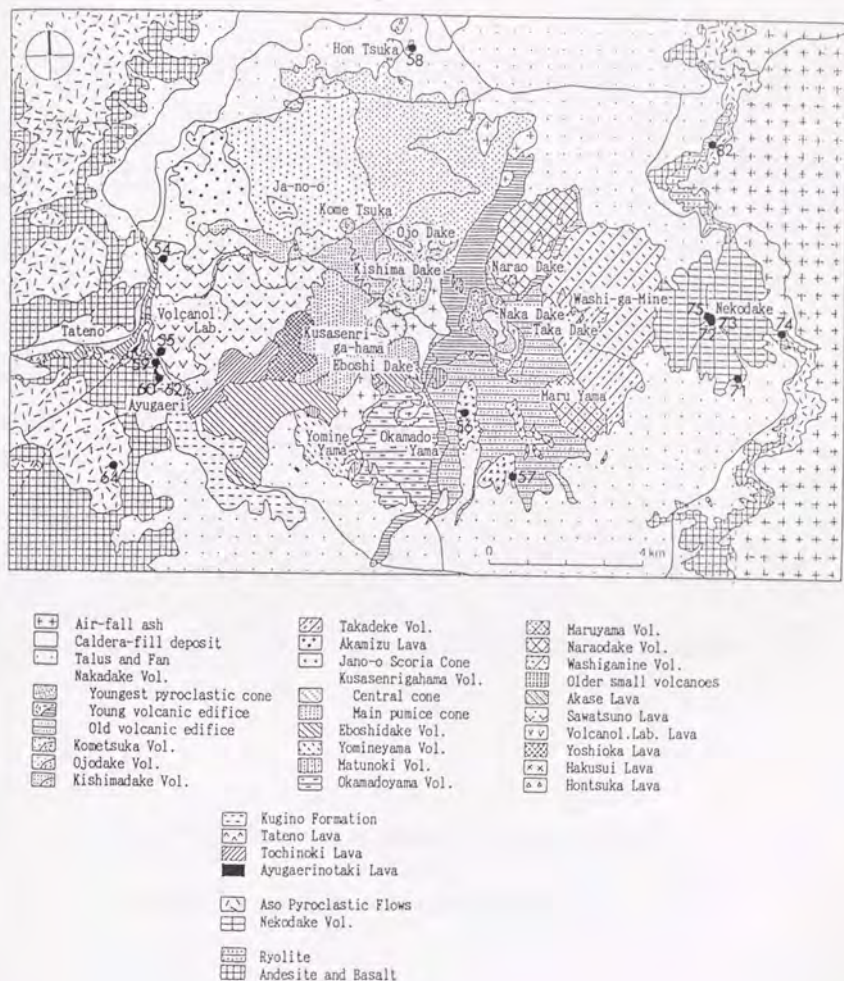


Fig.V-12. Geological map and localities of samples in the Aso Caldera.

Geological map is after Ono and Watanabe(1985).

The number in the figure corresponds to Sample No of Table V-7.

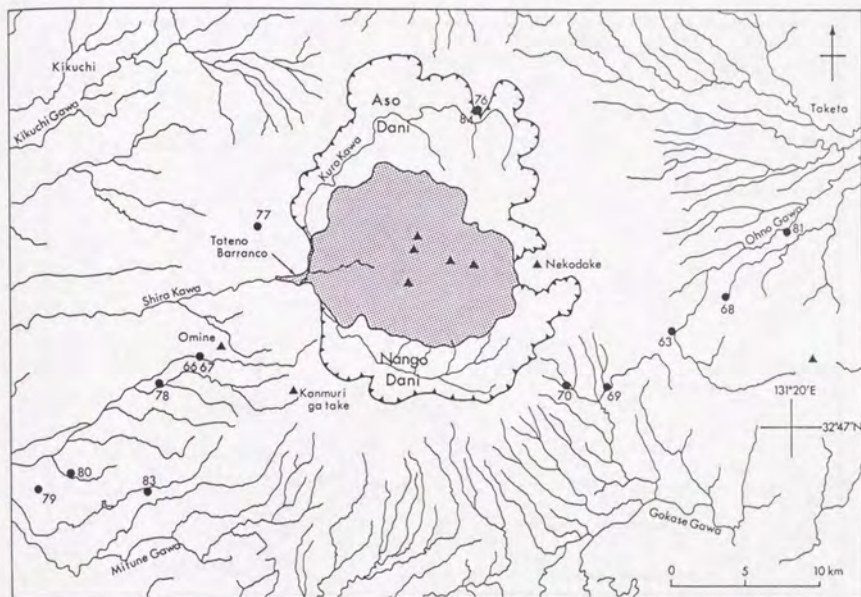


Fig.V-13. Localities of samples around the Aso Caldera.

The number in the figure corresponds to Sample No of TableV-7.

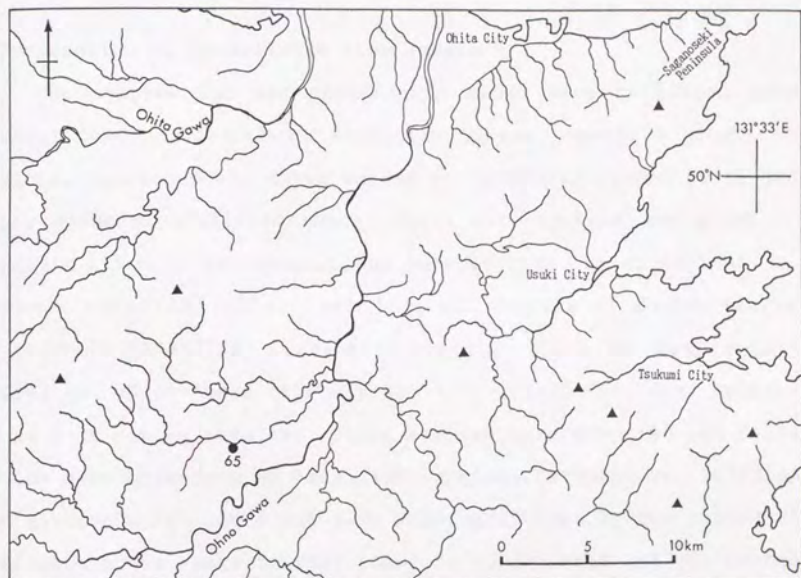


Fig.V-14. Localities of Aso-4 Pyroclastic Flow sample.

The number in the figure corresponds to Sample No of Table V-7.

dikes were prepared and determined by the same procedure as Ontake volcanic rocks, while those from pyroclastic flows were prepared as follows.

< Preparation of pyroclastic flow sample >

The samples for Aso pyroclastic flows were collected from several components such as essential lenses, obsidian blocks in breccia, homogeneously dense welded or secondary flowed parts and vapor phase crystallized parts. Their descriptions are given in Appendix III and the preparations were carried out as follows.

Aso-4 : Essential glass from lens and matrix of dense vitric welded tuff (64AS210A), essential obsidian block in breccia (81-KC664) and vapor phase crystallized part (61IK118AP) were selected as K-Ar dating samples. These samples were prepared and dated by the same procedure as lava flow samples. Furthermore, 64AS219A and 81KC664 which could not give meaningful ages by the procedure mentioned above, were crushed finer to 80-100 mesh and pre-heated at 150° C for 100 hours in order to decrease minute bubble inclusions and the atmospheric argon adsorped on the surface as much as possible.

Aso-3 : Three essential obsidian lenses (64TD232, 78TM200 and KWTM-1) were selected from dense welded tuffs. These sample were firstly prepared and dated in the same procedure as lava flow samples. The samples (78TM200 and KWTM-1) were further prepared and dated by the secondary procedure of Aso-4 (64AS219A and 81KC-664).

Aso-2 : Three whole rock samples were selected from homogeneously dense welded (69AS396A3) and secondary flowed (KWKC741 and 72MF-100) parts. They were prepared and dated by the same procedure as

lava flow samples.

Aso-1 : Two essential lenses (67MF22L1 and 69AS398A1) were selected from dense welded tuff and lithic breccia. These samples were prepared and dated by the same procedure as lava flow samples.

V-2-3. Result of K-Ar dating

K-Ar ages of Aso and nearby coeval volcanic rocks that erupted before the fallout of AT ash are given in Table V-8 with uncertainties of 1 σ . Fig.V-15 also summarizes their K-Ar ages consisting with volcanostratigraphies. The successive concordance with volcanostratigraphies and the eruptive history of Aso Volcano based on K-Ar ages are discussed in the following.

< Central Cones >

K-Ar age determinations for central cones have been made on the six volcanic products that erupted before the fallout of AT ash. Of these products, the Sawatsuno, Hokusui and Hontsuka Lavas are directly covered with AT ash (Ono and Watanabe, 1985). The five products except for the Ayugaerinotaki Lava have given significant K-Ar ages, while three samples of the Ayugaerinotaki Lava contained so large amount of total ^{40}Ar that they could not give significant ages. K-Ar ages of the Sawatsuno, Hokusui and Hontsuka Lavas covered with AT ash (27 ± 6 , 30 ± 6 and $46 \pm 9\text{ka}$) are consistent with the ^{14}C age of AT ash (22ka), and the ages of the Sawatsuno, Volcanological Laboratory and Tochinoki Lavas (27 ± 6 , 51 ± 5 and $73 \pm 10\text{ka}$) are successively concordant with volcanostratigraphies.

The Tochinoki Lava flowed into the "Tateno Barranco" (Fig.V-

Table V-8. K-Ar ages of Aso and nearby coeval volcanic rocks.

Sample Name	Sample Wt. (g)	K ₂ O (%)	³⁹ Ar/ ³⁶ Ar	⁴⁰ Ar/ ³⁶ Ar	Total ⁴⁰ Ar (10 ⁻⁹ mlSTP/g)	Rad. ⁴⁰ Ar (10 ⁻⁹ mlSTP/g)	Atm. ⁴⁰ Ar (%)	Age (ka)
【Sawatsuno Lava】								
54. KWKC736 LV	2.039	4.06	0.1858±0.0005	299.5±0.2	140 ± 6	3.50±0.76	97.5	27 ± 6
【Volcanological Laboratory Lava】								
55. KWKC740 LV	2.052	5.26	0.1861±0.0015	350.2±0.6	53.1±2.1	8.68±0.78	83.7	51 ± 5
【Hakusui Volcano】								
56. KWAS610 LV	2.168	4.25	0.1868±0.0016	321.0±0.8	50.8±2.0	4.07±0.81	92.0	30 ± 6
57. KWAS603A LV	1.256	—	—	—	>600	—	—	—
【Hontsuka Volcano】								
58. KWAS609B LV	2.089	4.27	0.1869±0.0004	302.7±0.3	26.5±1.1	6.31±1.21	97.6	46 ± 9
【Tochinoki Lava】								
59. KWKC739 LV	2.282	3.36	0.1864±0.0008	312.9±0.4	130 ± 5	7.88±1.11	93.9	73 ± 10
【Ayugaerinotaki Lava】								
60. 72WF304 LV	0.984	1.32	—	—	>520	—	—	—
61. KWKC737 LV	2.021	1.31	—	—	>470	—	—	—
62. KWKC738 LV	2.005	1.62	—	—	>400	—	—	—
【Aso-4 Pyroclastic Flow】								
63. 64AS210A GL	1.069 0.383	4.27	0.1891±0.0003	306.2±0.3	>1600 964 ± 39	11.6±3.4	98.8	85 ± 25
64. 81KC664 OB	0.998 0.755	5.16	0.1836±0.0003	286.2±0.3	>1200 3320±130	13±11	99.6	77 ± 67
65. 61K118AP VP	0.506 2.463	3.64	0.1870±0.0042 0.1871±0.0009	328.0±1.7 336.0±0.3	102 ± 4 88.3±3.5	10.0±4.1 10.5±0.9	90.2 88.1	85 ± 35 89 ± 7

Lv: Lava flow, Gl: Essential glass from lens and matrix, OB: Obsidian block in breccia, VP: Vapor phase crystallized part. * 80-100 mesh (Other samples were crushed to 32-60 mesh)

(Continued)

Sample Name	Sample Wt. (g)	K ₂ O (%)	³⁹ Ar/ ³⁶ Ar	⁴⁰ Ar/ ³⁶ Ar	Total ⁴⁰ Ar _g (10 ⁻⁹ mlSTP/g)	Rad. ⁴⁰ Ar	Atm. ⁴⁰ Ar (%)	Age (ka)
[Omine Volcano]								
66. MF72A1	LV	2.103	3.59	0.1871±0.0007	348.6±0.3	67.7±2.7	10.2±0.6	84.9
67. MF72B2	LV	2.085	3.59	0.1855±0.0006	330.2±0.3	90.4±3.6	10.7±0.7	99.2
[Aso-3 Pyroclastic Flow]								
68. 64TD232	LN	1.750	5.94	0.1883±0.0004	347.7±0.3	171 ± 7	23.6±1.2	86.3
69. 78TM200	LN	1.045	5.79	—	>70000	—	—	—
		0.755*	—	—	>62000	—	—	—
70. KWTM-1	LN	1.034	4.89	—	>15000	—	—	—
		1.008*	—	—	>12000	—	—	—
[Nekodake Volcano]								
71. 82AS707L1	LV	1.252	1.40	0.1851±0.0008	310.3±0.6	74.3±3.0	4.88±0.68	93.4
		2.821	—	0.1863±0.0005	312.8±0.3	67.3±2.7	4.13±0.40	93.9
72. 82AS785B	DK	2.796	1.02	0.1865±0.0010	307.7±0.4	68.1±2.7	2.99±0.69	95.6
		3.012	—	0.1866±0.0005	306.0±0.2	86.4±3.5	3.22±0.49	96.3
73. 82AS786T1	DK	2.974	0.931	0.1862±0.0014	324.4±0.5	34.8±1.4	3.34±0.49	90.4
74. KW81NK6	LV	0.997	1.31	0.1862±0.0015	303.2±0.5	122 ± 5	3.92±1.94	96.8
		2.912	—	0.1865±0.0004	303.3±0.2	116 ± 5	3.47±0.48	97.0
75. NK-103	DK	3.018	1.39	0.1852±0.0006	318.1±0.4	38.9±1.6	3.42±0.26	91.2
[Aso-2 Pyroclastic Flow]								
76. 69AS396A3	DW	0.505	—	—	>1800	—	—	—
77. KWK741	SC	2.967	4.18	0.1873±0.0005	349.7±0.4	125 ± 5	18.9±1.0	84.9
78. 72MF100	SC	3.017	3.70	0.1875±0.0006	352.2±0.3	109 ± 4	17.0±0.9	84.4
								142 ± 8

Lv: Lava flow, DK: Dike, LN: Essential lens, DW: Homogeneously dense welded part, SC: Secondary flowed part.

* 80-100 mesh (Other samples were crushed to 32-60 mesh)

(Continued)

Sample Name	Sample Wt. (g)	K ₂ O (%)	³⁶ Ar/ ³⁹ Ar	⁴⁰ Ar/ ³⁹ Ar	Total ⁴⁰ Ar (10 ⁻⁹ mlSTP/g)	Rad. ⁴⁰ Ar (10 ⁻⁹ mlSTP/g)	Atm. ⁴⁰ Ar (%)	Age (ka)
【Akaï Volcano】								
79. KWHF221	LV 2.020	3.36	0.1858±0.0007	342.0±0.4	110 ± 4	16.1±1.0	85.4	149± 9
80. KWHF222	LV 2.018	3.39	0.1870±0.0005	327.9±0.3	164 ± 7	16.1±1.1	90.2	147±10
【Aso-2/1 Lava】								
81. 67TD469	LV 2.065	4.19	0.1872±0.0005	345.6±0.3	138 ± 6	19.6±1.0	85.8	145± 8
82. KWAS612	LV 2.022	2.14	0.1870±0.0005	306.2±0.3	452 ± 18	15.4±2.3	96.6	223±34
【Aso-1 Pyroclastic Flow】								
83. 67MF22L1	LN 0.839 0.421	5.02	0.1880±0.0007 0.1886±0.0003	312.5±0.2 314.7±0.2	942 ± 38 945 ± 38	40.4±7.1 39.6±3.7	95.7 95.8	249±44 245±23 246±25
84. 69AS398A1	LN 1.001	4.96	0.1866±0.0006	369.8±0.4	214 ± 9	43.4±2.0	79.7	271±13

Lv: Lava flow, LN: Essential lens.

* 80-100 mesh (Other samples were crushed to 32-60 mesh)

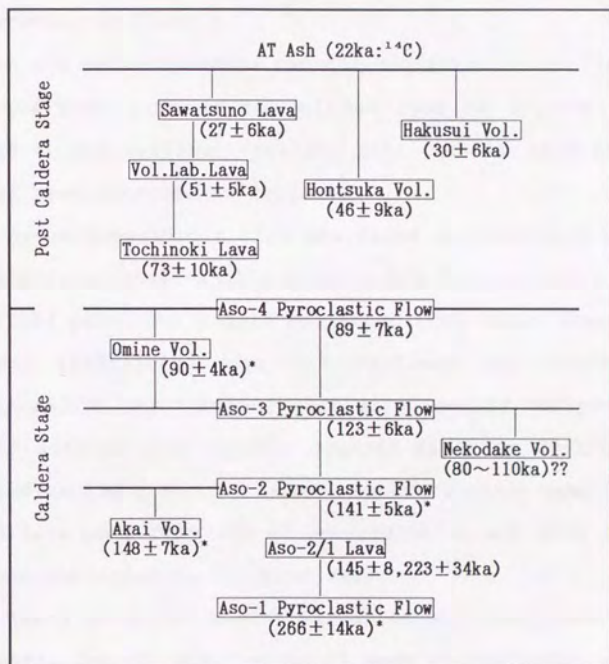


Fig. V-15. K-Ar ages of Aso and nearby coeval volcanic rocks, consisting with volcanostratigraphy.

Volcanostratigraphy is after Ono and Watanabe(1985).

* K-Ar ages of these samples are given in weighted means.

10 and 12) which was formed in the early Post Caldera Stage by tectonic movements. Hence, K-Ar age of the Tochinoki Lava (73 ± 10 ka) leads to a conclusion that the present Aso caldera was formed and activities of central cones started at least older than 60ka.

< Aso Pyroclastic Flows >

K-Ar age determinations for the Aso pyroclastic flows (Aso-1 to 4) have been made on the eleven samples by the procedure mentioned in the previous section. K-Ar ages of each pyroclastic flow have been obtained as follows.

Aso-4 : Aso-4 pyroclastic flow was dated on essential glass from lens and matrix, obsidian block in lithic breccia and vapor phase crystallized part. The sample collected from vapor phase crystallized part (61IK118AP) gave a significant age (89 ± 7 ka), while others (64AS210A and 81KC664) also gave ages by the procedure in which the samples were further crushed finer to 80-100 mesh and pre-heated at 150°C for 100 hours. However, these ages (85 ± 25 and 77 ± 67 ka) have more than 30% of uncertainties and were not enough to discuss the accurate eruption age.

Aso-3 : Aso-3 pyroclastic flow was dated on three essential obsidian lenses. One of them (64TD232) gave a meaningful age (123 ± 6 ka) by the same procedure as lava flow samples, while others (78TM200 and KWTM-1) could not give ages even by the secondary procedure mentioned in Aso-4 (64AS210A and 81KC664).

Aso-2 : K-Ar ages of Aso-2 pyroclastic flow were obtained for two samples collected from secondary flowed components (Aso-2R : KWKC741 and 72MF100). These ages (140 ± 7 and 142 ± 8 ka) are in agreement with each other. However, another sample collected from homogeneously dense welded component (69AS396A3) contained too

much total ^{40}Ar to obtain a significant age.

Aso-1 : Two essential lenses (67MF22L1 and 69AS398A1) collected from dense welded tuff and lithic breccia were determined by the same procedure as lava flow samples and meaningful ages were obtained. These K-Ar ages (246 ± 25 and $271 \pm 13\text{ka}$) are in agreement with each other within their uncertainties.

As is clear from these results, meaningful ages were obtained for the samples collected from some of the essential obsidian lenses, secondary flowed components and vapor phase crystallized parts. The samples which could not give meaningful ages were further crushed finer to 80-100 mesh and pre-heated at 150°C for 100 hours. However, this procedure was not so effective to decrease the amount of total ^{40}Ar and get meaningful ages. Essential obsidian lenses and secondary flowed components have been expected as the suitable samples for K-Ar dating of pyroclastic flows and some of them collected from Aso pyroclastic flows could give significant ages. Furthermore, it has been clarified in this study that vapor phase crystallized parts also can be used as a suitable sample for K-Ar dating of pyroclastic flows.

K-Ar ages of the Aso pyroclastic flows (Aso-1 to 4) directly clarified that they erupted at about 270, 140, 120 and 90ka, respectively. The interval between Aso-1 and 2 continued more than 1×10^5 years, while other intervals (Aso-3/2 and Aso-4/3) are estimated to be much shorter as at most 2.7×10^4 and 4.7×10^4 years, respectively, within uncertainties (1 σ) for K-Ar ages of these pyroclastics. The stratigraphic relations between Aso-4 and Younger Ontake volcanic products have been clarified through the stratigraphic position of Aso-4 ash (a widespread fallout tephra

that erupted accompanied by Aso-4 pyroclastic flow) in the Younger Ontake Tephra Group (Takemoto et al., 1987). The eruption age of Aso-4 will be further discussed in V-3, by comparing it with K-Ar ages of some Younger Ontake volcanic rocks whose relations with Aso-4 ash have been clarified.

< Other products erupted during Caldera Stage >

K-Ar age determinations for the Aso volcanic products except for pyroclastics and the nearby coeval volcanics, that erupted between Aso-1 and 4, have been made on the Aso-2/1 Lava, Nekodake, Omine and Akai Volcanoes. These ages except for Nekodake Volcano are consistent with the stratigraphic relations to Aso pyroclastic flows as shown in Fig.V-13. K-Ar ages of these products have clarified the following.

The periods of Akai and Omine Volcanoes have been estimated from the stratigraphic relations with Aso pyroclastic flows that Akai Volcano erupted between Aso-1 and 2 (Ono et al., 1981) and that Omine Volcano erupted between Aso-3 and 4 (Watanabe and Ono, 1969). Itaya et al. (1984) dated two lava flows of Omine Volcano (MF72A1 and MF72B2). However, these ages scattered as 123 ± 10 and 89 ± 10 ka, respectively. In this study, K-Ar age determination for Omine Volcano was made on the same samples as Itaya et al. (1984) and the determination for Akai Volcano was made on two lava flows (KWMF221 and KWMF222) collected from the Togawa Lava. The ages obtained in the present study ($Av. 90 \pm 4$ and 148 ± 7 ka) clarified that the activities of these nearby monogenetic volcanoes occurred just before the eruptions of Aso-2 and 4 (K-Ar : 141 ± 5 and 89 ± 7 ka), respectively. On the other hand, K-Ar ages of the Aso-2/1 Lava that erupted between Aso-1 and 2 (Ono, 1965) suggest a possi-

bility that they would consist of at least two groups ; the one erupted just before Aso-2 as Akai Volcano and the other in the significantly older age. Because K-Ar age of 67TD469 (145 ± 8 ka) can be regarded to be the same as that of Akai Volcano, while the age of KWAS612 (223 ± 34 ka) is significantly older than that of 67TD469 beyond 1 σ of uncertainties.

K-Ar age determinations for Nekodake Volcano have been made on five samples. Of these samples, two samples (82AS707L1 and KW-81NK6) were collected from lava flows and three (82AS785B, 82AS-786T1 and NK-103) from dikes. K-Ar ages of these samples scatter as 96 ± 9 , 96 ± 13 , 111 ± 16 , 83 ± 24 and 76 ± 6 ka without significant difference between lava flows and dikes. Furthermore, these ages except for 82AS786T1 are significantly younger than that of Aso-3 (123 ± 6 ka) beyond 1 σ of uncertainties and are inconsistent with the field observation that Nekodake Volcano was built at the earlier stage than Aso-3 (Ono et al., 1982). Such a large deviation in K-Ar ages of Nekodake Volcano would result from lower K₂O contents of Nekodake volcanics (0.9-1.4%) than those of other Aso volcanics, because the uncertainties for K-Ar ages relatively increase with the decreases of K₂O contents. On the other hand, as the reasons why K-Ar ages of Nekodake Volcano are inconsistent with the volcanostratigraphy, the following would be considered. (1) The stratigraphic relation between Aso-3 and Nekodake Volcano (Ono and Watanabe, 1985) would not be adequate, because it was not based on their direct contact and estimated from the geographical situation. (2) K-Ar age of Aso-3 was obtained only for one sample (64TD232), so there remains a possibility that the sample might contain excess ⁴⁰Ar and the real eruption age would be younger

than the age obtained in the present study. More intensive field observations for Aso-3 and Nekodake Volcano especially to find their direct contact and more K-Ar ages for Aso-3 may clarify the stratigraphic relation between Aso-3 and Nekodake Volcano.

< Summary >

Systematic K-Ar age determinations for Aso and nearby coeval volcanic products also showed the usefulness of new K-Ar dating technique based on MFCM for volcanics in the order of 10-100ka. K-Ar ages of these products that erupted between Aso-1 and the fallout of AT ash are successively concordant with their volcano-stratigraphies except for Nekodake Volcano. As the Aso pyroclastic flows (Aso-1 to 4) have given meaningful ages from essential obsidian lenses, secondary flowed components and vapor phase crystallized part, these components can be used as the suitable samples for K-Ar dating of other pyroclastic flows. For Nekodake Volcano and Aso-3 pyroclastic flow whose ages are inconsistent with the stratigraphic relation, their direct contact should be found and it should be confirmed whether Aso-3 pyroclastic flow dated in the present study contained excess ^{40}Ar or not.

v-3. Eruption ages of some widespread fallout tephras estimated from K-Ar ages of Ontake, Aso and other volcanics

Widespread fallout tephras are distributed in the extremely wide areas (Fig.V-16) and are useful as key beds to correlate tephra layers distributed in the different provinces. Of these widespread fallout tephras, Kikai-Akahoya ash (K-Ah), Ulreung-Oki ash (U-Oki), AT ash and Shikotsu pumice fall-1 (Spfa₁) have been dated intensively by the ¹⁴C method and their ages are recommended as 6.3, 9.3, 22 and 32ka, respectively (Endo et al.,1986). On the other hand, Daisen Kurayoshi pumice (DKP), Aso-4 ash and Pm-I were also dated by the FT and the Io methods. However, their ages had considerably large analytical uncertainties and scattered as shown in Table V-9 (Machida and Suzuki,1971 ; Okaguchi,1978 ; Tamanyu,1979 ; Omura et al.,1988). In tephrochronology, the eruption age of Pm-I has been estimated to be 70-90ka on the basis of FT ages (73 \pm 4, 77 \pm 8, 78 \pm 10, 82 \pm 10 and 95 \pm 5ka : Machida and Suzuki,1971), while those of Aso-4 ash and DKP have been estimated to be about 70 and 48ka, respectively, from the stratigraphic relations with some tephra layers in the standard sequence of South Kanto and the eastern foot of Ontake volcano which gave FT ages (Machida et al.,1985 ; Takemoto et al.,1987).

In this study, K-Ar age was obtained on the vapor phase crystallized part (64IK118AP : 89 \pm 7ka) of Aso-4 pyroclastic flow that erupted with Aso-4 ash, and on some of the Ontake and Aso volcanic products. Such products also have clarified the stratigraphic relations with DKP, Aso-4 ash and Pm-I (Ono and Watanabe, 1985 ; Takemoto et al.,1987 ; Yamada and Kobayashi,1988). Furthermore, the Tamadono Lava of Tateyama Volcano and the Ikeno-



Fig.V-16. Distribution of some widespread fallout tephras (after Endo et al., 1986).

Table V-9. Radiometric ages of DKP, Aso-4 ash and Pm-I.

	Method	Age (ka)	Reference
DKP	Io	43 ± 8	Omura et al.(1988)
Aso-4 ash	FT	29 ± 14	Okaguchi(1978)
	FT	84 ± 25	Tamanyu(1979)
	Io	80 ± 2	Omura et al.(1988)
Pm-I	FT	$73 \pm 4, 77 \pm 8, 78 \pm 10,$ $82 \pm 10, 95 \pm 5$	Machida and Suzuki(1971)
	Io	82 ± 5	Omura et al.(1988)

FT: Fission-Track method, Io: ^{230}U - ^{230}Th disequilibrium method

taira-bokujo Lava of Yatsugatake Volcano have clarified that they erupted before the fallout of DKP and Pm-I, respectively (Machida and Arai, 1979 ; Collaborative Research Group for Yatsugatake ed., 1988). On the basis of these stratigraphic relations with DKP, Aso-4 ash and Pm-I, their eruption ages are further discussed in this section. K-Ar ages of the Tamadono and the Ikenotaira-bokujo Lavas are given in Table V-10, and K-Ar ages of the products in Ontake, Aso, Tateyama and Yatsugatake Volcanoes whose stratigraphic relations with widespread fallout tephra have been clarified, are summarized in Fig.V-17.

< Pm-I >

As mentioned in the K-Ar age determinations for Ontake Volcano (V-1-1), phenocrysts (hornblende and biotite) extracted from the Pm-I Pumice Fall Deposit contained excess ^{40}Ar and could not give meaningful K-Ar ages. However, the eruption age was estimated to be at least older than 80ka from K-Ar ages of the other Mamahahadake Volcano Group that erupted after Pm-I.

On the other hand, stratigraphic relations of the following volcanic products dated in the present study with Pm-I have been clarified. (1) Aso-4 ash (K-Ar: 89 ± 7 ka) was found in the Younger Ontake Tephra Group at the foot of Ontake Volcano and fell out after the eruption of Pm-I (Takemoto et al., 1987). (2) The Ikenotaira-bokujo Lava of Yatsugatake Volcano (K-Ar: 124 ± 11 ka) has been covered with Pm-I tephra layer (Collaborative Research Group for Yatsugatake ed., 1988). ; K-Ar age of Aso-4 ash (89 ± 7 ka) supports the estimation based on K-Ar ages of the other Mamahahadake Volcanic products that Pm-I erupted at least older than 80ka, while K-Ar age of the Ikenotaira-bokujo Lava (124 ± 11 ka) restricts the

Table V-10. K-Ar ages of Yatsugatake and Tateyama volcanic rocks.

Sample Name	Sample Wt. (g)	K ₂ O (%)	³⁹ Ar/ ³⁶ Ar	⁴⁰ Ar/ ³⁶ Ar	Total ⁴⁰ Ar (10 ⁻⁹ mlSTP/g)	Rad. ⁴⁰ Ar (10 ⁻⁹ mlSTP/g)	Atm. ⁴⁰ Ar (%)	Age (ka)
【Yatsugatake Vol. Ikenotaira-bokujo Lava】								
85. TAT8914	2.028	1.99	0.1866±0.0008	327.7±0.4	79.0±3.2	7.98±0.73	89.9	124±11
86. TAT8915	2.020	2.30	0.1861±0.0011	341.7±0.5	71.2±2.8	10.1±0.83	85.7	137±11
87. TAT8916	2.021	1.80	—	—	>470	—	—	—
【Tateyama Vol. Tamadono Lava】								
88. TTYN-03	1.999	3.35	—	—	>1500	—	—	—
89. TTYN-04	2.011	3.09	0.1868±0.0018	326.2±0.9	49.3±2.0	4.68±0.09	90.5	47±9
89. TTYN-11	3.024	3.91	—	—	>510	—	—	—

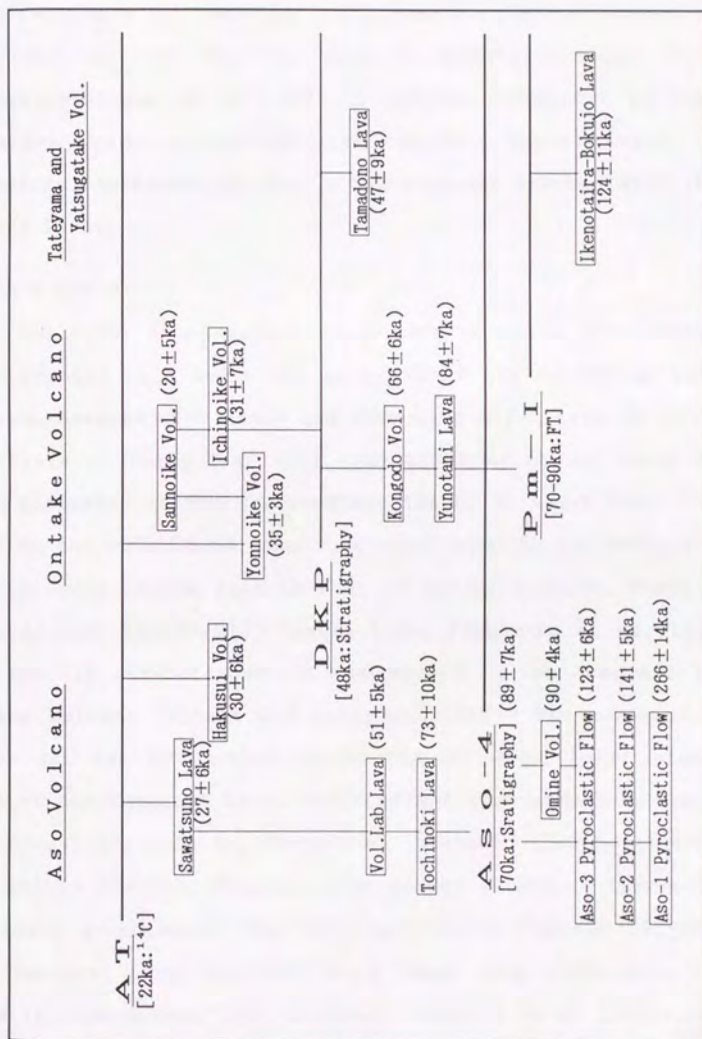


Fig. V-17. Stratigraphic correlation between four volcanoes using some widespread fallout tephra layers as maker beds.

upper limit of Pm-I to be at most younger than 120ka. The eruption age of Pm-I can be estimated to be at most within 80-120ka from K-Ar ages of these products, however, it is somewhat older than the age that has been used in tephrochronology (70-90ka). The eruption age of Pm-I will be further restricted by K-Ar ages of other products covered with the Pm-I tephra layer. It is, therefore, necessary to find other products covered with the Pm-I tephra layer.

< Aso-4 ash >

The vapor phase crystallized part of Aso-4 pyroclastic flow that erupted with Aso-4 ash gave a K-Ar age of 89 ± 7 ka and Omine Volcano covered with Aso-4 ash also gave a K-Ar age of 90 ± 4 ka. On the basis of these K-Ar ages, the eruption age of Aso-4 ash has been estimated in the previous section to be about 90ka.

On the other hand, Aso-4 ash was found in the Younger Ontake Tephra Group at the eastern foot of Ontake Volcano, where it was covered with the Pm-III' tephra layer (Takemoto et al., 1987). As the Pm-III' tephra layer also coexisted in the Yunotani Lava of Ontake Volcano (Yamada and Kobayashi, 1988), the eruption age of Aso-4 ash can be further restricted to be at least older than that of the Yunotani Lava. The Yunotani Lava gave K-Ar age of 84 ± 7 ka (Fig.V-17) ; it is, therefore, concluded that Aso-4 ash erupted within 80-90ka. However, such an age estimated from K-Ar ages of Aso-4 pyroclastic flow (89 ± 7 ka), Omine Volcano (90 ± 4 ka) and the Yunotani Lava (84 ± 7 ka) is at least 10ka older than the age used in tephrochronology (ca.70ka : Machida et al., 1985). The age of Aso-4 ash used in tephrochronology was based on the stratigraphic position in the standard sequence of South Kanto, where Aso-

4 ash was found at the intermediate horizon between Pm-I (FT:70-90ka) and Obaradai Pumice (FT:66 \pm 6ka), and it was estimated to be about 70ka on the assumption that the sedimentary rate of tephras between Pm-I and Obaradai Pumice was constant and that their ages were regarded as 66 and 81ka (the means of their FT ages), respectively. The eruption age of Pm-I estimated from K-Ar ages of Ontake and Yatsugatake volcanics was within 80-120ka, so the assumption (Machida et al.,1985) that Pm-I would have erupted at 81ka, might be underestimated and would produce a discrepancy between the age of Aso-4 ash estimated in the present study (80-90ka) and the one used in tephrochronology (ca.70ka).

< D K P >

The eruption age of DKP used in tephrochronology (ca.48ka : Takemoto et al.,1987) was based on the stratigraphic relation in Kanto where DKP was located just on the Tokyo Pumice (FT:49 \pm 5ka, Machida and Suzuki,1971). On the other hand, stratigraphic relations of the following volcanics with DKP have been clarified. (1) The Tamadono Lava of Tateyama Volcano is covered with DKP (Machida and Arai,1979). (2) In the Younger Ontake Tephra Group at the eastern foot of Ontake Volcano, DKP was found in the horizon between Yashikino (Ys) and Yanagimata (Yn) tephra layer (Takemoto et al.,1987). Kongodo and Ichinoike Volcanoes of the Marishiten Volcano Group were regarded as the sources of Ys and Yn tephra layer, respectively (Yamada and Kobayashi,1988). Hence it can be estimated that DKP erupted earlier than Ichinoike Volcano and later than the Tamadono Lava and Kongodo Volcano.

K-Ar ages of the Tamadono Lava, Ichinoike and Kongodo Volcano (47 \pm 9, 31 \pm 7 and 66 \pm 6ka) suggest that DKP erupted within 25-

55ka. However, the uncertainty for such an age (25-55ka) is too large to be compared with the one used in tephrochronology (ca.48 ka). It is, therefore, necessary to find other volcanics covered with or covering on DKP and to get as many K-Ar ages as possible in order to further restrict the eruption age of DKP.

< Summary >

Eruption ages of Pm-I, Aso-4 ash and DKP have been discussed based on K-Ar ages of volcanics whose stratigraphic relations with these widespread fallout tephra were clarified. The eruption age of DKP estimated from K-Ar ages of Ontake and Tateyama volcanic rocks (25-55ka) had too much uncertainty to be compared with the age used in tephrochronology (about 48ka). On the other hand, eruption ages of Aso-4 ash and Pm-I estimated from K-Ar ages of Ontake, Aso and Yatsugatake volcanics (Aso-4 ash : 80-90ka, Pm-I : 80-120ka) were older than the ages used in tephrochronology (Aso-4 ash : about 70ka, Pm-I : 70-90ka). The ages of Aso-4 ash and Pm-I used in tephrochronology might be underestimated and might be revised to be older by more than 10^4 years.

v-4. Radiometric ages for Aso-4 ash and Pm-I, and their implications for the late Quaternary sea level fluctuations in South Kanto

In the Quaternary sea level fluctuations, maximum phases of transgressions were estimated from radiometric ages (e.g., FT, Io and ^{14}C ages) of tephra layers covering terraces. Maximum phases of transgressions in South Kanto have also been estimated from FT ages of some tephra layers covering terraces, in which Pm-I and Aso-4 ash played an important role as key beds to determine a maximum phase. In this section, it is discussed how the differences between ages of Pm-I and Aso-4 ash estimated in the present study (80-120 and 80-90ka) and the ones used in tephrochronology (70-90 and ca.70ka) have an influence on the late Quaternary sea level fluctuation in South Kanto.

The late Quaternary sea level fluctuations in South Kanto have been summarized by Machida (1973,1977) as shown in Fig.V-18. He divided the late Quaternary coastal terraces into five groups in the order of Shimosueyoshi (S), Hikihashi (M), Obaradai (O), Misaki (M) and Tachikawa-1 (T_c-1) terrace, and considered that these terraces were constructed in high sea level stages. Of these terraces, the marine Shimosueyoshi terrace is more widely distributed and concluded to have formed in the last great interglacial stage. On the other hand, the post-Shimosueyoshi terraces (H, O, M and T_c-1 terraces) are mostly developed as fluvial terraces in the inland area and the marine surfaces are limited in the coastal region (Miura peninsula and its contiguous region). Maximum phases of Shimosueyoshi, Hikihashi, Obaradai and Misaki transgressions have been estimated from FT ages of some

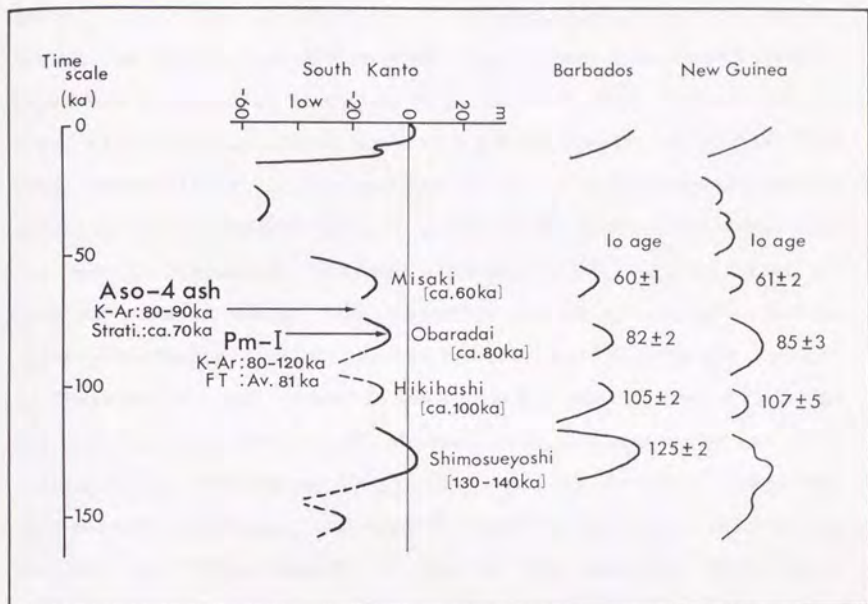


Fig.V-18. The late Quaternary sea level fluctuation in South Kanto, Barbados and New Guinea (modified after Machida, 1973).

Maximum phases of transgressions in South Kanto were estimated from FT ages of tephra layers whose stratigraphic relations with these terraces have been clarified (Machida and Arai, 1971 ; Machida, 1977).

Pm-I erupted at the maximum phase of Obaradai transgression and Aso-4 ash at the regression stage between Obaradai and Misaki transgression. Eruption age of Pm-I was estimated from FT ages of zircon extracted from Pm-I pumice fall deposit (Machida and Arai, 1971), while Aso-4 ash was estimated from stratigraphic relations with the other tephra layers which gave FT ages (Machida et al., 1985).

Lo ages of coral reef terraces in Barbados and New Guinea are after Mesollella et al., 1969, James et al., 1971 and Bloom et al., 1974.

tephra layers as follows (Machida and Suzuki, 1971 ; Machida, 1977), i.e., (1) The surface of Shimosueyoshi terrace formed during the fallout of K1P pumice layers, and the TAU-12 pumice layer was included in the upper most part of this terrace. K1P-6, 8 and TAU-12 pumice layers gave FT ages as 128 ± 11 , 132 ± 10 and 145 ± 7 ka, respectively, so the maximum phase of Shimosueyoshi transgression was estimated to have occurred at about 130-140 ka. (2) The maximum phase of Hikihashi transgression was estimated to have occurred at about 100 ka, based on the FT age of KmP-1 pumice layer (98 ± 12 ka) directly covering the terrace. (3) As the surface of Obaradai terrace formed between the fallout of Pm-I (FT: Av. 81 ka) and Obaradai Pumice (FT: 66 ± 6 ka), the maximum phase of this transgression was estimated to have occurred at about 80 ka. (4) The surface of Misaki terrace formed between the fallout of Yoshioka and Miura Pumice. FT age of the Obaradai Pumice that erupted before the Yoshioka Pumice was 66 ± 6 ka and FT age of the Tokyo Pumice that erupted after the Miura Pumice was 49 ± 5 ka, so the maximum phase of Misaki transgression was estimated to have occurred at about 60 ka. Furthermore, these maximum phases of transgressions have been correlated with those of coral reef terraces in Barbados and New Guinea which have given 10 ages (Mesolellia et al., 1969 ; James et al., 1971 ; Bloom et al., 1974).

As it has been mentioned above, Pm-I fell out at the maximum phase of Obaradai transgression. On the other hand, Aso-4 ash was found in the Obaradai tephra formation in which it was located at the intermediate horizon between Pm-I and Obaradai Pumice. This horizon corresponds to the regression stage between Obaradai and Misaki transgressions (Fig.V-18). The maximum phase of Obaradai

transgression usually has been considered to be about 80ka on the mean (81ka) of FT ages for Pm-I (73 ± 4 - 95 ± 5 ka : Machida and Suzuki, 1971) and Io ages of the coral reef terraces in Barbados and New Guinea (82 ± 2 and 85 ± 3 ka) corresponding to the Obaradai terrace. However, as discussed in the previous section (V-3), the eruption ages of Pm-I and Aso-4 ash has been estimated from K-Ar ages of some volcanics to be within 80-120 and 80-90ka, respectively. It is, therefore, concluded that the regression after Obaradai transgression had already commenced at least earlier than 80ka and the maximum phase of Obaradai transgression occurred earlier than 80ka which has been considered in the sea level fluctuation based on FT and Io ages.

As the maximum phase of Obaradai transgression was estimated simply from the mean of FT ages for Pm-I (73 ± 4 , 77 ± 8 , 78 ± 10 , 82 ± 10 and 95 ± 5 ka : Machida and Suzuki, 1971), it is not necessarily abroad to assume that the maximum phase might be $(1-2) \times 10^4$ years older than the conventional age (ca. 80ka) because of the uncertainties for FT ages of Pm-I. On the other hand, although Io ages of coral reef terraces in Barbados and New Guinea (82 ± 2 and 85 ± 3 ka) corresponding to the Obaradai terrace had extremely small analytical uncertainties and were in good agreement with the mean of FT ages for Pm-I, yet analytical uncertainties for these Io ages were considered only for a counting of ^{234}U and ^{230}Th . So it can be expected that the uncertainties for Io ages of coral reef terraces which are considered for other factors become considerably larger than the one considered only for a counting. Furthermore, coral samples used in the Io dating (Mesolellia et al., 1969 ; Bloom et al., 1974) were affected more than 1% of phase

transition (aragonite to calcite) and there remains a possibility that these samples did not keep a closed system for uranium and thorium, i.e., ^{234}U and ^{230}Th might be released from or added to samples in the phase transition. Io ages of these coral samples might be unreliable ones.

The maximum phase of Obaradai transgression will be clarified when the eruption age of Pm-I estimated from K-Ar ages of some volcanics (80-120ka) would be further restricted by K-Ar ages of other volcanics.

CONCLUSIONS

A new K-Ar dating technique applicable to volcanic rocks that erupted in the order of 10^4 years ago has been developed. This technique makes it possible to discuss systematic eruptive histories of Quaternary volcanoes whose life time are within 10^5 - 10^6 years by the combination of K-Ar and ^{14}C dating methods.

In this K-Ar dating technique, the initial $^{40}\text{Ar}/^{36}\text{Ar}$ ratio of a dated sample was always estimated from a stable $^{38}\text{Ar}/^{36}\text{Ar}$ ratio based on the fact that argon isotopic ratios of historic volcanics mostly lie on a theoretical mass fractionation from the present-day atmospheric one. It has been estimated from argon isotopic ratios of historic volcanics that the samples containing 2% of K_2O give significant K-Ar ages when more than twenty thousand years has passed after their eruptions. Some lava flows directly covered with the Aira-Tn ash have given concordant K-Ar ages with the ^{14}C age of Aira-Tn ash (22ka: ^{14}C).

Systematic K-Ar age determinations for Ontake and Aso Volcanoes indicated successive concordances with their volcanostratigraphies and gave the following important information for their eruptive histories.

1. Activities of Older Ontake Volcano initiated at least older than 700ka and finished before 400ka. It has been clarified that the "Kuragoehara Lava" used as a key bed to construct the volcanostratigraphy of Older Ontake Volcano (Yamada and Kobayashi, 1988) consists of two kinds of lava flows that erupted in quite different ages. Some lava flows classified into the same layers from stratigraphic relations with the Kuragoehara Lava and petrology (e.g., the Makuiwagawa and

Nunokawa Lavas) had different ages in each area. The Sengendaru Lava may have erupted in the Younger Ontake Period, because it had extremely young K-Ar age compared with other Older Ontake volcanics. The volcanostratigraphy of Older Ontake Volcano (Yamada and Kobayashi, 1988) should be revised based on K-Ar ages of volcanics distributed in each area.

2. Activity of Younger Ontake Volcano started at about 80-90ka after more than 3×10^5 years of inactive period. The following activities of the Marishiten Volcano Group started at about 80ka just after finishing of the Mamahahadake Volcano Group and it continued to about 20ka.
3. Aso pyroclastic flows (Aso-1 to 4) have given significant K-Ar ages (Aso-1: 266 ± 14 , Aso-3: 141 ± 5 , Aso-3: 123 ± 6 , Aso-4: 89 ± 7 ka) from essential lenses, secondary flowed matrixes and vapor phase crystallized part. Activities of nearby coeval monogenetic volcanoes (Akai and Omine Volcanoes) occurred just before Aso-2 and Aso-4, respectively. Furthermore, K-Ar ages of central cones clarified that the present shape of Aso caldera formed at least older than 60ka.
4. The eruption ages of Pm-I and Aso-4 ash estimated from K-Ar ages of some Ontake and Aso volcanics (Pm-I : 80-120ka, Aso-4 ash : 80-90ka) were at least 10^4 years older than the ages used in tephrochronology. Such eruption ages gave an information to the late Quaternary sea level fluctuation in South Kanto that the regression after Obaradai transgression would have already commenced at least older than 80ka.

ACKNOWLEDGMENTS

The author wishes to thank Professors Shigeo Aramaki and Ichiro Kaneoka for his constant supervisions and encouragements throughout the course of this study. He also thanks Drs. Ken Shibata and Kozo Uto for their critical discussions and encouragements. Professors T.Kobayashi and K.Watanabe, and Messrs. K.Ono and T.Soya are thanked for providing many Ontake and Aso volcanic rocks and geological information. Many historic volcanic rocks are also offered from the following persons ; Drs. N. Isshiki, S.Suto, Y.Kinugasa and Mr. S.Nakano. The author also shows cordial thanks to Mr. H.Aoyama for his help in sample preparation. He is also indebted to the following persons for fruitful discussions and encouragement at the various stage of the study ; Professor N.Takaoka, Drs. T.Tanaka, S.Togashi and N. Yamada.

APPENDIX I

(Correction of hot blank)

$$(^{36}\text{Ar})_s = (^{40}\text{Ar})_s / (^{40}\text{Ar}/^{36}\text{Ar})_s$$

$$(^{38}\text{Ar})_s = (^{36}\text{Ar})_s \cdot (^{38}\text{Ar}/^{36}\text{Ar})_s$$

$$(^{36}\text{Ar})_b = (^{40}\text{Ar})_b / (^{40}\text{Ar}/^{36}\text{Ar})_b$$

$$(^{38}\text{Ar})_b = (^{36}\text{Ar})_b \cdot (^{38}\text{Ar}/^{36}\text{Ar})_b$$

$$(^m\text{Ar})_{\text{cor.}} = (^m\text{Ar})_s - (^m\text{Ar})_b$$

$$(^m\text{Ar}/^{m'}\text{Ar})_{\text{cor.}} = (^m\text{Ar})_{\text{cor.}} / (^{m'}\text{Ar})_{\text{cor.}}$$

m : Mass number

$(^m\text{Ar})_s$: Intensity of ^mAr determined in sample analysis

$(^m\text{Ar})_b$: Intensity of ^mAr determined in hot blank analysis

$(^m\text{Ar}/^{m'}\text{Ar})_s$: $^m\text{Ar}/^{m'}\text{Ar}$ ratio determined in sample analysis

$(^m\text{Ar}/^{m'}\text{Ar})_b$: $^m\text{Ar}/^{m'}\text{Ar}$ ratio determined in hot blank analysis

$(^m\text{Ar})_{\text{cor.}}$: Intensity of ^mAr in a sample when hot blank is corrected

$(^m\text{Ar}/^{m'}\text{Ar})_{\text{cor.}}$: $^m\text{Ar}/^{m'}\text{Ar}$ ratio of a sample when hot blank is corrected

(Correction of mass discrimination)

$$(^m\text{Ar}/^{m'}\text{Ar})_f = \frac{(^m\text{Ar}/^{m'}\text{Ar})_{\text{cor.}} \cdot (^m\text{Ar}/^{m'}\text{Ar})_{\text{Nier}}}{(^m\text{Ar}/^{m'}\text{Ar})_{\text{air}}}$$

$(^m\text{Ar}/^{m'}\text{Ar})_{\text{cor.}}$: $^m\text{Ar}/^{m'}\text{Ar}$ ratio of a sample when hot blank is corrected

$(^m\text{Ar}/^{m'}\text{Ar})_{\text{Nier}}$: $^m\text{Ar}/^{m'}\text{Ar}$ ratio of the atmosphere defined by Nier(1950)

$(^m\text{Ar}/^{m'}\text{Ar})_{\text{air}}$: $^m\text{Ar}/^{m'}\text{Ar}$ ratio determined in air standard analysis

$(^m\text{Ar}/^{m'}\text{Ar})_f$: $^m\text{Ar}/^{m'}\text{Ar}$ ratio of a sample when mass discrimination is corrected

<Error for correction of hot blank>

$$\sigma_{36a}^2 = \sigma_{40a}^2 + \sigma_{(40/36)a}^2$$

$$\sigma_{38a}^2 = \sigma_{36a}^2 + \sigma_{(38/36)a}^2$$

$$\sigma_{36b}^2 = \sigma_{40b}^2 + \sigma_{(40/36)b}^2$$

$$\sigma_{38b}^2 = \sigma_{36b}^2 + \sigma_{(38/36)b}^2$$

$$\sigma_{mc} = \frac{[(^{36}\text{Ar}_a \cdot \sigma_{ma})^2 + (^{38}\text{Ar}_b \cdot \sigma_{mb})^2]^{1/2}}{(^{36}\text{Ar}_a - ^{38}\text{Ar}_b)}$$

$$\sigma_{(m/m')c}^2 = \sigma_{mc}^2 + \sigma_{m'c}^2$$

σ_{ma} : Relative error for intensity of ^{36}Ar determined in sample analysis

σ_{mb} : Relative error for intensity of ^{38}Ar determined in hot blank analysis

$\sigma_{(m/m')a}$: Relative error for $^{36}\text{Ar}/^{38}\text{Ar}$ ratio determined in sample analysis

$\sigma_{(m/m')b}$: Relative error for $^{36}\text{Ar}/^{38}\text{Ar}$ ratio determined in hot blank analysis

$^{36}\text{Ar}_a$: Intensity of ^{36}Ar determined in sample analysis

$^{38}\text{Ar}_b$: Intensity of ^{38}Ar determined in hot blank analysis

σ_{mc} : Relative error for intensity of ^{36}Ar in a sample when hot blank is corrected

$\sigma_{(m/m')c}$: Relative error for $^{36}\text{Ar}/^{38}\text{Ar}$ ratio of a sample when hot blank is corrected

<Error for correction of mass discrimination>

$$\sigma_{(m/m')r}^2 = \sigma_{(m/m')c}^2 + \sigma_{(m/m')air}^2$$

$\sigma_{(m/m')c}$: Relative error for $^{36}\text{Ar}/^{38}\text{Ar}$ ratio of a sample when hot blank is corrected

$\sigma_{(m/m')air}$: Relative error for $^{36}\text{Ar}/^{38}\text{Ar}$ ratio determined in air standard analysis

$\sigma_{(m/m')r}$: Relative error for $^{36}\text{Ar}/^{38}\text{Ar}$ ratio in a sample when mass discrimination is corrected

APPENDIX II

<Calculation of apparent radiogenic ^{40}Ar >

$$\text{App.Rad. } ^{40}\text{Ar} = \text{Total } ^{40}\text{Ar} (1 - R_o' / R)$$

$$R_o' = R_A (1 + 4\delta)$$

$$\delta = (r / r_A - 1) / 2$$

App.Rad. ^{40}Ar : Concentration of apparent radiogenic ^{40}Ar

Total ^{40}Ar : Concentration of total ^{40}Ar

R_o' : Apparent initial $^{40}\text{Ar}/^{36}\text{Ar}$ ratio of a sample estimated from $^{38}\text{Ar}/^{36}\text{Ar}$ ratio

R : $^{40}\text{Ar}/^{36}\text{Ar}$ ratio determined of a sample

R_A : $^{40}\text{Ar}/^{36}\text{Ar}$ ratio of the present-day atmosphere

δ : Degree of mass fractionation per a unit of mass difference

r : $^{38}\text{Ar}/^{36}\text{Ar}$ ratio determined of a sample

r_A : $^{38}\text{Ar}/^{36}\text{Ar}$ ratio of the present-day atmosphere

<Error for calculation of apparent radiogenic ^{40}Ar >

$$\sigma_{\text{APP. AR}}^2 = [\sigma_X^2 + \frac{A_c^2}{(1 - A_c)^2} (\sigma_R^2 + \sigma_{R_o'}^2)]$$

$$\sigma_{R_o'} = [2 r \sigma_r / (2 r - r_A)]$$

$$A_c = [(2 r - r_A) R_A / r_A R]$$

$\sigma_{\text{APP. AR}}$: Error for calculation of apparent radiogenic ^{40}Ar

σ_X : Error for total ^{40}Ar analysis (4%)

σ_R : Error for $^{40}\text{Ar}/^{36}\text{Ar}$ ratio analysis

$\sigma_{R_o'}$: Error for estimation of apparent initial $^{40}\text{Ar}/^{36}\text{Ar}$ ratio

σ_r : Error for $^{38}\text{Ar}/^{36}\text{Ar}$ ratio analysis

A_c : Fraction of atmospheric ^{40}Ar

APPENDIX III

< Petrographic description of Ontake volcanic rocks >

1. PEAK-6'-1 (Sannoike Vol.)

Locality : 35° 54' 15" N, 137° 29' 25" E,
Sample : Olivine-bearing clinopyroxene-orthopyroxene-
hornblende andesite (lava flow)
Phenocryst : Pl > Hb > Opx > Cpx > Op >> Ol
Groundmass : Gl > Pl > Cpx > Opx > Op > Af > Hb
Texture : Hyalopilitic
All minerals are fresh.

2. PEAK-16 (Sannoike Vol.)

Locality : 35° 54' 04" N, 137° 31' 41" E
Sample : Olivine-bearing hornblende-clinopyroxene-ortho-
pyroxene andesite (lava flow)
Phenocryst : Pl > Opx > Cpx > Op > Hb > Ol
Groundmass : Pl > Gl > Opx > Cpx > Op
Texture : Intersertal
All minerals are fresh.

3. NITK-72 (Sannoike Vol.)

Locality : 35° 55' 07" N, 137° 32' 06" E
Sample : Hornblende-clinopyroxene-orthopyroxene andesite
(lava flow)
Phenocryst : Pl > Opx > Cpx > Op > Hb
Groundmass : Gl > Pl > Op > Opx > Cpx
Texture : Hyalopilitic
All minerals are fresh.

4. PEAK-145 (Yonnoike Vol.)

Locality : 35° 54' 37" N, 137° 29' 08" E
Sample : Olivine-hornblende-bearing clinopyroxene-ortho-
pyroxene andesite (lava flow)
Phenocryst : Pl > Opx > Cpx > Op >> Hb > Ol
Groundmass : Gl > Pl > Cpx > Op > Opx
Texture : Hyalopilitic
All minerals are fresh.

5. PEAK-146 (Yonnoike Vol.)

Locality : 35° 54' 31" N, 137° 29' 09" E
Sample : Clinopyroxene-orthopyroxene andesite (lava flow)
Phenocryst : Pl > Opx > Cpx > Op
Groundmass : Gl > Pl > Opx > Op > Cpx
Texture : Hyalopilitic
All minerals are fresh.

6. NIGRG-206 (Yonnoike Vol.)

Locality : 35° 55' 07" N, 137° 27' 29" E
Sample : Olivine-bearing orthopyroxene-clinopyroxene andesite
(lava flow)
Phenocryst : Pl > Cpx > Opx > Op >> Ol
Groundmass : Pl > Si > Cpx > Opx > Op
Texture : Pilotaxitic
All minerals are fresh.

7. PEAK-170 (Ichinoike Vol.)

Locality : 35° 53' 30" N, 137° 28' 44" E
Sample : Clinopyroxene-orthopyroxene andesite (lava flow)
Phenocryst : Pl > Opx > Cpx > Op
Groundmass : Gl > Pl > Opx > Op > Cpx
Texture : Hyalopilitic
All minerals are fresh.

8. NGRKW-20 (Ichinoike Vol.)

Locality : 35° 51' 08" N, 137° 27' 56" E
Sample : Hornblende-bearing olivine-orthopyroxene-clino-
pyroxene andesite (lava flow)
Phenocryst : Pl > Cpx > Opx > Ol > Op >> Hb
Groundmass : Pl > Gl > Opx > Cpx > Op
Texture : Intersertal
All minerals are fresh.

9. NITK-11 (Mamakodake Vol.)

Locality : 35° 54' 25" N, 137° 31' 17" E
Sample : Olivine-quartz-hornblende bearing orthopyroxene-
clinopyroxene andesite (Lava flow)
Phenocryst : Pl > Cpx > Opx > Op >> Hb > Qz > Ol
Groundmass : Pl > Si > Cpx > Opx > Gl > Op
Texture : Intersertal
All minerals are fresh.

10. NITK-134 (Mamakodake Vol.)

Locality : 35° 55' 16" N, 137° 31' 18" E
Sample : Clinopyroxene-orthopyroxene andesite (lava flow)
Phenocryst : Pl > Opx > Op > Cpx
Groundmass : Gl > Pl > Op > Opx > Cpx > Tr > Bi
Texture : Hyalopilitic
All minerals are fresh.

11. PEAK-180 (Kusakidani Vol.)

Locality : 35° 54' 06" N, 137° 29' 07" E
Sample : Olivine-bearing orthopyroxene-clinopyroxene andesite

(lava flow)
Phenocryst : Pl > Cpx > Opx > Op >> Ol
Groundmass : Gl > Pl > Opx > Op
Texture : Hyalopilitic
All minerals are fresh.

12. PEAK-185 (Kusakidani Vol.)

Locality : 35° 54'15"N, 137° 29'13"E
Sample : Clinopyroxene-orthopyroxene andesite
(dense-welded agglutinate)
Phenocryst : Pl > Opx > Cpx > Op >> Ap
Groundmass : Gl > Pl > Op > Opx
Texture : Hyalopilitic
All minerals are fresh.

13. PEAK-178 (Okunoin Vol.)

Locality : 35° 53'04"N, 137° 29'01"E
Sample : Orthopyroxene-bearing clinopyroxene-olivine andesite
(lava flow)
Phenocryst : Pl > Ol > Cpx > Op >> Opx
Groundmass : Gl > Pl > Cpx > Op > Opx > Tr > Ol > Bi
Texture : Hyalopilitic
All minerals are fresh.

14. TNHR-09 (Okunoin Vol.)

Locality : 35° 52'36"N, 137° 29'25"E
Sample : Orthopyroxene-clinopyroxene andesite
(dense-welded agglutinate)
Phenocryst : Pl > Cpx > Opx > Op >> Ap
Groundmass : Pl > Cpx > Opx > Op > Af > Tr
Texture : Pilotaxitic
All minerals are fresh.

15. AKGW-05 (Kongodo Vol.)

Locality : 35° 52'36"N, 137° 28'27"E
Sample : Clinopyroxene-orthopyroxene andesite (lava flow)
Phenocryst : Pl > Opx > Cpx > Op
Groundmass : Pl > Si > Cpx > Opx > Op > Af
Texture : Pilotaxitic
All minerals are fresh.

16. AKGW-06 (Kongodo Vol.)

Locality : 35° 52'37"N, 137° 28'33"E
Sample : Olivine-bearing hornblende-clinopyroxene-ortho-
pyroxene andesite (lava flow)
Phenocryst : Pl > Op > Opx > Cpx > Hb >> Ol

Groundmass : Gl > Pl > Cpx > Opx > Op > Af
Texture : Hyalopilitic
All minerals are fresh.

17. AKGW-10 (Kongodo Vol.)

Locality : 35° 52' 50"N, 137° 28' 43"E
Sample : Clinopyroxene-orthopyroxene-hornblende andesite
(dense-welded agglutinate)
Phenocryst : Pl > Hb > Op > Opx > Cpx > Ap
Groundmass : Gl > Pl > Opx > Cpx > Op > Ap
Texture : Hyalopilitic
All minerals are fresh.

18. NITK-116 (Kongodo Vol.)

Locality : 35° 53' 48"N, 137° 32' 38"E
Sample : Clinopyroxene-orthopyroxene andesite (lava flow)
Phenocryst : Pl > Opx > Cpx > Op
Groundmass : Gl > Pl > Op > Opx > Cpx
Texture : Hyalopilitic
All minerals are fresh.

19. NGRG-28-3 (Nigorigo Vol.)

Locality : 35° 54' 31"N, 137° 27' 49"E
Sample : Orthopyroxene-clinopyroxene andesite (lava flow)
Phenocryst : Pl > Op > Cpx > Opx
Groundmass : Gl > Pl > Cpx > Opx > Op > Af
Texture : Hyalopilitic
All minerals are fresh.

20. NGRG-28-4 (Nigorigo Vol.)

Locality : 35° 54' 31"N, 137° 27' 50"E
Sample : Olivine bearing orthopyroxene-clinopyroxene andesite
(lava flow)
Phenocryst : Pl > Cpx > Opx > Op >> Ol
Groundmass : Pl > Si > Cpx > Opx > Op > Af
Texture : Pilotaxitic
All minerals are fresh.

21. NGRG-106 (Nigorigo Vol.)

Locality : 35° 56' 33"N, 137° 25' 47"E
Sample : Orthopyroxene-bearing olivine-clinopyroxene andesite
(lava flow)
Phenocryst : Pl > Cpx > Ol >> Opx > Op
Groundmass : Pl > Cpx > Opx > Si > Op
Texture : Pilotaxitic
All minerals are fresh.

22. NGRG-118 (Nigorigo Vol.)

Locality : 35° 54'06"N, 137° 28'04"E
Sample : Orthopyroxene-clinopyroxene andesite (lava flow)
Phenocryst : Pl > Cpx > Opx > Op
Groundmass : Pl > Si > Cpx > Opx > Gl > Op
Texture : Intersertal
All minerals are fresh.

23. SMKRSW-13 (Miureyama Lava)

Locality : 35° 52'11"N, 137° 27'11"E
Sample : Hornblende-bearing clinopyroxene-orthopyroxene
dacite (lava flow)
Phenocryst : Pl > Opx > Cpx > Op >> Hb
Groundmass : Gl > Pl > Opx > Cpx > Op > Tr > Bi
Texture : Hyalopilitic (Glass is devitrified.)
All minerals are fresh.

24. SMKRSW-19 (Miureyama Lava)

Locality : 35° 52'46"N, 137° 26'56"E
Sample : Clinopyroxene-hornblende-orthopyroxene dacite
(lava flow)
Phenocryst : Pl > Opx > Op > Hb > Cpx
Groundmass : Pl > Si > Op > Opx > Af > Bi
Texture : Pilotaxitic (with felsitic spots)
All minerals are fresh.

25. SMKRSW-20 (Miureyama Lava)

Locality : 35° 52'34"N, 137° 27'00"E
Sample : Clinopyroxene-hornblende-orthopyroxene dacite
(lava flow)
Phenocryst : Pl > Opx > Op > Hb >> Cpx
Groundmass : Gl > Pl > Si > Op > Opx > Bi
Texture : Hyalopilitic (Glass is devitrified.)
All minerals are fresh.

26. NIGRG-240 (Nigoridaki Pyroclastic Flow)

Locality : 35° 56'52"N, 137° 24'12"E
Sample : Clinopyroxene-bearing orthopyroxene-hornblende
rhyolite (Essential fragment in pyroclastic flow)
Phenocryst : Pl > Hb > Opx > Op > Cpx
Groundmass : Gl > Pl > Opx > Cpx > Op
Texture : Hyalopilitic
All minerals are fresh.

27. NGRKW-25 (Yunotani Lava)

Locality : 35° 52' 29"N, 137° 27' 53"E
Sample : Orthopyroxene-hornblende rhyolite (lava flow)
Phenocryst : Pl > Hb > Opx > Op >> Ap
Groundmass : Gl > Pl > Si > Opx > Op > Cpx
Texture : Hyalopilitic (Glass is devitrified.)
All minerals are fresh.

28. NIGRG-28-1 (Yunotani Lava)

Locality : 35° 54' 29"N, 137° 27' 40"E
Sample : Orthopyroxene-hornblende rhyolite (lava flow)
Phenocryst : Pl > Hb > Opx > Op >> Zr
Groundmass : Gl >> Pl > Opx > Bi > Ap
Texture : Hyaline
All minerals are fresh.

29. NIGRIG-127 (Shintani Lava)

Locality : 35° 53' 56"N, 137° 27' 47"E
Sample : Clinopyroxene-orthopyroxene dacite (lava flow)
Phenocryst : Pl > Opx > Op > Cpx
Groundmass : Pl > Tr > Opx > Op > Af > Bi
Texture : Pilotaxitic
All minerals are fresh.

30. 800N-08 (Pm-I Pumice Fall)

Locality : 35° 53' 39"N, 137° 32' 57"E
Sample : Zircon-bearing biotite-orthopyroxene-hornblende
rhyolitic pumice
Phenocryst : Pl > Hb > Opx > Bi > Op >> Zr
Groundmass : Gl

31. OHTK-25 (Mikasayama Lava)

Locality : 35° 51' 55"N, 137° 31' 03"E
Sample : Olivine-bearing hornblende-clinopyroxene-ortho-
pyroxene andesite (lava flow)
Phenocryst : Pl > Opx > Cpx > Op > Hb >> Ol
Groundmass : Gl > Pl > Opx > Cpx > Op > Tr > Bi
Texture : Hyalopilitic (Glass is devitrified.)
All minerals are fresh.

32. MZGCGW-09 (Mikasayama Lava)

Locality : 35° 51' 44"N, 137° 30' 40"E
Sample : Olivine-bearing orthopyroxene-clinopyroxene andesite
(lava flow)
Phenocryst : Pl > Cpx > Opx > Op >> Ol

Groundmass : Gl > pl > Opx > Cpx > Op > Tr > Bi > Si
Texture : Hyalopilitic (Glass is devitrified.)
Orthopyroxene is slightly altered to mica minerals.

33. MZGCGW-05 (Mizoguchigawa Lava)

Locality : 35° 51' 32"N, 137° 30' 37"E
Sample : Clinopyroxene-orthopyroxene andesite (lava flow)
Phenocryst : Pl > Opx > Cpx > Op
Groundmass : Gl > Pl > Opx >> Cpx >>> Bi
Texture : Hyalopilitic
All minerals are fresh.

34. ASH-27 (Nunokawa Lava)

Locality : 35° 56' 07"N, 137° 28' 38"E
Sample : Clinopyroxene-olivine basic andesite (lava flow)
Phenocryst : Pl > Ol > Op > Cpx
Groundmass : Pl > Cpx > Op > Ol > Af
Texture : Pilotaxitic
All minerals are fresh.

35. TKN-51 (Nunokawa Lava)

Locality : 35° 57' 21"N, 137° 28' 48"E
Sample : Clinopyroxene-bearing olivine basic andesite
(lava flow)
Phenocryst : Pl > Ol > Op >> Cpx
Groundmass : Pl > Cpx > Op > Ol
Texture : Intergranular
All minerals are fresh.

36. MZGCGW-03 (Suzugasawa Lava)

Locality : 35° 51' 05"N, 137° 30' 49"E
Sample : Orthopyroxene-clinopyroxene andesite (lava flow)
Phenocryst : Pl > Cpx > Opx > Op
Groundmass : Gl > Pl > Opx > Cpx > Op > Af > Bi
Texture : Hyalopilitic
All minerals are fresh.

37. TKN-29 (Sengendaru Lava)

Locality : 35° 56' 39"N, 137° 30' 22"E
Sample : Olivine-bearing hornblende-clinopyroxene-ortho-
pyroxene andesite (lava flow)
Phenocryst : Pl > Opx > Cpx > Op > Hb >> Ol
Groundmass : Gl > Pl > Opx > Cpx > Op > Bi
Texture : Hyalopilitic
All minerals are fresh.

38. TKN-46 (Sengendaru Lava)

Locality : 35° 56'28"N, 137° 30'24"E
Sample : Hornblende-bearing olivine-orthopyroxene-clinopyroxene andesite (lava flow)
Phenocryst : Pl > Cpx > Opx > Op > Ol >> Hb
Groundmass : Gl > Pl > Opx > Cpx > Op
Texture : Hyalopilitic
All minerals are fresh.

39. TCUR-22 (Kuragoehara Lava)

Locality : 35° 50'53"N, 137° 25'18"E
Sample : Hornblende andesite (lava flow)
Phenocryst : Pl > Hb > Op
Groundmass : Gl > Pl > Cpx > Opx > Op
Texture : Hyalopilitic (Glass is devitrified.)
Groundmass is very slightly altered to mica minerals.

40. TCUR-33 (Kuragoehara Lava)

Locality : 35° 51'20"N, 137° 25'57"E
Sample : Hornblende andesite (lava flow)
Phenocryst : Pl > Hb > Op
Groundmass : Gl > Pl > Cpx > Opx > Op
Texture : Hyalopilitic (Glass is devitrified.)
Groundmass is very slightly altered to mica minerals.

41. NGRKW-73 (Kuragoehara Lava)

Locality : 35° 49'11"N, 137° 29'11"E
Sample : Hornblende andesite (lava flow)
Phenocryst : Pl > Hb > Op
Groundmass : Gl > Pl > Cpx > Opx > Op
Texture : Hyalopilitic (Glass is devitrified.)
Groundmass is very slightly altered to mica minerals.

42. OHTK-18 (Kuragoehara Lava)

Locality : 35° 50'07"N, 137° 32'50"E
Sample : Hornblende andesite (lava flow)
Phenocryst : Pl > Hb > Op
Groundmass : Gl > Pl > Cpx > Opx > Op
Texture : Hyalopilitic
All minerals are fresh.

43. SZGSW-06 (Kuragoehara Lava)

Locality : 35° 50'50"N, 137° 30'05"E
Sample : Hornblende andesite (lava flow)
Phenocryst : Pl > Hb > Op

Groundmass : Gl > Pl > Cpx > Opx > Op
Texture : Hyalopilitic (Glass is devitrified.)
Groundmass is very slightly altered to mica minerals.

44. ASH-20 (Kuragoehara Lava)

Locality : 35° 56' 22"N, 137° 28' 38"E
Sample : Olivine-hornblende-bearing andesite (lava flow)
Phenocryst : Pl > Op > Hb > Ol
Groundmass : Pl > Cpx > Opx > Si > Op
Texture : Pilotaxitic
All minerals are fresh.

45. TKN-41 (Kuragoehara Lava)

Locality : 35° 56' 36"N, 137° 31' 05"E
Sample : Clinopyroxene-orthopyroxene andesite (lava flow)
Phenocryst : Pl > Cpx > Opx > Op
Groundmass : Pl > Cpx > Opx > Op
Texture : Pilotaxitic
All minerals are fresh.

46. HNTN-36 (Makuiwagawa Lava)

Locality : 35° 53' 29"N, 137° 26' 24"E
Sample : Orthopyroxene-bearing olivine-clinopyroxene basaltic andesite (lava flow)
Phenocryst : Pl > Cpx > Ol > Op >> Opx
Groundmass : Pl > Cpx > Op > Ol
Texture : Intergranular
All minerals are fresh.

47. TKN-30 (Makuiwagawa Lava)

Locality : 35° 56' 23"N, 137° 30' 21"E
Sample : Clinopyroxene-bearing olivine basic andesite (lava flow)
Phenocryst : Pl > Ol > Op >> Cpx
Groundmass : Pl > Cpx > Op > Ol > Af
Texture : Intergranular
All minerals are fresh.

48. TCUR-14 (Hakodani Lava)

Locality : 35° 52' 33"N, 137° 26' 23"E
Sample : Hornblende-orthopyroxene dacite (lava flow)
Phenocryst : Pl > Opx > Hb > Op
Groundmass : Pl > Opx > Si > Op > Bi > Ap
Texture : Pilotaxitic
All minerals are fresh.

49. TCUR-09 (Shiranunodani Lava)

Locality : 35° 51' 36"N, 137° 25' 35"E
Sample : Clinopyroxene-orthopyroxene-hornblende andesite
(Lava flow)
Phenocryst : Pl > Hb > Opx > Cpx > Op >> Ap
Groundmass : Pl > Opx > Op > Si > Bi
Texture : Pilotaxitic
All minerals are fresh.

50. HNTN-16 (Shiranunodani Lava)

Locality : 35° 53' 42"N, 137° 26' 25"E
Sample : Hornblende-orthopyroxene-clinopyroxene andesite
(Lava flow)
Phenocryst : Pl > Cpx > Opx > Hb > Op
Groundmass : Pl > Opx > Op > Af > Bi > Tr
Texture : Pilotaxitic
All minerals are fresh.

51. HNTN-12 (Tsuchiuragawa Lava)

Locality : 35° 53' 34"N, 137° 24' 57"E
Sample : Clinopyroxene basic andesite (Lava flow)
Phenocryst : Pl > Cpx > Op
Groundmass : Pl > Si > Cpx > Op > Af >> Bi
Texture : Felty
All minerals are fresh.

52. YKW-13 (Tsuchiurazawa Lava)

Locality : 35° 53' 39"N, 137° 32' 07"E
Sample : Hornblende-orthopyroxene-clinopyroxene andesite
(Lava flow)
Phenocryst : Pl > Opx > Cpx > Hb > Op
Groundmass : Pl > Opx > Cpx > Op > Bi
Texture : Pilotaxitic
All minerals are fresh.

53. TCUR-01 (Tsuchiurazawa Lava)

Locality : 35° 51' 20"N, 137° 24' 06"E
Sample : Olivine-clinopyroxene basaltic andesite (Lava flow)
Phenocryst : Pl > Cpx > Ol > Op
Groundmass : Pl > Gl > Ol > Cpx > Op
Texture : Intersertal
All minerals are fresh.

Pl : Plagioclase,	Cpx : Clinopyroxene,	Opx : Orthopyroxene,
Ol : Olivine,	Hb : Hornblende,	Bi : Biotite,
Qz : Quartz,	Ap : Apatite,	Zr : Zircon,
Gl : Glass,	Tr : Tridymite,	Af : Alkali feldspar,
Op : Opaque mineral,	Si : Silica mineral	

< Description of Aso pyroclastic flows >

64AS210A (Aso-4)

Locality : 32° 50' 18"N, 131° 14' 58"E. Abandoned quarry at roadside 300m southeast of Katayama, Takamori-machi, Aso-gun, Kumamoto-ken.

Sample : Black essential glass from lens and matrix of dense vitric welded tuff (pyroxene hornblende dacite). Accidental lithic fragments, included a few percent in the matrix, were picked out.

Field occurrence : Ca.8m section of welded tuff of Aso-4B pyroclastic flow, upper 3m partially welded and lower 5m welded to homogeneously dense black glass, lies on non-welded Aso-4A pyroclastic flow. The sample is from lower dense portion of Aso-4B.

Phenocrysts : Small amount of plagioclase, hornblende, orthopyroxene, clinopyroxene, magnetite. (Plagioclase content is ca.8%.)

Matrix : Pale brown clear glass. No clay minerals.

81KC664 (Aso-4)

Locality : 32° 51' 04"N, 130° 59' 04"E. Roadcut at the top of Nanamagari, Kugino-machi, Aso-gun, Kumamoto-ken.

Sample : Whole rock of obsidian block (rhyolite) in lithic breccia of Aso-4.

Field occurrence : At this locality, Aso-4 is represented only by the lithic breccia, a few meters thick, lying on Aso-2 welded tuff. Blocks in the breccia are mainly of accidental, pyroxene andesite of pre-Aso volcanics and basement plutonic and sedimentary rocks, with small amount of fresh obsidian as analyzed

specimen. The obsidian blocks are probably essential material by their freshness, mineralogy and chemistry. Sandy matrix is mostly composed of essential material of Aso-4, phenocrystic plagioclase and hornblende and minor amount of white pumice.

Phenocrysts : Small amount of plagioclase, pyroxene, magnetite.
(Plagioclase content is ca.5%.)

Matrix : Colorless clear glass with small amount of crystallite.
No clay minerals.

61IK118AP (Aso-4)

Locality : 33° 02'00"N, 131° 34'45"E. Road cut 500m north of Tabarudono near Akane River, Chitose-machi, Ono-gun, Oita-ken.

Sample : Devitrified matrix of pumice block, partially collapsed by welding and intensely altered by vapor phase crystallization. Very fragile as collapsible under fingers. The sample is collected from vapor phase crystallized parts as much as possible.

Field occurrence : A section, 16m thick, of Aso-4A welded tuff ; in ascending order; 5m : dense, devitrified dark-colored welded tuff, 5m : less dense welded tuff with obsidian lenses in gray devitrified matrix, 3m : partially welded gray devitrified welded tuff, 3m : zone of vapor phase crystallization(analyzed sample collected). This zone gradates into vitric zone composed of dark-colored, partially welded vitric tuff, laterally at the same height but probably away from the side contact to the valley wall.

Phenocrysts : Small amount of plagioclase, hornblende, orthopyroxene, magnetite. (Plagioclase content is 5-8%.)

Matrix : Very porous cluster of microspherulitic aggregate of accicular sanidine and granular cristobalite. No clay minerals.

64TD232 (Aso-3)

Locality : 32° 51'33"N, 131° 17'12"E. Roadcut 500m northeast of Nagano, Takamori-machi, Aso-gun, Kumamoto-ken.

Sample : Nearly non-porphyritic, essential obsidian lens in purplish-gray-colored, dense welded tuff (px high-K dacite) of Aso-3A pyroclastic flow.

Field occurrence : A few to 10m thick welded tuff layer covers on Miocene Sobosan Volcanic Complex.

Phenocrysts : Small amount of plagioclase, clinopyroxene, orthopyroxene and magnetite. (Plagioclase content is ca.5%.)

Matrix : Clear pale brown glass. No clay minerals.

78TM200 (Aso-3)

Locality : 32° 48'18"N, 131° 12'07"E. Roadside at the hair-pin corner of Rt.325 1km west of Kigo, Takamori-machi, Aso-gun, Kumamoto-ken.

Sample : Nearly non-porphyritic black obsidian lens in red-colored dense welded tuff (high-K dacite) of Aso-3A pyroclastic flow deposit.

Field occurrence : Exposed section of Aso-3 pyroclastic flow deposit here is ca.16m thick. In ascending order ; Aso-3A ; bottom 3m on preceding air-fall pumice bed : dense vitric welded tuff, lenses and matrix similarly converted to homogeneous black glass. 6m : dense welded tuff of red matrix and markedly flattened black lenses (analyzed specimen). 4m : dense, red-

colored, mostly devitrified welded tuff. Two pulled-apart gaps, nearly vertical to the foliation plane of the welded tuff, opened in the welded tuff and essential lenses (KWTM-1) were squeezed-out into the gaps from their walls. Throughout the section of Aso-3A secondary flowage structure is conspicuous. Aso-3B ; 1.5m : Mostly devitrified dense welded tuff of nearly non porphyritic andesite. Aso-3C ; 1.5m : agglutinated deposit of dark-red-colored blocks of plagioclase-porphyritic andesite, and matrix of same kind ash and some accidental blocks.

Phenocrysts : Small amount of plagioclase, clinopyroxene, orthopyroxene, magnetite. (Plagioclase content is ca.5%.)

Matrix : Pale brown glass. No clay minerals.

KWTM-1 (Aso-3)

Locality : 32° 48' 18"N, 131° 12' 07"E. Roadside 200m at the hair-pin corner of Rt.325 1km west of Kigo (same as that of 78TM200), Takamori-machi, Aso-gun, Kumamoto-ken.

Sample : An essential lens squeezed-out from the wall of pulled-apart tension gaps in dense welded tuff of Aso-3A. It is dark-red-colored, devitrified, nearly non porphyritic high-K dacite.

Field occurrence : See the description of 78TM200.

Phenocrysts : Small amount of plagioclase, clinopyroxene, orthopyroxene, magnetite. (Plagioclase content is ca.5%.)

Matrix : Very fine-grained aggregate of felsic minerals. No clay minerals.

69AS396A3 (Aso-2)

Locality : 32° 58' 25"N, 131° 06' 37"E. Roadcut south of zoga-hana,

north rim of the Aso Caldera, at 670m height, Ichinomiya-machi, Aso-gun, Kumamoto-ken.

Sample : Whole rock of dense obsidian (welded tuff of non-porphyrific andesite) from base of Aso-2 pyroclastic flow deposit. It is completely welded to dense, black and homogeneous glass.

Field occurrence : More than 100m section of Aso-1 to Aso-2 in ascending order ; Aso-1 ; 6m+ : lithic breccia (horizon of 69-AS398A1). 8m+ : dense welded tuff. Aso-2/1 lava flow ; ca.10m: non-porphyrific andesite lava. Aso-2A ; 1.3m : dense obsidian (welded tuff of non-porphyrific andesite, sample horizon) with basal partially welded zone of 5cm thick. 30m : platy-jointed dense crystalline welded tuff with zone of coarse lenses near the top. ca.20m : talus cover. Aso-2B ; ca.30m : non-welded scoria flow deposit of non-porphyrific andesite.

Phenocrysts : Very small amount of plagioclase, pyroxene and magnetite. (Plagioclase content is ca.3%.)

Matrix : Brown glass. No clay minerals.

KWKC741 (Aso-2R)

Locality : 32° 54' 17"N, 130° 57' 15"E. Roadcut near Toge, Ozu-machi, Kikuchi-gun, Kumamoto-ken.

Sample : Whole rock of compact, gray, flow-banded, non-porphyrific andesite.

Field occurrence : A few meters section of irregularly jointed lava-looking body.

Phenocrysts : Very small amount of plagioclase, pyroxene and magnetite. (Plagioclase content is ca.1%)

Matrix : Very fine grained aggregate of felsic minerals and

microlite of pyroxene showing fluidal texture. No clay minerals.

72MF100 (Aso-2R)

Locality : 32° 48' 22"N, 130° 52' 53"E. Roadcut 500m west of Akita, Nishihara-machi, Kamimashiki-gun, Kumamoto-ken.

Sample : Whole rock of compact, gray, flow-banded, non-porphyritic andesite.

Field occurrence : Aso-2R here is ca.15m thick. Central compact layer is platy-jointed, blue-gray to purplish gray andesite (analyzed specimen) with surface and bottom radish brown clinker layers, each 1m thick. To the west, Aso-2R covers on Aso-1 welded tuff with air-fall ash layers between. To the east, surface clinker of Aso-2R is overlain and stuck by the bottom of densely welded Aso-2A, which is 1m thick and, in turn, covered by weakly welded, oxidized Aso-2B scoria flow deposit of more than 10m thick.

Phenocrysts : Very small amount of plagioclase, pyroxene, magnetite. (Plagioclase content is ca.1%.)

Matrix : Very fine grained aggregate of felsic minerals and microlite of pyroxene showing fluidal texture. No clay minerals.

67MF22L1 (Aso-1)

Locality : 32° 44' 47"N, 130° 52' 22"E. Abandoned quarry at the roadside, 200m east of a bridge south of Tonoue, Mifune-machi, Kamimashiki-gun, Kumamoto-ken.

Sample : A large obsidian lens, 20cm in length, in gray dense

vitric welded tuff of Aso-1 pyroclastic flow deposit.

Field occurrence : Dense welded tuff, more than 5m thick, is exposed.

Phenocryst : Small amount of plagioclase, pyroxene, magnetite.
(Plagioclase content is ca.6%.)

Matrix : Pale brown glass. No clay minerals.

69AS398A1 (Aso-1)

Locality : 32° 58' 17"N, 131° 06' 32"E. Roadcut south of zoga-hana, north rim of the Aso Caldera, at 630m high, Ichinomiya-machi, Kumamoto-ken.

Sample : A large, devitrified, gray, essential lens in lithic breccia of Aso-1 (high-K dacite).

Field occurrence : More than 100m section of Aso-1 to Aso-2 (see the description of 69AS396A3, Aso-2). The bottom of Aso-1 is concealed. Exposed lower, 6m thick section of Aso-1 is coarse, unconsolidated, accidental lithic breccia with small amount of essential lenses(analyzed specimen). The upper 8m thick section of Aso-1 is characteristic alternation of dense welded tuff, 1 to 2m thick, and unconsolidated lithic breccia, 20 to 70cm thick.

Phenocryst : Small amount of plagioclase, pyroxene, magnetite.
(Plagioclase content is ca.5%.)

Matrix : Very fine-grained aggregate of felsic minerals. Tridymite fills mialolitic cavities. No clay minerals.

[Description of Aso and nearby coeval volcanic rocks except for pyroclastics]

Sample name	Latitude	Longitude	Ol	Phenocrysts			Rock name
				Cpx	Opx	Hb	
Sawatsuno Lava	KWK736	32° 53' 40" N 130° 59' 40" E	*	*	*	*	opx-cpx-dacite (glassy lava)
Vol. lab. Lava	KWK740	32° 52' 15" N 130° 59' 39" E	*	*	+	*	bi-rhyolite (obsidian)
Hakusui Vol.	KWAS610	32° 51' 31" N 131° 04' 49" E	*	*	*	*	opx-cpx-dacite (compact lava)
	KWAS603A	32° 50' 38" N 131° 05' 35" E	*	*	*	*	opx-cpx-dacite (compact lava)
Hontsuka Vol.	KWAS609B	32° 56' 38" N 131° 03' 55" E	*	*	*	*	hb-bg cpx-opx-dacite (glassy lava)
Tochinoki Vol.	KWK734	32° 52' 06" N 130° 59' 39" E	*	*	*	+	opx-cpx-andesite (compact lava)
Ayugaerinotaki Lava	72MF304	32° 51' 58" N 130° 59' 40" E	*	+	*	*	opx-ol-cpx-basalt (very compact lava)
	KWK737	32° 51' 57" N 130° 59' 40" E	*	+	*	*	opx-ol-cpx-basalt (very compact lava)
	KWK738	32° 51' 59" N 130° 59' 41" E	*	+	*	*	opx-ol-cpx-basalt (very compact lava)
Omine Vol.	MF72A1	32° 49' 33" N 130° 54' 34" E	*	*	*	*	cpx-opx-hb-andesite (glassy lava)
	MF72B2	32° 49' 33" N 130° 54' 34" E	*	*	*	*	cpx-opx-hb-andesite (compact lava)
Nekodake Vol.	82AS707L1	32° 52' 00" N 131° 08' 23" E	+	++	++	+	ol-opx-cpx-andesite (compact lava)
	82AS785B	32° 52' 46" N 131° 08' 59" E	++	++	++	+	opx-ol-cpx-andesite (compact block from dike)
	82AS786T1	32° 52' 48" N 131° 08' 59" E	+	++	++	+	opx-cpx-andesite (compact block from dike)
	KW81NK6	32° 52' 38" N 131° 10' 07" E	*	++	+	*	ol-opx-cpx-andesite (compact lava)
	NK-103	32° 52' 51" N 131° 08' 54" E	+	++	++	*	opx-cpx-andesite (compact block from dike)
Aso-2/1 Lava	67TD463	32° 54' 08" N 131° 19' 47" E	*	*	*	*	opx-cpx-andesite (compact lava)
	KWAS612	32° 55' 13" N 131° 08' 00" E	*	+	*	*	opx-ol-cpx-andesite (porous lava)
Akai Vol.	KWMF221	32° 44' 50" N 130° 47' 28" E	*	*	*	*	opx-cpx-andesite (very compact lava)
	KWMF222	32° 45' 15" N 130° 49' 05" E	*	*	*	*	opx-cpx-andesite (very compact lava)

Ol : olivine, Cpx : clinopyroxene, Opx : orthopyroxene, Bi : biotite, Hb : hornblende, Mt : magnetite, P. : plagioclase.
 +++ : 30~10 %, ++ : 10~3 %, + : 3~1 %, * : less than 1 %
 In every sample, all minerals are fresh.

References

- Ando, A., Mita, N. and Matsumoto, A. (1989) 1987 complication of K_2O concentrations in seventeen GSJ rock reference samples, "Igneous rock series". Bull. Geol. Surv. Japan, 40, 19-45.
- Bloom, A.L., Broecker, W.S., Chappell, J.M.A., Matthews, R.K. and Mesolelia, K.J. (1974) Quaternary sea level fluctuations on a tectonic coast : New $^{230}Th/^{234}U$ dates from the Huon Peninsula, New Guinea. Quaternary Research, 4, 185-205.
- Cassignol, C. and Gillot, P. Y. (1982) Range and effectiveness of unspiked potassium-argon dating : experimental groundwork and applications. Numerical dating in stratigraphy. ed. by Odin, G. S., Wiley and Sons, Chichester, 159-179.
- Collaborative Research Group for Yatsugatake ed. (1988) Quaternary system around Mts. Yatsugatake. Monograph Assoc. Geol. Collab. Japan, 34, 179-190. (in Japanese with English abstract).
- Dalrymple, G.B. (1968) Potassium-argon ages of Recent rhyolites of the Mono and Inyo Craters, California. Earth Planet. Sci. Lett., 3, 289-298.
- Dalrymple, G.B. (1969) $^{40}Ar/^{36}Ar$ analyses of historic lava flows. Earth Planet. Sci. Lett., 6, 47-55.
- Dodson, M.H. (1978) A linear method for second-degree interpolation in cyclical data collection. J. Phys. E : Sci. Instrum., 11, 296.
- Endo, K., Fukuoka, T., Miyaji, N. and Sumita, M. (1986) Recent progress in tephra study. Bull. Volcanol. Sci. Japan. 30, S237-S266. (in Japanese with English abstract).

- Flish, M. (1982) Potassium - argon analysis. Numerical dating in stratigraphy. ed. by Odin, G.S., Wiley and Sons, Chichester, 154-158.
- Fukuoka, T. and Kigoshi, K. (1974) Discordant ^{106}Ag -ages and the uranium and thorium distribution between zircon and host rocks. *Geochem. J.*, 8, 117-122.
- Fukuoka, T. and Terada, H. (1984) Age determination of tephras by the ionium and fission track methods. Conservation science and cultural-natural science on archaeological objects. ed. by Watanabe, N., 929-939. (in Japanese).
- Gillot, P. Y., Labeyrie, J., Laj, C., Valladas, G., Guerin, G., Poupeau, G. and Delibrias, G. (1979) Age of the Laschamp Paleomagnetic excursion revisited. *Earth Planet. Sci. Lett.*, 42, 444-450.
- Gillot, P.Y., Chiesa, S., Pasquare, G. and Vezzoli, L. (1982) < 3300-yr. K-Ar dating of the volcano-tectonic horst of the Isle of Ischia, Gulf of Naples. *Nature*, 299, 242-245.
- Gladney, E.S. and Burns, C.E. (1983) 1982 compilation of elemental concentrations in eleven United States Geological Survey rock standards. *Geostandard Newsletter*, 7, 3-226.
- Hall, C. M. and York, D. (1978) K-Ar and $^{40}\text{Ar}/^{39}\text{Ar}$ age of the Laschamp geomagnetic polarity reversal. *Nature*, 274, 462-464.
- Hayakawa, Y. and Yui, M. (1989) Eruptive history of the Kusatsu Shirane Volcano. *The Quaternary Research*, 28, 1-17. (in Japanese with English abstract).
- Hayatsu and Carmichael (1970) K-Ar isochron method and initial argon ratios. *Earth Planet. Sci. Lett.*, 8, 71-76.
- Hurford, A.J. and Hammerschmidt, K. (1985) $^{40}\text{Ar}/^{39}\text{Ar}$ and K/Ar

dating of the Bishop and Fish Canyon Tuffs : Calibration ages for fission-track dating standards. *Chem. Geol.*, **58**, 23-32.

Itaya, T., Nagao, K., Nishida, H. and Ogata, K. (1984) K-Ar age determination of Late Pleistocene volcanic rocks. *J. Geol. Soc. Japan*, **90**, 899-909.

Itaya, T. and Nagao, K. (1988) K-Ar age determination of volcanic rocks younger than 1 Ma. *Mem. Geol. Soc. Japan*, No29, 143-161. (in Japanese with English abstract).

Jäger, E., Ji, C.W., Hurford, A.J., Xin, L.R., Hunziker, J.C. and Ming, L.D. (1985) BB-6 : A Quaternary age standard for K-Ar dating. *Chem. Geol.*, **52**, 275-279.

James, N.P., Mountjoy, E.W. and Omura, A. (1971) An early Wisconsin reef terrace at Barbados, West Indies, its climatic implications. *Geol. Soci. America Bull.*, **82**, 2011-2018.

Kaneko, T., Shimizu, S. and Itaya, T. (1989) K-Ar chronological study of the Quaternary volcanic activity in Shin-etsu Highland. *J. Min. Petr. Econ. Geol.*, **84**, 211-225. (in Japanese with English abstract).

Kaneoka, I. (1980) Rare gas isotopes and mass fractionation : An indicator of gas transport into or from a magma. *Earth Planet. Sci. Lett.*, **48**, 284-292.

Kaneoka, I., Mehnert, H., Zashu, S. and Kawachi, S. (1980) Pleistocene volcanic activities in the Fossa Magna region, central Japan - K-Ar age studies of the Yatsugatake volcanic chain. *Geochem. J.* **14**, 249-257.

Kobayashi, T. (1974) The petrochemical characteristics of Ontake volcano. *J. Coll. Lib. Arts, Toyama Univ.*, **7**, 71-85.

- Kobayashi, T. (1980) Ontake volcano and its activity of 1979. Excursion guide-book, The 3rd meeting IGU commission of field experiments in geomorphology, 151-156.
- Kobayashi, T. (1982) The Stratigraphy and its age of Ontake tephra layers. "Monbusho Kagaku-Kenkyuhi", Comprehensive research on the Shimosueyoshi Terrace, no.1, "Shimosueyoshi Terrace", 103-110. (in Japanese).
- Kobayashi, T. and Soya, T. (1981) Petrochemical changes of Ontake during the late Pleistocene. Abstracts of 1981 IAVCEI Symposium - Arc volcanism -, 182-183.
- Kobayashi, T., Omori, E. and Omori, S. (1975) Bull. Geol. Surv. Japan, 26, 497-512. (in Japanese with English abstract).
- Kobayashi, T., Takagi, N. and Fujii, T. (1977) Representative columnar section of Younger Ontake tephra layer, Ontake Volcano. "Karuishigaku Zasshi", no.4, 37-41. (in Japanese).
- Kozu, T. (1907) Report for the geological survey on Kiso-Ontake Volcano. "Sinsai Yobo Chousakai Hokoku", no.71, 71p. (in Japanese).
- Krummenacher, D. (1970) Isotope composition of argon in modern surface volcanic rocks. Earth Planet. Sci. Lett., 8, 109-117.
- Machida, H. (1973) Tephrochronology of coastal terraces and their tectonic deformation in South Kanto. J. Geography, 82, 53-76. (in Japanese with English abstract).
- Machida, H. (1977) "Kazanbai wa Kataru". Shoju Shobo, Tokyo, 209-296. (in Japanese).
- Machida, H. and Suzuki, M. (1971) Absolute ages of tephras and chronology of the late Pleistocene. Kagaku, 41, 263-270. (in

Japanese).

- Machida, H., Arai, F., Murata, A. and Hakamata, K. (1974) Correlation and Chronology of the middle Pleistocene tephra layers in South Kanto. *J. Geography*, **83**, 302-338. (in Japanese with English abstract).
- Machida, H. and Arai, F. (1979) Daisen Kurayoshi Pumice : Stratigraphy, chronology, distribution and implication to Late Pleistocene events in central Japan. *J. Geography*, **88**, 33-50. (in Japanese with English abstract).
- Machida, H., Arai, F. and Momose, M. (1985) Aso-4 ash : a wide-spread tephra and its implications to the events of Late Pleistocene in and around Japan. *Bull. Volcanol. Sci. Japan*, **30**, 49-70. (in Japanese with English abstract).
- Matsumoto, A. (1989) Improvement for determination of potassium in K-Ar dating. *Bull. Geol. Surv. Japan*, **40**, 65-70. (in Japanese with English abstract).
- Matsumoto, A., Uto, K. and Shibata, K. (1989) Argon isotopic ratios in historic lavas - Improvement of correction for the initial argon in K-Ar dating of young volcanic rocks -. *Mass Spectroscopy*, **37**, 353-363. (in Japanese with English abstract).
- McDougall, I., Polach, H.A. and Stipp, J.J. (1969) Excess radiogenic argon in young subaerial basalts from the Auckland volcanic field, New Zealand. *Geochim. Cosmochim. Acta*, **33**, 1485-1520.
- Mesolechia, K.J., Matthews, R.K., Broecker, W.S. and Thurber, D.L. (1969) The astronomical theory of climatic change : Barbados data. *J. Geology*, **77**, 250-274.
- Momose, K. and Kobayashi, K. (1972) Thermomagnetic properties of

ferromagnetic minerals extracted from the pumice-fall deposit "Pm-I" of the Ontake volcano. *J.Geomag. Geoelectr.*, 24, 127-131.

Nagao,K. and Itaya,T.(1988) K-Ar age determination. *Mem.Geol.Soc. Japan*, No.29, 5-21. (in Japanese with English abstract).

Nier,A.O. (1950) A redetermination of the relative abundances of the isotopes of carbon, nitrogen, oxygen, argon and potassium. *Phys. Rev.*, 77, 789-793.

Okaguchi,M. (1978) Fission track dating of the obsidians from pyroclastic flow deposits. *Bull. Volcanol. Soc. Japan*, 23, 231-240. (in Japanese with English abstract).

Omura,A., Kawai,S. and Tamanyu,S. (1988) Dating of volcanic products by the radioactive disequilibrium system between ^{238}U and ^{230}Th . *Bull. Geol. Surv. Japan*, 39, 559-572. (in Japanese with English abstract).

Ono,K. (1965) Geology of eastern Aso Caldera. *J. Geol. Soc. Japan*, 71, 541-553. (in Japanese with English abstract).

Ono,K., Kubota,A. and Ota,K. (1981) Aso volcano, in *Field Exc. Guid to Sakurajima, Kirishima and Aso volcanoes*, IAVCEI Symposium on Arc Volcanism, Japan, 33-50.

Ono,K., Shibata,K. and Watanabe,K. (1982) Nekodake volcano is not a central cone of Aso Caldera. *Bull. Volcanol. Soc. Japan*, 27, 155-156. (in Japanese).

Ono,K. and Watanabe,K. (1985) Geological Map of Aso Volcano at 1:50000. *Geol. Surv. Japan*, 8p. (in Japanese with English abstract).

Sakai,J. (1981) Late Pleistocene climatic changes in Central Japan. *J. Fac. Sci., Shinshu Univ.*, 16, 1-64.

- Samejima, T. (1958) Geology of Kiso-Ontake Volcano. "Kiso Kyoiku Kai", 19-96. (in Japanese).
- Shibata, H. (1963) Geology of the Kisodani district. With Geological Sheet Map at 1:50000, Nagano Forestry Department, 16p. (in Japanese).
- Shimizu, S., Yamazaki, M. and Itaya, T. (1988) K-Ar ages of Plio - Pleistocene volcanic rocks in the Ryohaku-Hida mountains area, Japan. Bull. Hiruzen Res. Inst., Okayama Univ. Sci., 14, 1-36. (in Japanese with English abstract).
- Steiger, R.H. and Jäger, E. (1977) Subcommittee on Geochronology : convention on the use of decay constants in geo- and cosmochronology. Earth Planet. Sci. Lett., 36, 359-362.
- Suto, S., Sakaguchi, K., Matsubayashi, O., Kamata, H., Katoh, K. and Yamamoto, T. (1984) Cooling history of the 1983 lava in Miyake-jima, Japan. Bull. Volcanol. Soc. Japan. 29, S253-S265. (in Japanese with English abstract).
- Takaoka, N. (1985) Study of volcanic gas by isotopic analysis of noble gas for eruption prediction by geochemical techniques. Bull. Volcanol. Soc. Japan. 30, 185-195 (in Japanese with English abstract).
- Takaoka, N., Konno, K., Oba, Y. and Konda, T. (1989) K-Ar dating of lavas from Zao Volcano, North-eastern Japan. J. Geol. Soc. Japan, 95, 157-170. (in Japanese with English abstract).
- Takemoto, H., Momoshe, M., Hirabayashi, K. and Kobayashi, T. (1987) Stratigraphy and correlation of the Yonger Ontake tephra group - an implication to the Late Pleistocene chronology in central Japan. The Quaternary Research, 25, 337-352. (in Japanese with English abstract).

- Tamanyu, S. (1979) Fission track age determination by using volcanic glass. Report in short time symposium for Fission track detection method. Nuclear Reactor Lab. Kyoto Univ., 43-44. (in Japanese).
- Togashi, S. and Matsumoto, E. (1987) Radiocarbon dating methods for the samples of 40000 to 50000 years B.P. using benzene-liquid scintillation. Bull. Geol. Surv. Japan, 39, 525-535. (in Japanese with English abstract).
- Tsukui, M., Nishido, H. and Nagao, K. (1985) K-Ar ages of the Hiruzen Volcano Group and the Daisen Volcano. J. Geol. Soc. Japan, 91, 279-288 (in Japanese with English abstract).
- Uchida, T. and Hirao, Y. (1987) Preparation of sample and standard solutions by mass. Bunseki, 93-96. (in Japanese).
- Uchiumi, S. and Shibata, K. (1980) Errors in K-Ar age determination. Bull. Geol. Surv. Japan, 31, 267-273. (in Japanese with English abstract).
- Watanabe, K. and Ono, K. (1969) Geology of the vicinity of Omine on the western flank of the Aso caldera. J. Geol. Soc. Japan, 75, 365-374. (in Japanese with English abstract).
- Yamada, N. and Kobayashi, T. (1988) Geology of the Ontakesan district. With Geological Sheet Map at 1:50000, Geol. Surv. Japan, 136p. (in Japanese with English abstract).

同位体分別補正法による第四紀火山岩のK-Ar年代測定

- 測定法の開発と御嶽・阿蘇火山への応用 -

松 本 哲 一

約1万年前に噴出した火山岩まで適応可能なK-Ar年代測定法を開発し、K-Ar法と ^{14}C 法を併用することによって、第四紀火山の現世までの噴火史を系統的に論ずることが可能となることを目標とした。

測定法の開発では、現世に噴出した歴史溶岩類のアルゴン同位体比を分析し、大部分の試料のアルゴン同位体比が、現在の大気アルゴン同位体比からの同位体分別直線上に散在していることを見い出した。この結果を普遍的なものと仮定し、年代未知試料に対するアルゴン同位体比分析では、初生 $^{40}\text{Ar}/^{36}\text{Ar}$ 比を安定同位体比である $^{38}\text{Ar}/^{36}\text{Ar}$ 比から推定した。このため、放射起源 ^{40}Ar の定量は、従来の同位体希釈法によらず感度法で行なった。カリウム定量についても、積分法とリチウム内部標準法を併用した測定法により、精度と確度の改良を行なった。

新しいK-Ar法によって、どこまで若い火山岩の年代測定が可能かを歴史溶岩類のアルゴン同位体比から理論的に見積ったところ、 K_2O 含量2%の試料では、噴出後約2万年程度の時間が経過すれば有意のK-Ar年代が得られることが判明した。また、 ^{14}C 法によって噴出年代が詳細に求められている始良Tn火山灰に直接覆われる複数の溶岩試料について、K-Ar年代測定を行なったところ、始良Tn火山灰の ^{14}C 年代(22ka)と調和的な値を得ることができた。

さらに、本測定法の火山層序との連続的な整合性を確認するため、また、K-Ar年代に基づく特定火山の噴火史解明の一例として、御嶽・阿蘇火山を選び、それら噴出物に対して系統的なK-Ar年代測定を行なった。その結果、両火山とも一部の例外を除き、2万年以前の噴出物に対して火山層序と整合的な年代を得ることができた。そして、各火山の噴火史について新たに次のことが判明した。(1) 古期御嶽火山の活動は、約70万年前に始まり、40万年前までに終了した。古期御嶽火山岩類の層序を組み立てる際に鍵層とした倉越原溶岩

層には、噴出年代の全く異なる2種類の溶岩層が共存している。(2)新期御嶽火山の活動は、8~9万年前の継母岳火山群の連続的な活動から始まった。それにつづく摩利支天火山群の活動も、約8万年前に開始し、2万年前まで続いた。(3)阿蘇火山起源の火砕流(Aso-1~Aso-4)の噴出年代を、火砕流中の本質レンズ・二次流動強溶結部・気相再結晶部のK-Ar年代(Aso-1: 266 ± 14 , Aso-2: 141 ± 5 , Aso-3: 123 ± 6 , Aso-4: 89 ± 7 ka)から求めた。阿蘇火山周辺の単成火山(赤井・大峰火山)の活動は、それぞれ阿蘇火砕流(Aso-2・Aso-4)の噴出直前であった。また、現在の阿蘇カルデラは少なくとも6万年以前に形成された。

御嶽・阿蘇火山は、それぞれ広域テフラPm-IとAso-4 ashの給源であり、年代測定を行なった御嶽・阿蘇火山岩の一部は、Pm-IとAso-4 ashさらにはDKPとの層序関係が判明していることから、広域テフラ(Pm-I・Aso-4 ash・DKP)の噴出年代をこれら火山岩のK-Ar年代を基に推定した。そしてさらに、K-Ar年代に基づく広域テフラの噴出年代が、南関東における第四紀後期の海水準変動の従来の時間軸にどの程度影響を及ぼすかを検討した。

K-Ar-Altersbestimmungen für quartären Vulkaniten

gegründet auf die Masse-Korrektion-Methode

- Entwicklungen der Methode und Anwendungen

auf die Vulkane Ontake und Aso -

Zusammenfassung

Der Zweck dieser Forschung lag in der Entwicklungen der K-Ar-Methode, die auf bis vor etwa 10000 Jahren ausgeworfens vulkanisches Gestein angewandt werden kann, um durch kombinierte Anwendung der K-Ar-Methode und der ^{14}C -Methode auf Vulkane mit einer Lebensdauer von etwa 10^5 bis 10^6 eine systematische Diskussion der Ausbruchgeschichte bis zur Gegenwart zu ermöglichen.

Für die Entwicklungen der Methode wurde das in der während gegenwärtiger Epoche ausgeworfen Lava enthaltene Argonisotopverhältnis analysiert, es wurde beurteilt, daß das anfängliche Argonisotopverhältnis der Proben auf fraktionierten Geraden aus den gegenwärtigen argonisotopverhältnissen in der Atmosphäre liegt, und auf Grund dieses Ergebnisses wurde für die Analyse des Argonisotopverhältnisses eine Methode verwendet, die jederzeit Schätzung des anfänglichen $^{40}\text{Ar}/^{36}\text{Ar}$ -Verhältnisses aus dem $^{38}\text{Ar}/^{36}\text{Ar}$ -Verhältnis als dem stabilen Isotopverhältnis ermöglicht. Auch für die Kaliumbestimmung werden die Präzision und der Genauigkeit durch die Methode unter kombinierter Verwendung von Integralmethode und Methode mit internem Lithiumstandard verbessert. In Bezug auf die Möglichkeit der Altersmessung für jüngere Proben nach der K-Ar-Methode wird durch eine Schätzung vom anfänglichen Argonisotopverhältnis her gezeigt, daß für Proben mit einem K_2O -Gehalt von 2% ein bedeutsames K-Ar-Alter erhalten werden kann,

wenn nach dem Auswurf etwa 20000 Jahre verstrichen sind.

Als Beispiele für die Klärung der Ausbrüche eines bestimmten Vulkans auf der Grundlage des K-Ar-Alters wurden die Vulkane Ontake und Aso ausgewählt, und systematische Altersmessungen wurden für die Auswürfe dieser Vulkane durchgeführt. Als Ergebnis war es möglich, mit einigen Ausnahmen, in Bezug auf die Auswürfe mit einem Alter über etwa 20000 Jahren mit der Stratigraphie in Übereinstimmung stehende Alterswerte zu erhalten. Weiterhin konnten einige neue Erkenntnisse in Bezug auf die Ausbruchsgeschichte dieser Vulkane erhalten werden. Die Vulkane Ontake und Aso sind die Quelle für Pm-I und Aso-4-Asche (Tephra), und da für einen Teil der Proben der stratigraphische Zusammenhang mit dieser Tephra geklärt ist, wurde das Auswurfalter für diese Tephra (Pm-I und Aso-4 Asche) auf der Grundlage des K-Ar Alters dieser Auswürfe geschätzt. Weiterhin wird dann geschätzt, welchen Einfluß diese Alterswerte auf die bisher für die eustatische Änderung des Meeresspiegels in der zweiten Hälfte des Quartärs im südlichen Kanto-Bereich verwendete Zeitachse hat.

